



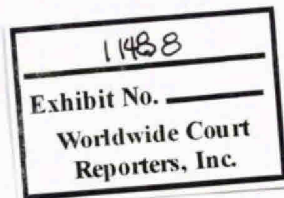
**In re: Oil Spill by the Oil Rig “Deepwater Horizon” in
the Gulf of Mexico, on April 20, 2010**

United States District Court
Eastern District of Louisiana
MDL No. 2179, Section J
Judge Barbier; Magistrate Judge Shushan

**Technical Review of US Government Expert Witness
Reports on Flow Rates from the MC252 Macondo Well**

Expert Report of A. E. Johnson PhD CEng MIMechE

May 1, 2013



CONFIDENTIAL

FEESA Ltd
FEESA Ltd, Westmead House, Farnborough, Hampshire GU14 7LP.
Tel: + 44 (0) 1252 372321 • E-mail: info@feesa.net

TREX 011488.0001

CONTENTS

1 EXECUTIVE SUMMARY	4
1.1 DR. GRIFFITHS' REPORT	4
1.2 DR. DYKHUIZEN'S REPORT	5
2 INTRODUCTION	7
3 QUALIFICATIONS AND EXPERIENCE	8
4 TECHNICAL EVALUATION OF DR. GRIFFITHS' REPORT.....	10
4.1 DR. GRIFFITHS' UNSUPPORTED ASSUMPTION OF A CONSTANT PRODUCTIVITY INDEX AFTER THE FIRST NINE HOURS COULD GENERATE INCORRECT RESULTS.	10
4.1.1 Dr. Griffiths incorrectly interprets the Appendix W data.	10
4.1.2 Using Dr. Griffiths' own methods with a non-constant PI assumption demonstrates the uncertainty range of his results is much wider than he claims.	11
4.2 APPLICATION OF DR. POOLADI-DARVISH'S METHODOLOGY PRIOR TO 8 TH MAY 2010 FURTHER INCREASES THE UNCERTAINTY AROUND DR. GRIFFITHS' ESTIMATE.	16
4.3 DR. GRIFFITHS' WELLBORE MODEL DOES NOT APPROPRIATELY REPRESENT THE GEOMETRY OF THE WELL AND THE EFFECTS OF MULTIPHASE FLOW WITHIN THAT GEOMETRY.....	19
4.3.1 Comparison of Dr. Griffiths' method with an industry-standard multiphase simulator demonstrates errors in Dr. Griffiths' calculations.	19
4.3.2 Dr. Griffiths' failure to represent multiphase flow in the two well flowpaths results in an inaccurate model.....	22
4.3.3 Dr. Griffiths' comparison of his model to PROSPER work done by a BP Engineer during the response is inappropriate and misleading.	25
4.3.4 Dr. Griffiths' use of constant discharge coefficients in his model is unjustified....	26
4.4 DR. GRIFFITHS IGNORES THE MANY PHYSICAL CHANGES THAT OCCURRED THROUGH THE SYSTEM OVER TIME.....	26
4.4.1 Dr. Griffiths ignores changes in the BOP through time.....	27
4.4.2 Dr. Griffiths ignores changes in the well through time.	28
4.5 DR. GRIFFITHS' ATTEMPTED VERIFICATION OF HIS BEST ESTIMATE FLOW RATE IS BASED ON FLAWED LOGIC AND CIRCULAR REASONING.....	30
4.6 THE OFFSET THAT DR. GRIFFITHS CALCULATED FOR PT-B IS INCORRECT.	31
4.7 DR. GRIFFITHS REACHES INCORRECT CONCLUSIONS IN HIS APPENDIX I REGARDING CHANGES IN THE SYSTEM GEOMETRY PRIOR TO 8 TH MAY 2010.	36
4.8 DR. GRIFFITHS' REPORT CONTAINS A NUMBER OF ADDITIONAL TECHNICAL ERRORS.	38
5 TECHNICAL EVALUATION OF DR. DYKHUIZEN'S REPORT.....	40
5.1 DR. DYKHUIZEN'S ANALYSES ARE BASED ON INCORRECT OR UNSUPPORTED ASSUMPTIONS IN CALCULATING THE FLOW RATE FROM THE TOP HAT.	40
5.1.1 Dr. Dykhuizen's Top Hat skirt flow estimate is highly inaccurate.....	41
5.1.2 Dr. Dykhuizen misrepresents his well flow rate estimate, based on the Top Hat vent flow calculation, as a lower bound.	42

5.2 DR. DYKHUIZEN’S TOP KILL ANALYSIS HAS SERIOUS TECHNICAL ERRORS THAT AFFECT THE VALIDITY OF HIS FLOW RATE CALCULATIONS..... 43

5.3 DR. DYKHUIZEN MADE INCORRECT ASSUMPTIONS IN CALCULATING THE FLOW RATE FROM THE WELL THROUGH TIME AND THE CUMULATIVE DISCHARGE. 48

6 CONCLUSIONS..... 49

7 FEDERAL RULES OF CIVIL PROCEDURE 51

8 REFERENCES 52

9 APPENDICES..... 54



1 EXECUTIVE SUMMARY

I am a consulting engineer working for FEESA Ltd, which provides technical analysis services to the oil and gas industry. BP retained FEESA to provide expert opinions in connection with the litigation stemming from the *Deepwater Horizon* drilling rig incident on 20th April 2010. In this report, I provide a technical review of the US Government expert witness reports relating to the estimated volume of oil discharged from the MC252 Macondo Well. My review focuses specifically on the reports of Dr. Stewart K. Griffiths and Dr. Ronald C. Dykhuizen.

1.1 Dr. Griffiths' Report

Dr. Griffiths purports to estimate the flow rate from the Macondo well and the resulting cumulative discharge from the well over the 86 days of the incident. To do this, he constructs an over-simplified and inaccurate model of the flow path (and associated resistances) from the reservoir to the sea, incorporating numerous incorrect and unsupported assumptions into his model. Dr. Griffiths' over-simplified model and incorrect assumptions are used to generate just one of many possible results with unrealistically small uncertainty ranges around that result. The following is a summary of findings and conclusions from my technical evaluation of Dr. Griffiths' report:

1. Dr. Griffiths' assumption that the productivity index ("PI") increased to 43.8 stock tank barrels per day per psi (stb/d/psi) during the first 8.6 hours following the blowout is a misinterpretation of available data and is incorrect. Dr. Griffiths' assumption that the PI then remained constant throughout the 86 days is unfounded. The constant PI Dr. Griffiths assumed is only one of many scenarios of how the PI may have changed over time. In the absence of an assumed constant PI, Dr. Griffiths' own methods generate a much wider uncertainty range than he claims.
2. Dr. Griffiths makes incorrect assumptions about the bottom of BOP pressure ("PT-B") prior to the first available data on the 8th May 2010. Application of Dr. Pooladi-Darvish's (a US Government expert witness) PT-B methodology prior to 8th May 2010 further increases the uncertainty around Dr. Griffiths' estimate by reducing Dr. Griffiths' "best estimate" by 10%. Combining Dr. Pooladi-Darvish's PT-B methodology with a non-constant PI in Dr. Griffiths' method further increases this uncertainty range of Dr. Griffiths' results, reducing his "best estimate" by more than 30%.
3. Dr. Griffiths' calculation methods are overly simplistic. They do not represent two critical features of the system that affected the flow rate (multiphase flow and the presence of two flow paths in the well caused by the drill pipe in the well) sufficiently to calculate the flow rate accurately. Comparison to an industry-standard multiphase simulator demonstrates the errors in Dr. Griffiths' calculations.
4. Dr. Griffiths' model determines the well and BOP discharge coefficients using only a few hours of capping stack data from the end of the flowing period. Dr. Griffiths then assumes that this model (with constant well and BOP discharge coefficients) based on a few hours at the end of the incident can be applied to the prior 86 days of the incident.

This is contrary to the physical evidence which indicates that numerous changes in the flow path occurred throughout the incident.

5. The two alternative methods that Dr. Griffiths used to “validate” his model were derived from the same set of data from which his initial model was based. Therefore, they do not (and cannot) present any form of validation of his “best estimate” case. Dr. Griffiths’ use of these two alternative models is a self-fulfilling circular argument. Furthermore, the application of these “validation” methods to the entire 86 day flow period offers no validation of Dr. Griffiths’ cumulative discharge results.
6. Dr. Griffiths has not demonstrated that his adjustments of the PT-B readings are correct. The uncertainty surrounding the proper correction (or corrections) to be applied to PT-B indicates that the overall uncertainty of Dr. Griffiths’ flow estimates is much greater than he acknowledges.
7. Dr. Griffiths’ analysis of the flow rates and cumulative discharge prior to 8th May 2010 is mainly conjecture and the estimates for this period could be incorrect by a factor of approximately 2.

1.2 Dr. Dykhuizen’s Report

Dr. Dykhuizen presents three calculations that he asserts are lower bound flow rates. The first calculation is based on BOP pressure and Top Kill data from the Top Kill period on 28th May 2010. The second and third calculations are based on flow from the Top Hat. These calculations include a number of technical errors and incorrect assumptions, which lead to incorrect results. Dr. Dykhuizen also briefly reviews calculations that he performed during and immediately following the response effort, wherein he calculated a cumulative discharge over the 86 days of the incident and highlights reasons for changes in his estimate on account of updated data. The following is a summary of findings and the conclusions from my technical evaluation of Dr. Dykhuizen’s report:

1. Dr. Dykhuizen’s calculation of a lower bound flow rate, based on the flow from the vents on the Top Hat, was incorrect outside of a narrow time frame. Dr. Dykhuizen added the result of the calculation to the collection flow rate just prior to the installation of the capping stack, when the collection rate from the Top Hat was higher than it had been at earlier times. At earlier times in the Top Hat period this lower bound flow rate would have been about 20,000 stb/d. Dr. Dykhuizen’s lower bound estimate is, therefore, only a lower bound near the capping stack period.
2. Dr. Dykhuizen’s June 2010 calculation of flow from the skirt at the base of the Top Hat is subject to large uncertainties in two key parameters used in the analysis: the skirt geometry and pressure data. Dr. Dykhuizen’s flow rate estimate for the flow from the skirt at the base of the Top Hat is a gross overestimate, by a factor of at least 10.
3. Dr. Dykhuizen’s calculation of a lower bound flow rate based on the Top Kill period is incorrect. When I performed a calculation using Dr. Dykhuizen’s own method for an earlier Top Kill attempt, it yielded a result of 32,700 stb/d. Other uncertainties in the

calculation could result in an even lower flow rate than 32,700 stb/d. Given the uncertainties of mud flow direction and presence of junk shot materials during the Top Kill attempt on 28th May 2010, I do not believe that subset of later Top Kill data can be used for accurate flow rate estimation.

4. My analyses as to why Dr. Griffiths' calculation of flow rate over the 86 days is incorrect equally apply to Dr. Dykhuizen's estimate (*i.e.*, Dr. Dykhuizen, like Dr. Griffiths, incorrectly assumes that restriction and PI were constant over time, and fails to account for the drill pipe in the well). Had Dr. Dykhuizen performed this calculation correctly (taking account of changing restrictions in the system, the drill pipe in the well, and multiphase effects) the results would not have indicated a decreasing flow rate with time.
5. Also, as in the case of Dr. Griffiths' calculation of the volume of oil leaked from the well, Dr. Dykhuizen's estimate is (at best) an order of magnitude estimate. And (although Dr. Dykhuizen does not quantify them) the uncertainty bands around the cumulative flow estimates are large.

2 INTRODUCTION

My analyses of Dr. Griffiths' and Dr. Dykhuizen's reports are based on many years of experience in modeling and analysis of oil and gas production systems within the oil industry, together with in-depth understanding of fluid flows under diverse conditions.

This report will discuss:

- **Section 3: Qualifications** – Presents my relevant qualification and experience.
- **Section 4: Technical Evaluation of Dr. Griffiths' Report** – Describes in detail the points of technical issues and deficiencies in this US Government Report.
- **Section 5: Technical Evaluation of Dr. Dykhuizen's Report** – Describes in detail the points of technical issues and deficiencies in this US Government Report.
- **Section 6: Conclusion** – Outlines the main technical conclusions drawn from my technical analyses.
- **Section 7: Federal Rules of Civil Procedure** – Required statements for an expert witness report.
- **Section 8: References** – List of documents referred to in this report.
- **Section 9: Appendices** – There are 8 appendices covering the in-depth technical details of each area of my technical analysis.

Throughout the report references to documents are given as a number in brackets – *e.g.*, (ref. 21) and the documents referenced are listed in section 8 of this report.



3 QUALIFICATIONS AND EXPERIENCE

This section outlines my qualifications and experience in analysis of flowing systems in various engineering environments, primarily in the oil and gas industry.

I am a chartered engineer with 29 years engineering experience, the last 24 years of which have been in the oil and gas industry.

My qualifications include:

- PhD in Mechanical Engineering – Studying complex turbulent flows – University of Surrey, 1990
- CEng (Chartered Engineer) – On the Engineering Council’s register as a practicing professional engineer, 1990
- MIMechE (Member of the Institution of Mechanical Engineers) – A full member of the Institution of Mechanical Engineers, 1990
- BSc in Mechanical Engineering – Specializing in Maritime and Offshore engineering – University of Surrey, 1985
- Ordinary National Diploma in Engineering from People’s College, Nottingham, 1981

My experience in the oil industry includes:

- Technical consulting and analysis, including:
 - FEESA (2010 to present)
 - Whitewood Ltd. (1999 to 2010)
 - BP Research & Engineering (1993 to 1999)

I have 20 years consulting experience specialising in understanding, analysing and modeling the hydraulic behaviour of oil and gas production and pipeline systems. I have performed key roles on major projects and in operations in pipelines and production flow assurance (*i.e.*, the technical evaluation of a flowing system to ensure there will not be any thermal or hydraulic problems with the design or operation). I have performed and led modeling work and field trials on international projects and studies for numerous locations (*e.g.*, Azerbaijan, Georgia, Turkey, United Kingdom, Gulf of Mexico, Angola, Oman, Algeria, Egypt, etc.).

I am now the consultancy manager who leads the technical consulting work for FEESA, leading a team of eight consultants in the modeling of production systems and pipelines for numerous projects including deep-water oil production, tight gas production systems, CO₂ sequestration, water injection, pipeline network analysis and uncertainty analysis.

- Investigative R&D at BP Research (1989 to 1993) - Including studying the structure of multiphase flow, the mechanical behaviour of flexible riser pipe, valve leak detection and testing of drill pipe protectors.

I have previous expert witness experience performing analysis of the failure of a drill-string disc brake on a deep-water exploration well, located offshore in West Africa. I have never testified as an expert witness.

I also have spent one year working in the nuclear industry.



4 TECHNICAL EVALUATION OF DR. GRIFFITHS' REPORT

This section describes in detail the technical issues found during my evaluation of Dr. Griffiths' report (ref. 1). Dr. Griffiths' study aimed to quantify flow rates and cumulative discharge of oil from the Macondo well via a very simplified model of the system. However, Dr. Griffiths assumed that restrictions throughout the system remained constant with time and he failed to incorporate key parts of the system, which seriously affected his results.

4.1 Dr. Griffiths' unsupported assumption of a constant productivity index after the first nine hours could generate incorrect results.

In this section, I show that Dr. Griffiths' assumptions about the PI at the time of the blowout are incorrect. I then demonstrate that Dr. Griffiths' assumption of a constant PI over the 86 days is only one possible scenario that matches the available data. Finally, I apply Dr. Griffiths' own analysis methods with different assumptions that are supported by the data to demonstrate that Dr. Griffiths' flow rate and discharge conclusions are only one of many possible solutions that can be reached using his model. In this way, I show that the range of "cumulative discharge" results from Dr. Griffiths' model are far greater than what Dr. Griffiths presents in his Report.

4.1.1 Dr. Griffiths incorrectly interprets the Appendix W data.

Dr. Griffiths assumes that the PI rapidly changes within the first 9 hours following the blowout and then remains constant over the 86 days (ref. 1, footnote 10, page 11). Essentially, then, Dr. Griffiths assumes that there was a constant PI during the entirety of the 86 days of the incident. This assumption of a constant PI is a fundamental input of Dr. Griffiths' model. If Dr. Griffiths is incorrect about this assumption then the results produced from his model will also be incorrect. As I explain in this section, Dr. Griffiths is not justified in assuming that the PI was constant. Once divorced from Dr. Griffiths' constant PI assumption, I demonstrate that there are a series (and in fact, an infinite number) of PIs that can exactly match the PT-B data and Dr. Griffiths' calculated flow rate for the Capping Stack.

Dr. Griffiths arrives at a PI using data from the period when the Capping Stack was installed. (ref. 1, page 31). Specifically, Dr. Griffiths performs a non-linear, least-squares analysis to obtain his PI and discharge coefficients. The PI Dr. Griffiths deduces from the Capping Stack period is 43.8 stb/day/psi¹ for his "best estimate" case.

Having calculated a PI based upon data from day 86, Dr. Griffiths then applies this PI backward in time to day 1 of incident, save for the first approximately 9 hours following the blowout. To support this constant PI assumption, Dr. Griffiths concludes that the PI changed from about 9 stb/day/psi to 43.8 stb/day/psi in just 8.6 hours (ref. 1, footnote 10, page 11). To support this assumption, Dr. Griffiths relies upon data and analysis presented in Appendix W (ref. 14) of the Deepwater Horizon Accident Investigation Report (See page 11, ref. 14,

¹ Dr. Griffiths calculated two PIs, but for purposes of my analysis, I will cite the 43.8 stb/d/psi because this is the value he used for his "best estimate".

footnote 10, page 11). Dr. Griffiths draws incorrect and unsupported conclusions from the Appendix W analysis that undermines his assumption of a constant PI.

As further described in Appendix W, ae add energy used drill string pressure data to model the flow of drilling mud and hydrocarbons on 20th April 2010, prior to the blowout. ae add energy is able to match the drill string pressure data by using, among other parameters, an exposed reservoir of about 13 feet. ae add energy achieves this match of pressure data and exposed reservoir for the period from 15:00 to 21:30 (ref. 14, Fig. 3.32, page 55). Then, at 21:30, in order to match the drill string pressure data (when the mud pumps were turned off), ae add energy must increase the exposed reservoir from 13 feet to 16.5 feet. With that instantaneous change in the exposed reservoir from 13 feet to 16.5 feet, ae add energy matches the drill string pressure from 21:30 until 21:49, when the blowout occurs.

Dr. Griffiths interpreted this data to mean that there was a failure of downhole restrictions such that the “effective productivity index increased by over 25% between 21:00 and 21:30” (ref. 1, page 11). Dr. Griffiths concluded that a “continued failure at this rate” would result in an increase of the PI from about 9 stb/d/psi to his 43.8 stb/d/psi within 8.6 hours. Dr. Griffiths seems to link this “failure” to erosion of the downhole cement (ref. 1, footnote 11, pages 11-12).

Dr. Griffiths made a fundamental error in his interpretation of this data that affects his assumption of a constant PI of 43.8 stb/d/psi throughout the 86 days. Dr. Griffiths treats the change from 13 feet to 16.5 feet as a continuous change at a rate of 7 feet per hour, as if the exposed reservoir was opening up from 13 feet to 16.5 feet over this 30 minute period. However, ae add energy applied an instantaneous change to the exposed reservoir at exactly 21:30 in order to match the drill string pressure. Indeed, ae add energy matched the drill string pressure with a constant assumption of 13 feet for the period from 15:00 to 21:30. Thus, no rate change was required during this time period. Additionally, for the period between 21:30 and 21:49, ae add energy matched the drill string pressure with a constant assumption of 16.5 feet. Again, no “rate change” was required during this time period in order to match the pressure data, even for the large pressure increase approaching the blowout.

Dr. Griffiths argues that the change in the exposed reservoir at 21:30 from 13 feet to 16.5 feet supports his assumption that there were rapid changes to the downhole restrictions leading up to the blowout. Yet, the ae add energy analysis does not support this conclusion. Rather, ae add energy matched the pressure data with a constant exposed reservoir (albeit 13 feet and 16.5 feet) for the period prior to 21:30 and the period following 21:30. Thus, there is no support for Dr. Griffiths extrapolation of a rate of change associated with the instantaneous change in exposed reservoir.

4.1.2 Using Dr. Griffiths’ own methods with a non-constant PI assumption demonstrates the uncertainty range of his results is much wider than he claims.

The ae add energy analysis contained in Appendix W implies a productivity index of 9.4 stb/d/psi at 21:49 on 20 April. The ae add energy analysis does not tell us anything about how the productivity index may have changed over time from 21:49 on 20 April until the well was shut-in on 15th July 2010. Indeed, the ae add energy work tends to suggest that for the period of its analysis, the productivity index was constant apart from the step change when the mud

pumps were shut down. If I assume that Dr. Griffiths is correct that the PI on 15th July 2010 was 43.8 stb/d/psi, I can draw any number of profiles between a PI of 9.4 stb/d/psi on 20th April 2010 and 43.8 stb/d/psi on 15th July 2010, and still match the pressure data at the BOP, as Dr. Griffiths does in his model.

In the absence of any additional constraints, an infinite number of alternative PI profile assumptions could be made using a recreation of Dr. Griffiths' model that would be consistent with the available pressure data. These different scenarios would result in very different flow rate profiles through time and, therefore, very different volumes leaked to the sea overall.

The PI assumptions used to demonstrate the discussion here are given in Figure 1. Each of the assumed PI scenarios in Figure 1 is a possible fit for the data.

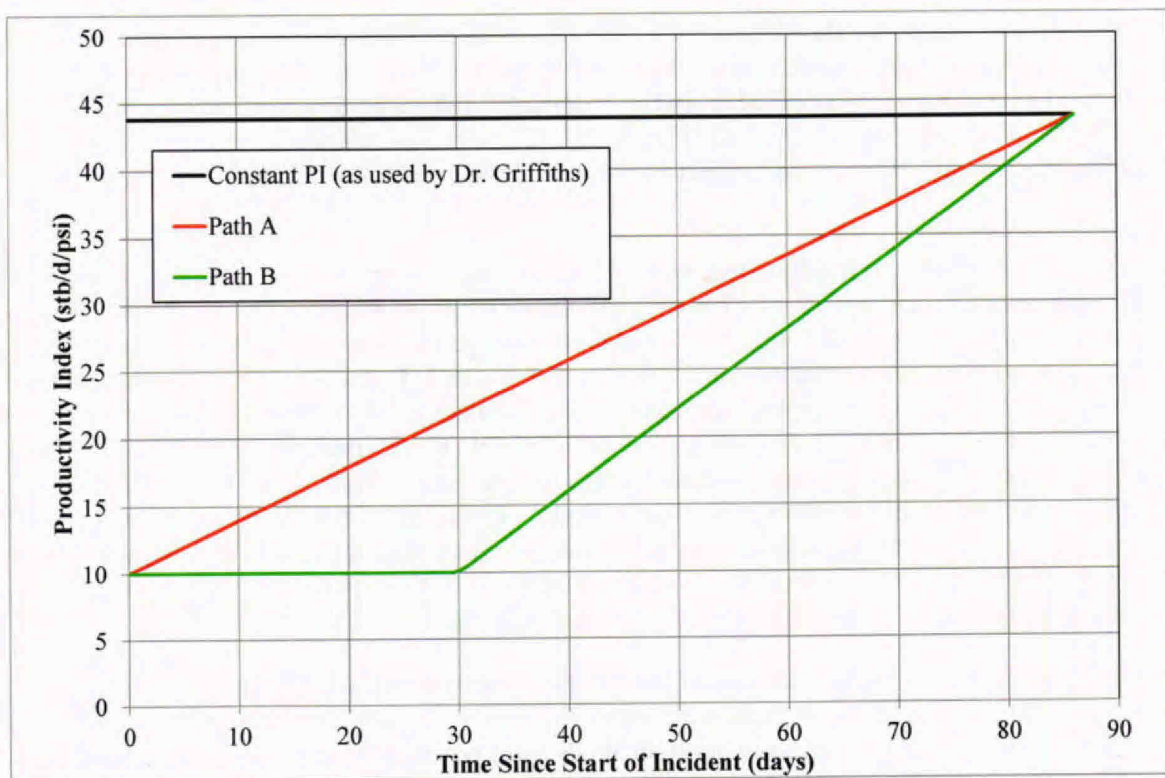


Figure 1. Possible PI Profiles

As discussed above, there is an infinite number of curves that could be drawn over the range shown in Figure 1 (and perhaps an even greater range) with little or no evidence that any particular curve is correct. Certainly, there is no evidence that the assumption of a constant PI, which Dr. Griffiths' assumed was the case, is correct. In fact, Paths A and B in Figure 1 are based on the PI inferred from Appendix W (ref. 14). Appendix W implies a PI at the time of the blowout of 9.4 stb/d/psi (rounded to 10 stb/d/psi in Figure 1).

The profile associated with Path B is further constrained in that it matches the PI to produce the flow rate calculated by Dr. Zaldivar. Dr. Zaldivar calculates a flow rate range of approximately

30 Mstb/d to 35 Mstb/d from 13th May 2010 to 20th May 2010, and I calculate that this flow rate requires a PI of about 10 stb/d/psi. Thus, Dr. Zaldivar's work is evidence that Path B presents the more likely PI profile for the 86 day period of the PI profiles presented in Figure 1.

In Figure 2, below, I present flow rate profiles based upon the PI profiles from Figure 1 and PT-B data. For the analysis presented in Figure 2, I use Dr. Griffiths' extrapolation of PT-B data to the pre-8th May 2010 period. However, it is important to note that there is no PT-B data available before the 8th May 2010. As I further discuss in Section 4.2, below, the data points generated using Dr. Griffiths' method for the pre-8th May 2010 period are wrong. Nevertheless, for the purpose of demonstration, I have used Dr. Griffiths' extrapolated value of PT-B in calculating the flow rate at the time of the blowout in Figure 2, even though it is incorrect.

Using the PI profiles given in Figure 1, I calculate the wide range of potential flow rate profiles that can be generated. Figure 2 shows the resulting flow rate profiles from this analysis. Only one of the profiles is consistent with Dr. Griffiths' results (see details of the calculation in Appendix B), but all are possible based on the available data. All of the flow rate profiles converge at the capping stack period because the constants (*i.e.*, PI, k_{well} , k_{BOP} , etc.) in Dr. Griffiths' model were set by regression analysis to the capping stack flow rate data.

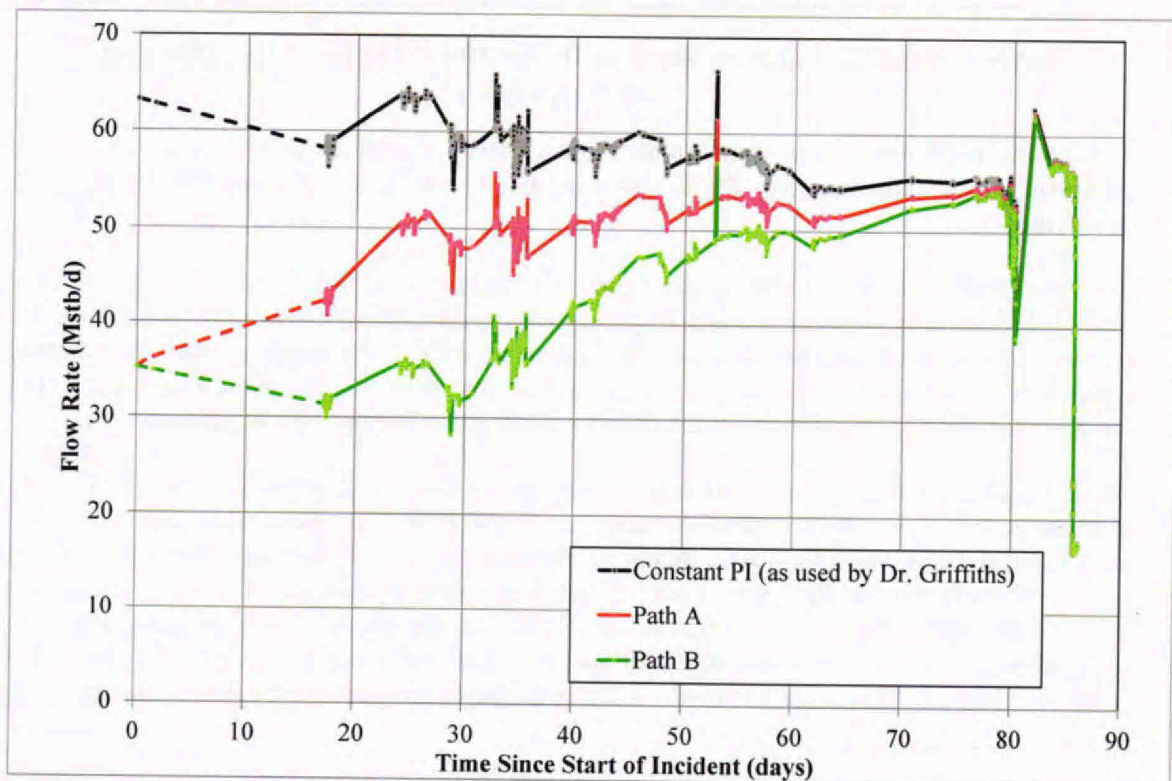


Figure 2. Flow Rate Profiles Using Dr. Griffiths' Method And Different PI Assumptions

For the analysis in Figure 2, there is no PT-B data available before the 8th May 2010. Dr. Griffiths assumed a pressure at the bottom of the BOP at the time of the blowout by extrapolation backwards of his least-squares fit to a selectively picked data set² from the available PT-B data. This extrapolation of the PT-B data is a factually unsupported assumption. Indeed there is evidence to suggest that the pressure at the bottom of the BOP at the time of the blowout was much higher than Dr. Griffiths' value (see section 4.2).

From integration of the flow rate profiles presented in Figure 2, Table 1 shows the total predicted volume of oil released from the well over the incident and the total leaked to the sea (*i.e.*, subtracting the 0.81MMstb that BP collected during the incident (ref. 12) and subtracting the oil that was released and subsequently burned in the 1.5days prior to the *Deepwater Horizon* sinking (see ref. 13) that states that the first 2 days of flow from the well are not included in the volume of oil released to sea).

PI Path	Total Volume of Oil from Well (MMstb)	Volume of Oil to DWH (MMstb)	Collected Volume of Oil (MMstb)	Total Volume of Oil Leaked to Sea
Constant PI	5.0	0.10	0.81	4.1
Path A	4.2	0.05	0.81	3.3
Path B	3.7	0.05	0.81	2.8

Table 1. Total Oil Volumes Based on Dr. Griffiths' Method Using Different PI Assumptions

The results for Paths A and B in Table 1 are consistent with all of the available data, but eliminate the fundamental error Dr. Griffiths made when he assumed a constant PI throughout the incident.

The lower the PI of the well, the greater the flow restriction needed in the BOP³ to match the available PT-B data. That is, a lower PI gives (all else equal) lower flow rate, and a lower flow rate through the BOP requires a greater restriction to achieve the same pressure drop between PT-B and the ambient sea pressure. Large variations in PI would, therefore, require large variations in the loss coefficient⁴ in the BOP to result in the required PT-B pressure.

At first glance, it might seem that large variations in the loss coefficient in the BOP would mean large variations in the size of the openings in the BOP (*i.e.*, the eroded flow paths or the gaps between rams, etc.). However, this is not the case because of the shape of the curve for the loss coefficient versus the open area of the restriction as shown in Figure 3. The loss coefficients required to give a match to the PT-B data, for the low PI scenarios are all large (*i.e.*, between about 10,000 and 100,000) and are, therefore over to the left hand side of the curve in Figure 3. The steepness of the left hand side of the curve in Figure 3 illustrates how

² For example, Dr. Griffiths deleted high pressure data points at the end of the Top Hat period and low pressure data prior to the Top Kill period.

³ In this discussion the riser also provides a restriction, but has been omitted from the discussion for purposes of clarity.

⁴ Loss coefficient refers to the constant of proportionality between the pressure drop across the BOP and the flow rate squared through the BOP.

very small changes in the open area through the BOP cause large changes in the loss coefficient. As discussed above, the low PI scenarios are as valid as (if not more valid than) the constant PI scenario.

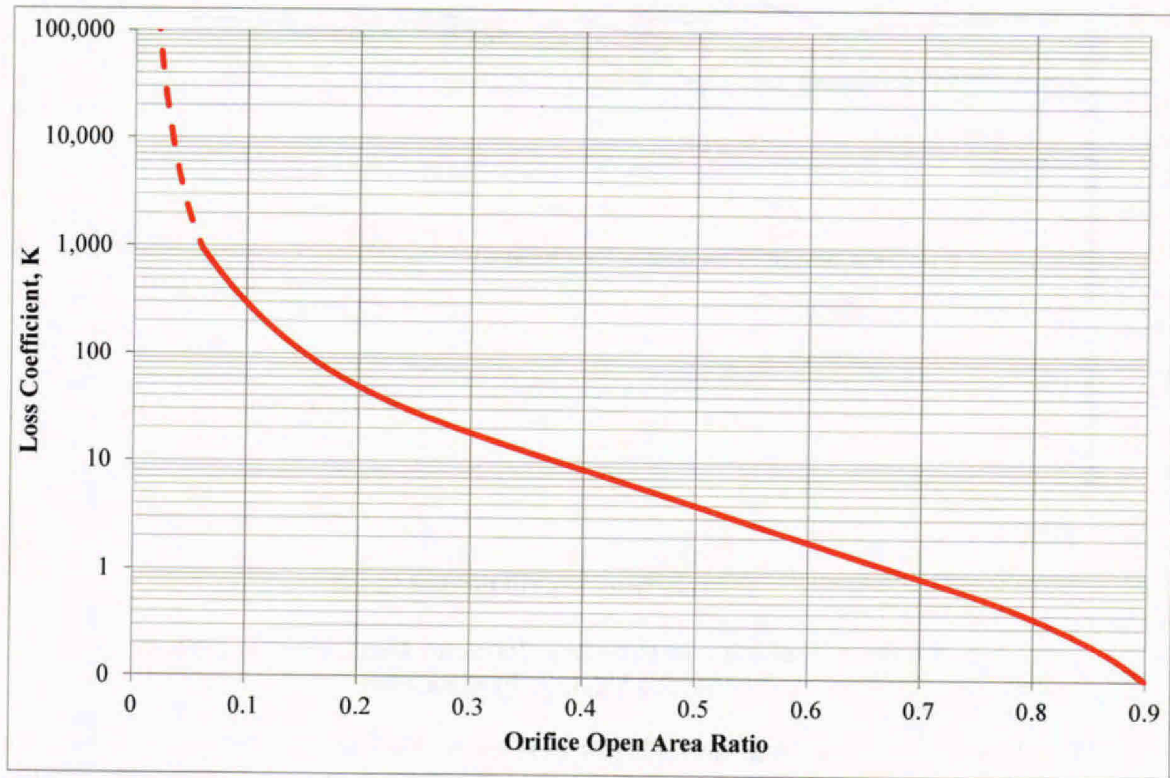


**Figure 3. Orifice Loss Coefficient Curve (from ref. 16, Fig. 14.3)
Extrapolated (as shown by the dotted section) for the BOP Open Area Ratio**

The effective diameters of the opening required to give the loss coefficients needed to match the PT-B data are shown for the various PI scenarios in Figure 4.

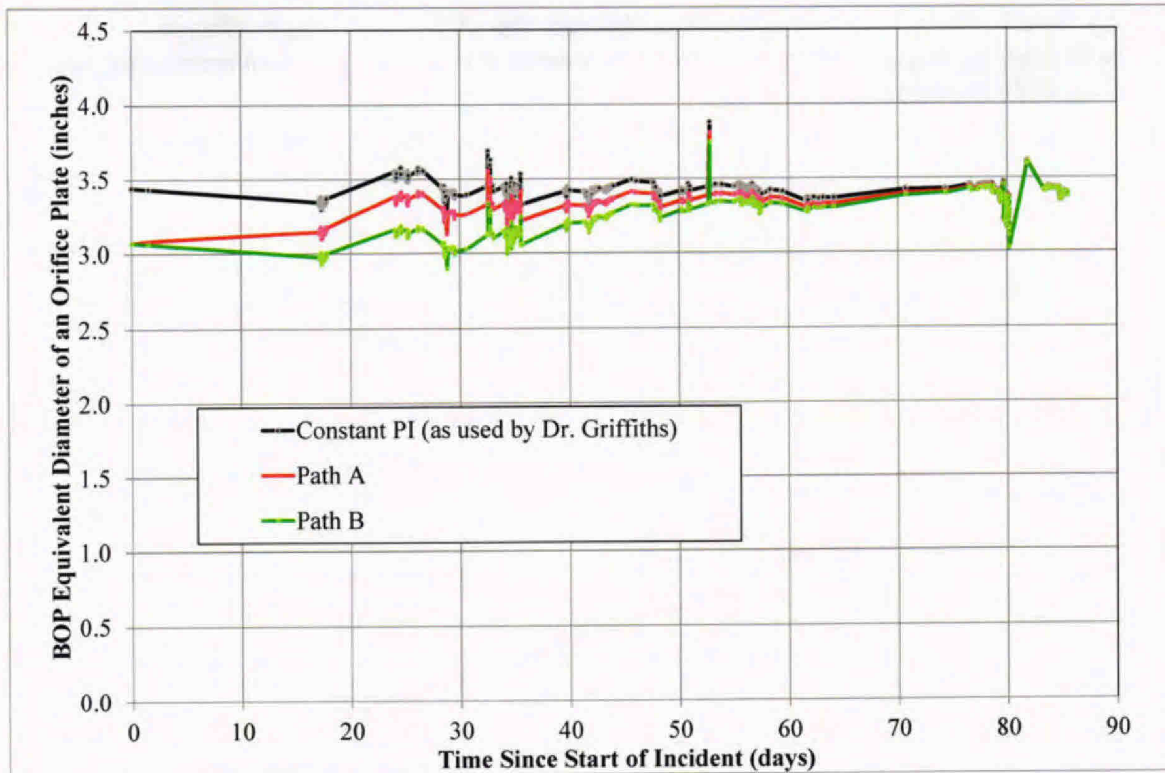


Figure 4. Variation of Effective Diameter Downstream of PT-B for the Various PI Scenarios

Figure 4 demonstrates that the greatest change in effective diameter required between any two of the scenarios shown in Figures 1, 2 and 4, is less than 1 inch. A 1 inch change in effective diameter could result from erosion, Top Kill blockages, or movement of rams.

Table 1 shows that the oil volumes leaked to sea vary by about 150% from the lowest to the highest. This uncertainty range is far greater than the -13.9% and +9.7% that Dr. Griffiths represented as the error bands for his calculations (see ref. 1, page 10). In fact, the total uncertainty range is greater than the snapshot presented in Table 1, given that there are other PI scenarios that could be postulated. My analysis demonstrates that Dr. Griffiths, had insufficient information to accurately predict the oil flow rate throughout the 86 days using his hydraulic analysis.

4.2 Application of Dr. Pooladi-Darvish's methodology prior to 8th May 2010 further increases the uncertainty around Dr. Griffiths' estimate.

As discussed in section 4.1 above, the 20th April 2010 PT-B pressure proposed by Dr. Griffiths is based (incorrectly) on extrapolation of a least squares fits of the PT-B data back to this date. The Sperry Sun data (ref. 36) at the time of the integrity test shows that the last pressure reading at the top of the drill pipe on 20 April 2010 was 5786 psia. From this drill pipe

pressure, I calculated a pressure at the PT-B position of about 8700 psia. The 8th May 2010 PT-B reading was 4565 psia (see refs. 7-11), using Dr. Griffiths' correction to PT-B of +740 psia. These data were adopted by Dr. Pooladi-Darvish in his expert report (ref. 37) where he suggests that the change from this high 20 April 2010 PT-B pressure to the lower value on 8th May 2010 represents a gradual erosion of the BOP (and effectively the riser kink, although this is not specifically mentioned by Dr. Pooladi-Darvish).

In a similar way to Dr. Pooladi-Darvish's analysis, I have produced a PT-B profile between 20th April 2010 and 8th May 2010 that varies linearly from the high value at the time of the integrity test to the first PT-B reading at 8th May 2010. Combining this declining PT-B profile prior to the 8th May 2010 with the PT-B data from 8th May to 15th July 2010 results in a new PT-B trend through the 86 days, as shown in Figure 5. Although I am producing a PT-B pressure profile pre-8th May 2010 in a similar way to that of Dr. Pooladi-Darvish, I am not commenting further on his work and am not endorsing it. Also shown in Figure 5 is the PT-B profile assumed by Dr. Griffiths.

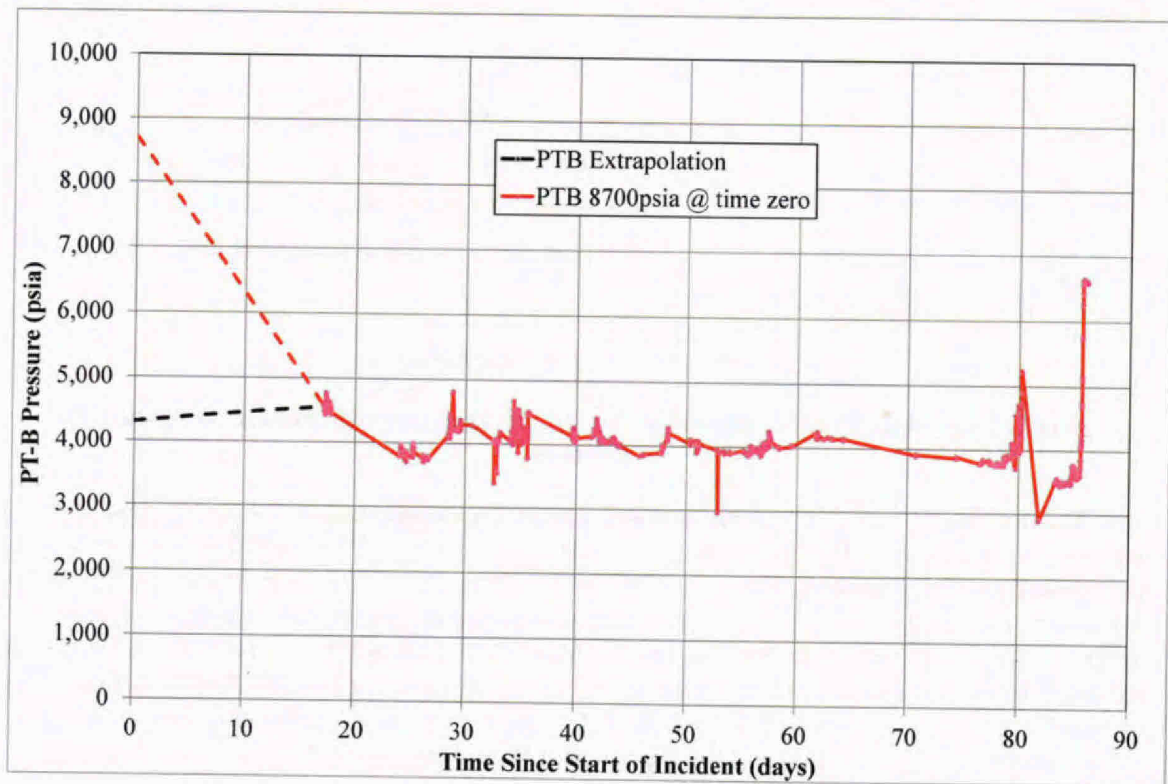


Figure 5. PT-B Profiles using the Dr. Pooladi-Darvish and Dr. Griffiths Approach

The new PT-B pressure profile shown in Figure 5, for the case of high 20 April 2010 PT-B pressure, is a more believable profile than the one based on Dr. Griffiths' extrapolation. The new profile matches the trend in the PT-B data for the few days after the 8th May 2010 and could even explain the decrease in the PT-B readings in mid-May (*i.e.*, days 24 to 26 in Figure 5).

I combined the constant PI profile and Path B PI profile, described above and shown in Figure 1, with the PT-B profiles shown in Figure 5 in the modeling method of Dr. Griffiths to produce four flow rate profiles as shown in Figure 6.

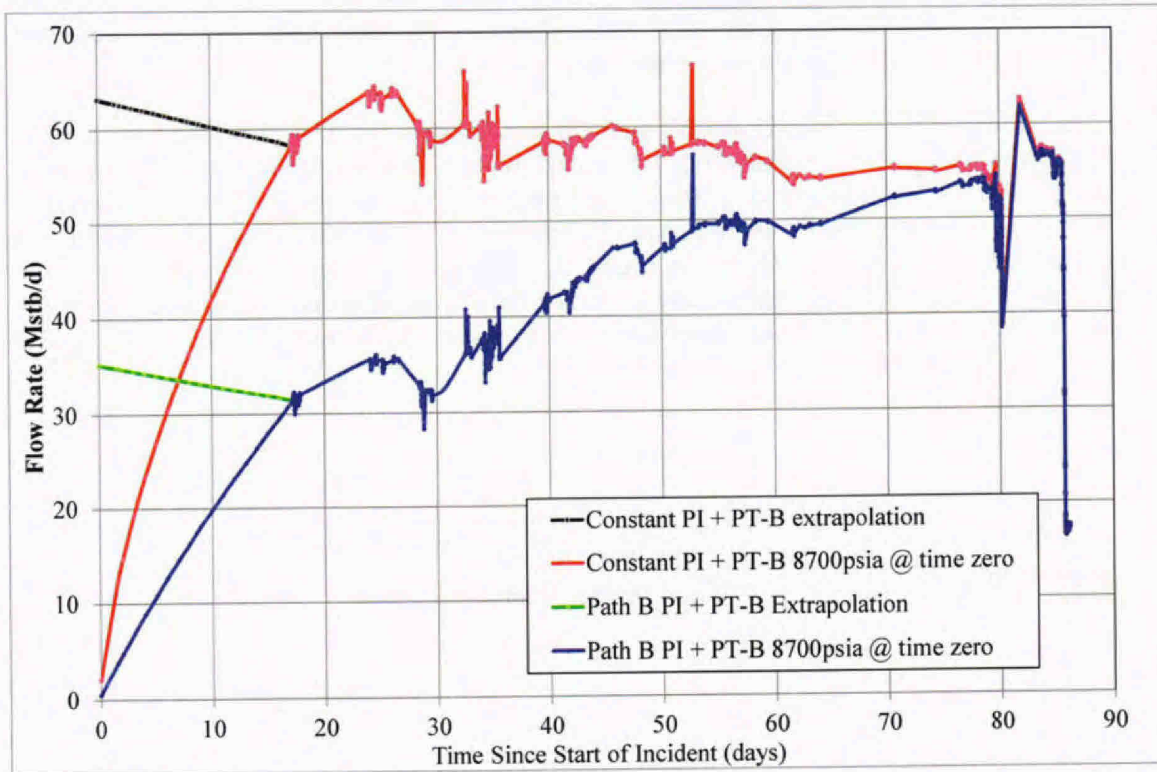


Figure 6. Flow Rate Profiles Based on the Dr. Pooladi-Darvish and Dr. Griffith PT-B Profiles

From 8th May 2010 to 15th July 2010 the flow rate profiles illustrated in Figure 6 are the same as those in Figure 2, above. Recall that Figure 2 also uses the same PT-B and PI inputs as used in the calculations for Figure 6. However, before 8th May 2010, only the black and the green profiles are the same as shown in Figure 2 above because they again use a constant PI and Dr. Griffiths' PT-B assumption for prior to the 8th May 2010. The two new cases, the red and blue profiles in Figure 6 representing the case of high PT-B pressure on the 20th April 2010, are very different. The flow rate on the 20th April 2010 for the high PT-B pressure cases is close to zero (*i.e.*, about 2000 stb/d and 500 stb/d for the constant PI and the Path B PI cases respectively).

Integration of the flow rate profiles in Figure 6 results in the cumulative discharge values given in Table 2.

Case	Total Volume of Oil from Well (MMstb)	Volume of Oil to DWH (MMstb)	Collected Volume of Oil (MMstb)	Total Volume of Oil Leaked to Sea (MMstb)
Constant PI + PT-B extrapolation	5.0	0.10	0.81	4.1
Constant PI + PT-B 8700psia @ time zero	4.5	0.01	0.81	3.7
Path B PI + PT-B Extrapolation	3.7	0.05	0.81	2.8
Path B PI + PT-B 8700psia @ time zero	3.4	0.00	0.81	2.6

Table 2. Cumulative Discharge Results Based on the Dr. Pooladi-Darvish and Dr. Griffith PT-B Profiles

As demonstrated in Table 2, the assumption of a steady decline in the PT-B pressure prior to 8th May 2010, compared with the Dr. Griffiths' assumption of PT-B pressure in this period, results in a decrease in the cumulative discharge from the well of about 500 Mstb from Dr. Griffiths' result – *i.e.*, 10% decrease. Dr. Griffiths fails to account for this variability in his uncertainty range.

4.3 Dr. Griffiths' wellbore model does not appropriately represent the geometry of the well and the effects of multiphase flow within that geometry.

In section 4.3, I use Dr. Griffiths' own analysis methods and compare them with results from an industry-standard multiphase simulation tool⁵ to demonstrate that Dr. Griffiths' methods do not represent the complex flow path geometry and complex flow conditions present in the Macondo well during the incident.

4.3.1 Comparison of Dr. Griffiths' method with an industry-standard multiphase simulator demonstrates errors in Dr. Griffiths' calculations.

I calculated, using industry-standard multiphase flow network simulation software called Maximus, with a detailed composition and the OLGAS two-phase flow correlation, the oil flow rate variation versus PT-B pressure for the following three conditions:

- No drill pipe present;
- With the drill pipe located at the top of the well;
- With the drill pipe located lower down in the well.

⁵ The industry-standard multiphase simulation tool used is FEESA's own life of field, steady state, network simulation software, Maximus. Maximus uses rigorous multiphase thermal hydraulic calculation. The software is widely used in the oil and gas industry for simulation of wells and pipeline networks on multi-billion dollar projects around the world.

I compared the results for each of the cases using Maximus to Dr. Griffiths' method. For each of these comparisons, I ran calculations both for the 8th May 2010 and 15th July 2010 reservoir pressures. I used a constant PI and Dr. Griffiths' PT-B offset for all of these comparisons (although I agree with neither the use of a constant PI, see Section 4.1 above, nor with Dr. Griffiths' PT-B offset, as discussed in Section 4.4 below). This analysis is discussed in detail in Appendix C of this report.

Figures 7, 8a, and 8b show that the form of the curves is different for the two methods of calculation, especially when the drill pipe is present. This is due to the Maximus model taking into account the multiphase phenomena that Dr. Griffiths has ignored in his assumption that the flow acts as if it is homogeneous and unchanging. That is, he ignores flow regime changes, slip between phases, density changes, interaction between frictional and gravitational pressure drop and the presence of the drill pipe as a second flow path. A significant finding is that for the 8th May period there is a significant difference for the cases where the drill pipe is present – despite Dr. Griffiths' calculation matching the data for the capping stack time period (which it must by definition, as his model is tuned to fit that period). This is due to the fact that Dr. Griffiths' simplified method does not account for the effect of changing temperatures and pressures on the vapor-liquid equilibrium (VLE). As a result, Dr. Griffiths' method does not account for the effect of these multiphase phenomena on the frictional and gravitational pressure drop in the two flow paths.

Also shown in Figures 7, 8a, and 8b are arrows drawn between the points at which the well was predicted to be operating on the respective curves on the 8th May 2010 and the operating point at the capping stack period (15th July 2010), for the respective models. As can be seen from these arrows in Figures 8a and 8b (where the drill pipe is present for the Maximus model), Dr. Griffiths' incorrect calculation results in a decrease in flow rate between 8th May 2010 and 15th July 2010. The more complete and accurate Maximus model predicts an increase in flow rate over this same period if the drill pipe remained at the top of the well or a constant flow rate if the drill pipe moved down the well. Figure 7 shows that the two models broadly agree for the operating points of the well when there is assumed to be no drill pipe present, suggesting that the main error in Dr. Griffiths' modeling is not accounting for the multiple flow paths present and, thus, the differing multiphase effects in those flow paths as outlined above. Dr. Griffiths' simplified model cannot represent the many multiphase effects in the two flow paths in the well and is, therefore wrong, as demonstrated here.

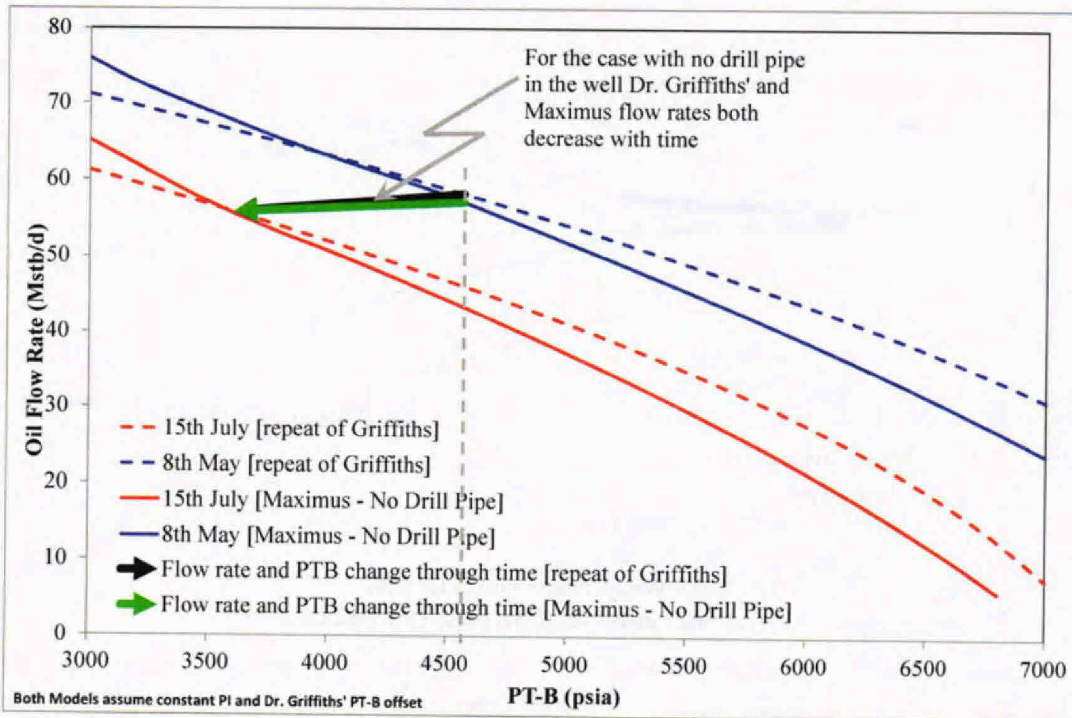


Figure 7. Flow Rate versus PT-B Pressure for Maximus and Repeat of Griffiths – No Drill pipe Present

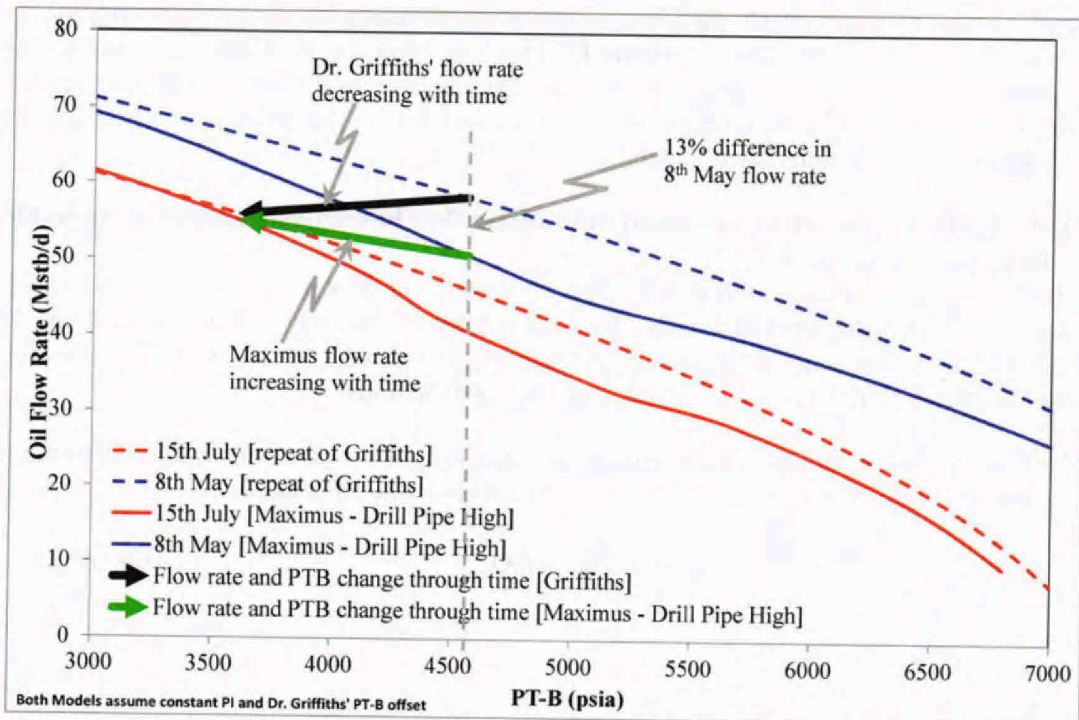


Figure 8a. Flow Rate versus PT-B Pressure for Maximus and Repeat of Griffiths – Drill pipe High in Well in Maximus

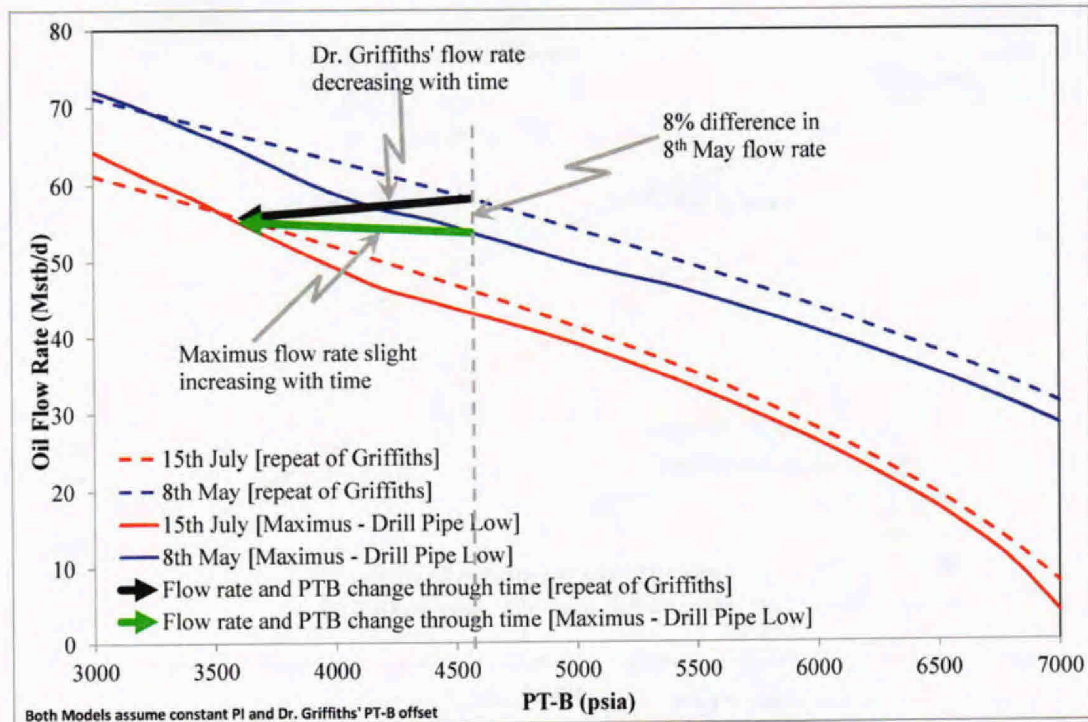


Figure 8b. Flow Rate versus PT-B Pressure for Maximus and Repeat of Griffiths – Drill pipe Low in Well in Maximus

Given the over-simplicity of Dr. Griffiths' model it is preordained to predict a decreasing flow rate over time, once one assumes a constant PI. This is because Dr. Griffiths' flow rate is solely dependent on the difference in pressure between the reservoir and PT-B – a difference that is decreasing with time. This sole dependency is incorrect due to the effect of the multiple flow paths on the VLE as demonstrated above.

4.3.2 Dr. Griffiths' failure to represent multiphase flow in the two well flowpaths results in an inaccurate model.

The flow from the Macondo well is a multiphase flow (as is flow in most wells), in which gas and liquids are flowing simultaneously. To model the well properly it must be modeled as a multiphase flow, especially considering the multiple flow paths in the well. This modeling should preferably be performed using industry-standard methods.

Dr. Griffiths' analysis assumes the frictional pressure drop throughout the system from bottom hole to the sea to be proportional to the oil stock tank flow rate squared, *i.e.*:

$$\Delta P_f = \beta \cdot Q_{st}^2 \quad (\text{Eq. 1})$$

where:

ΔP_f is the frictional pressure drop
 β is a constant of proportionality
 Q_{st} is the stock tank flow rate of oil

Dr. Griffiths' analysis also assumes that the gravitational and frictional pressure drops are independent of each other and can be separately dealt with in the calculation. Unlike Maximus, Dr. Griffiths' model assumes the gravitational pressure drop is a constant and that this pressure drop is not affected by the pressure in the well; this assumption is incorrect.

I have two decades of experience performing studies that involved analysis of flows in oil and gas systems. It is my opinion that Dr. Griffiths is incorrect in his assumptions that the gravitational pressure drop is constant and that the gravitational and frictional pressure drops are not affected by the pressure and temperature in the well. This is particularly true given his assumption of a single flowpath in the well. A comparison of Dr. Griffiths' model with the more sophisticated, nuanced, industry-standard model, Maximus, shows that Dr. Griffiths' model itself (even apart from the mistaken assumptions Dr. Griffiths makes in implementing that model) is not suited to evaluating a multiphase flow system of this complexity.

First, Dr. Griffiths uses an over-simplified equation. Dr. Griffiths' approach would be more applicable to a single phase flow (*e.g.*, a flow where there is only a liquid). But even for single phase flow, my decades of making and analyzing field measurements on real oil systems show that the relationship between pressure drop and flow rate would not be a squared one. Even if Dr. Griffiths' general approach was correct he is still applying the wrong exponent (*i.e.*, he erroneously assumes that the pressure drop is proportional to the square of the flow rate).

Second, the flow in the well is not homogeneous. Dr. Griffiths' model assumes that the flow throughout the entire system is homogenous – *i.e.*, an oil and gas flow that is thoroughly mixed such that both phases move together and act like single phase. This may be true for the points of discontinuity such as BOP rams and kink. It is not true for the long flow sections such as the well, drill pipe, and riser, where there will be significant slip between the liquid and gas phases. This is demonstrated in Figure 9 by plotting the mass fluxes in the well over the Hewitt-Roberts (ref. 26) mass flux map which indicates that the flow regime in the well and drill pipe in the well is some form of annular flow.

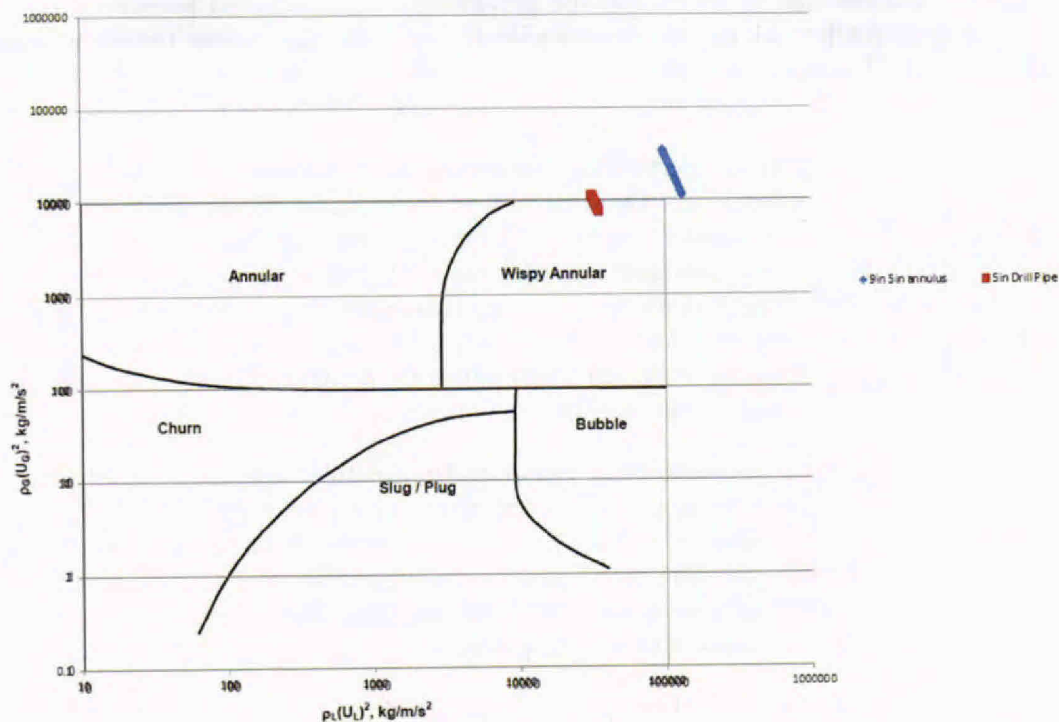


Figure 9. Well Flow Regime Using OLGAS and Hewitt-Roberts Mass Flux Map

where the variables in the axis labels of Figure 9 are:

- ρ_l is the liquid density
- ρ_g is the gas density
- U_l is the superficial liquid velocity
- U_g is the superficial gas velocity

Using the industry-standard OLGAS 2Ph correlation in a Maximus model of the well also indicates that the flow regime is annular rather than homogeneous.

Third, Dr. Griffiths incorrectly separates the gravitational and frictional pressure drops in the well, which is inappropriate for a multiphase flow through two flow paths (here, the casing and the drill pipe) where frictional and gravitational pressures in the two paths differ considerably. Considering the flow in the well, the pressure and temperature at any point dictate the amount of gas that comes out of solution and thus the amount of free gas present (*i.e.*, the vapor-liquid equilibrium, VLE). This affects the mixture density of the fluids which, in turn, affects the velocities of the fluids and the flow regime. Also, the PT-B pressure will affect at what elevation in the well gas begins to come out of solution. Therefore, both the frictional and gravitational pressure drops in the well will be affected by local pressure and temperature through the two flow paths that exist in the well. Dr. Griffiths assumes that gravitational pressure drop is constant and that frictional pressure drop varies only with stock tank oil flow

rate. He also assumes that the two are not connected, which is simply incorrect. Dr. Griffiths' analysis is inappropriate for a multiphase flow through two flow paths where frictional and gravitational pressures in the two paths differ (this was demonstrated in Section 4.3.1 where Dr. Griffiths' analysis was compared with the industry-standard Maximus model).

The Macondo well was not a fully completed production well and, as a result, it had factors (*i.e.*, dual flow paths and varying restrictions due to the BOP and riser) that made it all the more important that a detailed multiphase simulator be used for the analysis. The need to accurately model and predict the multiphase flow conditions in the oil and gas industry has resulted in the development of industry-standard multiphase simulators. The most appropriate method of modeling such a complex well as the Macondo well is to use one of these industry standard multiphase simulators such as Maximus, PROSPER, or OLGA.

4.3.3 Dr. Griffiths' comparison of his model to PROSPER work done by a BP Engineer during the response is inappropriate and misleading.

Apart from the significant inaccuracies and shortcomings of Dr. Griffiths' model in not appropriately representing the multiphase flow in the Macondo well, in figure 7 (ref. 1, page 13) of his report, Dr. Griffiths attempts to justify the assumption that frictional pressure drop is proportional to stock tank oil volumetric flow rate squared by comparison with PROSPER modeling done by Dr. Liao of BP. However, this comparison is inappropriate because:

1. Dr. Liao's work was done during the response to the Macondo incident. The exact reason this modeling was done is not explained by Dr. Griffiths (and, indeed, Dr. Liao cannot recall why it was done) (ref. 34) (sample 5), but Dr. Griffiths has used this work as if it is an authoritative and complete simulation of the well.
2. Dr. Griffiths achieves a good match to Dr. Liao's frictional pressure drop data, but Dr. Griffiths has to adjust his wellbore discharge coefficient (k_{well}) by about 22% to achieve this.
3. Dr. Liao's modeling did not include a drill pipe in the simulation and was simply a model of the flow in the casing with no restrictions. Even if the drill pipe had detached from the bottom of the BOP it would still have remained in the well, forming an obstruction and a second flow path up the well. This second flow path would affect the form of the pressure drop versus flow rate relationship and the frictional pressure drops and flow rate along the two paths would be very different (as demonstrated in section 4.3.1 above). This is because the friction factors in the two flow paths would differ greatly due to the large difference in the ratio of pipe roughness to diameter (*i.e.*, e/D , where e is pipe wall roughness and D is pipe diameter), which is a key ratio in determining the multiphase flow conditions (as discussed above) and frictional pressure drop. Figures 7, 8a, and 8b in section 4.3.1 show the results of the flow rate versus PT-B pressure for the Macondo well based on our Maximus model of the well with and without a drill pipe in it. Alongside the Maximus results in Figures 5, 6a, and 6b are my reproduction of Dr. Griffiths' results (without the drill pipe present). It can be seen from Figures 7, 8a, and 8b that the forms of the curves generated by Maximus and Dr. Griffiths' model, respectively, are very different, demonstrating the technical inaccuracy of Dr. Griffiths' comparison.

4. Although Dr. Griffiths' comparison in his figure 7, (ref. 1, page 13), matches the form (but not the values without adjustment) of the frictional pressure drop from the PROSPER modeling of the flow in the casing (without the drill pipe), it applies only to one point in time and one set of pressure and temperature conditions in the well. There would be many other such curves for other well conditions that would require different k_{well} values to achieve a match. Had Dr. Griffiths presented other such comparisons he would have demonstrated the error he has made in using a constant k_{well} . The same argument would apply for the other constant discharge coefficients assumed in the model, *i.e.*, k_{BOP} and k_{eff} .

4.3.4 Dr. Griffiths' use of constant discharge coefficients in his model is unjustified.

Dr. Griffiths' report presents an analysis that purports to show that his model's assumption of constant discharge coefficients is valid. This analysis does not stand up to scrutiny in a number of ways.

In Appendix C of his report, Dr. Griffiths applies the Lockhart-Martinelli formulation (ref. 27) to arrive at a $\Delta P_f \propto Q_{st}$ relationship of a similar form to the one he has used. However, Dr. Griffiths' analysis assumes that geometry and the friction factor are constant, even though (due to the presence of drill pipe in the well) we know they are not. Also, further into Appendix C (page 22 of his report) Dr. Griffiths recognizes that the Reynolds numbers are very high (implying high velocities and, therefore, high mass fluxes, suggesting that the flow regime would be some form of annular flow, as shown in section 4.3.2 above, and by the OLGAS correlation within Maximus) but then goes on to use work by Whalley (28) in his argument. However, the formula by Whalley was derived for the very special case (pages 54 and 55 of (28)) of homogeneous flow and for constant friction factor, neither of which are true for the Macondo well flow (as discussed above). I am not convinced that Dr. Griffiths realizes his mistake in this respect.

At the end of Appendix C, Dr. Griffiths admits that his analysis is negated if he failed to appropriately justify the use of a constant discharge coefficient: "Use of a discharge coefficient determined at one pressure to describe flow rates at others is (also) well justified and this is fundamental to calculating historical flow rates by the present method." (see page 29 of Dr. Griffiths' report). Despite the definitive language he uses in his report, Dr. Griffiths has not justified, and cannot justify, use of constant discharge coefficients through time, as shown above.

4.4 Dr. Griffiths ignores the many physical changes that occurred through the system over time.

A key assumption in Dr. Griffiths' analysis is that all changes to the sand face, cement, shoe track (these effectively for the PI in the Macondo well), well, BOP, and flow paths downstream occurred "rapidly over the first few days following the blowout" (page 4 of his report). This is a necessary condition of Dr. Griffiths' model because his analysis assumes that the geometry of the system was nominally unchanged over the 86 days of the incident. However, this is a factually flawed approach, as shown below.

Examination of the records and physical evidence indicates that changes in the geometry of the system occurred throughout the incident and it is, therefore, impossible that the resulting flow conditions remained constant throughout the incident.

4.4.1 Dr. Griffiths ignores changes in the BOP through time.

Evidence shows (*e.g.*, Appendix D of this report) that many changes occurred in the BOP through the duration of the incident. These changes include:

1. Activation and deactivation of the BOP rams - A BP spreadsheet (ref. 3) gives the activation of the BOP rams throughout the incident. Examples of activation of the rams are as follows:
 - a. The UVBR and MVBR were closed on 20th April 2010.
 - b. The BSR was not activated until 22nd April 2010.
 - c. The Test Ram was activated on 26th April 2010 and opened for the Top Kill attempts between 26th May 2010 and 30th May 2010 (with a brief period of closure on 28th May 2010).
 - d. The CSR was not activated until 29th April 2010 and pressure reapplied to the actuators at a number of points through the incident.

Closure of a ram in the BOP is designed to restrict or stop the well flow, so closure of rams would have had an impact on the restriction in the BOP and on the flow rate. Dr. Griffiths fails to account for these changes in his calculation.

2. Erosion of the Casing Shear Ram (CSR), Blind Shear Ram (BSR) and disintegration of the Test Ram - An examination of the evidence in my visit to the Michoud Assembly Facility (see Appendix D) showed numerous changes to the rams.
 - a. The pressure data through the BOP in between Top Kill attempts (ref. 4) – 26th May 2010 to 28th May 2010 – shows significant change in the pressure drop across the Test Ram (about 700psi change) as it is opened and closed. The fact that a substantial pressure drop across the Test Ram was maintained indicates that the Test Ram was largely intact at this point in time. This is in contrast to the condition of the Test Ram when the BOP was recovered after the incident. When the component was recovered, it was found that the Test Ram had largely disintegrated due to the erosion of the polymer sections that held the Test Ram together. Indeed, only two of the Test Ram elements (*i.e.*, the metal teeth that are designed to close around the drill pipe) were recovered, one jammed inside the bottom of the eroded drill pipe at the base of the BOP, as shown in Figure D-17 in Appendix D (the other as found in the BOP, but we are not sure where). Junk shot material was also jammed upstream of the VBR/Test Ram element in the drill pipe 148 (as designated in (23)) suggesting either (i) the VBR/Test Ram element found its way into the drill pipe during, or after, the Top Kill period, or (ii) the drill pipe below the BOP had already eroded away and detached by the end of the Top Kill period.

- b. The drag on the loose Test Ram elements (due to the well flow) was sufficient to lift the elements, so they would have moved around the base of the BOP or top of the well, causing a variable restriction to flow with time. Eventually they could have settled in a position and stayed there, from which point on the restriction due to them would have changed only by further erosion.
 - c. Much of the debris found in the pipe section 148 between the jammed VBR/Test Ram element and the CSR (Figure D-18 in Appendix D) is junk shot material, and there appears to be some cement. This suggests that the cement and, therefore, bottom hole conditions were changing after the first activation of the CSR - *i.e.*, some time after the start of the incident.
3. Between 20:38 26th May 2010 and 14:30 28th May 2010 various junk shot materials (see ref. 6 for the large list of materials injected) were injected into the BOP along with the Top Kill mud at varied flow rates (see 5 for a timeline of the Top Kill attempts). Significant amounts of junk shot material were found in the BOP when recovered (see ref. 30 for evidence of materials found in the BOP). This excludes material that would have dropped out of the BOP into the well on shut-in on 15th July 2010.

The changes in the system described above could result in significant changes in the effective area that the flow travels through. However, Dr. Griffiths' methodology ignores the potential impact of these changes to the system.

4.4.2 Dr. Griffiths ignores changes in the well through time.

Dr. Griffiths' method of calculating flow rates based on PT-B data, constant k_{well} (the discharge coefficient for the well), constant PI, and reservoir pressure necessarily assumes that there are no changes in the system below the location of PT-B (*i.e.*, between the reservoir and the bottom of the BOP). However, there is no evidence that the restriction below PT-B - *i.e.*, in the well or sand face - did not change over time, and therefore it is unrealistic to assume that everything below the BOP remained constant throughout the 86 days for such a dynamic situation. For example, down-hole changes could have resulted from:

1. Erosion of the sand face and cement barrier;
2. Blockage of the sand face or parts at bottom hole;
3. Movement of the drill pipe in the well; and/or
4. Blockage and unblockage of flow paths within the well, such as at the shoe track or the drill pipe within the well.

Dr. Griffiths' work takes no account of any of these potential changes in the well and simply dismisses them as having occurred in the first few hours or days after the blowout, despite evidence to the contrary. Dr. Griffiths acknowledges the detachment of the drill pipe below the BOP but contends that the drill pipe must have detached prior to the initial PT-B pressure measurements obtained on 8th May 2010. He contends there is no significant change in the

subsequent pressure data to show its later detachment. However, there are many large changes in the PT-B pressure data throughout the incident as shown in Figure 10.⁶ Setting aside the Top Kill period and final well shut in, the variations in the PT-B data are numerous and range over about 1400 psi (*i.e.*, 35% overall variation). Any one of the pressure changes depicted in Figure 10 could represent the point in time the drill pipe detached. Dr. Griffiths asserts that the PT-B data is accurate, apart from the need for the application of an offset. This combined with the fact there are significant changes in the PT-B data with time are inconsistent with Dr Griffiths' statement (on page 48 of his report) that "there is no evidence in the BOP pressure history that indicates it failed later".

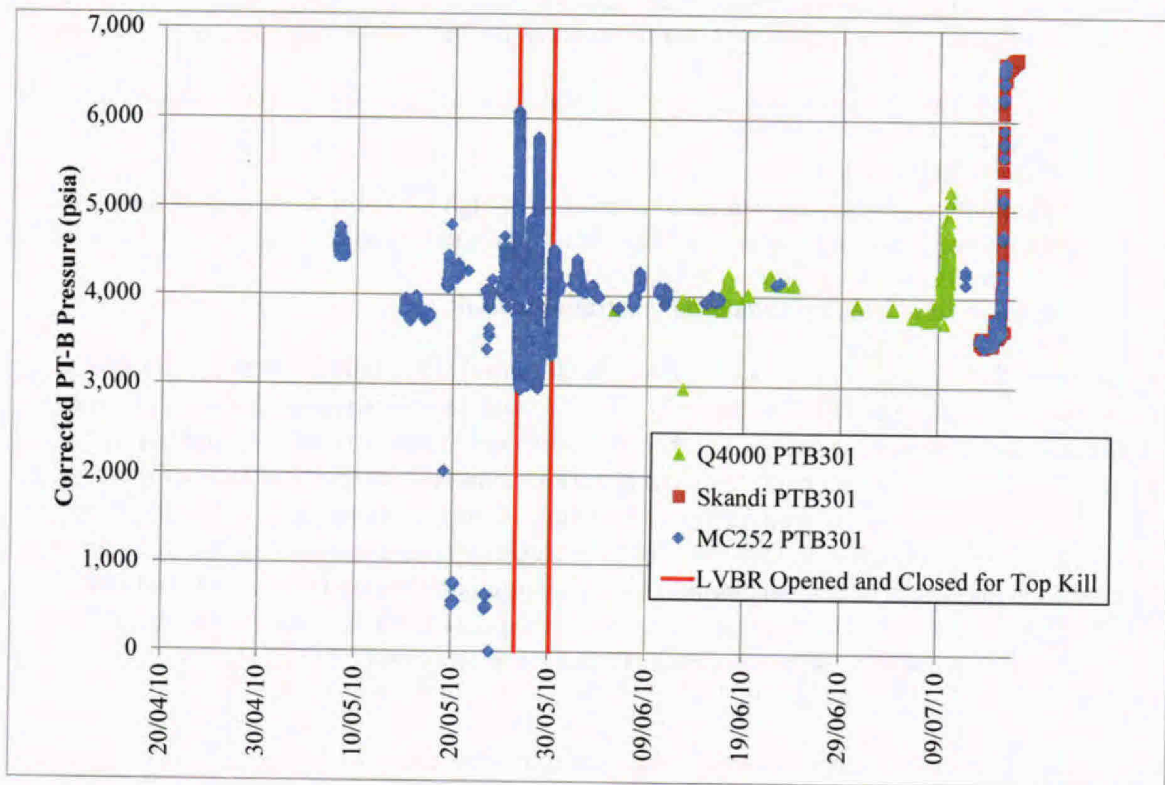


Figure 10. PT-B Pressure Data (adjusted using Dr. Griffiths' corrections)

Given this multitude of potential considerations, it is clear that Dr. Griffiths' model is based on merely one of many potential scenarios. Indeed, Dr. Griffiths' proposed scenario, of resistances in the system remaining constant after the first few days, is less realistic than other scenarios given the evidence.

⁶ Figure 10 shows data taken from (refs. 7, 8, 9, 10, 11) adjusted according to the corrections used by Dr. Griffiths. These corrections are discussed in Section 4.6.

4.5 Dr. Griffiths' attempted verification of his best estimate flow rate is based on flawed logic and circular reasoning.

Dr. Griffiths argues that his two "alternative" models validate his purported "best estimate" flow rate and cumulative discharge calculations. But Dr. Griffiths' "alternative" models are not alternatives at all; they were derived from the same set of data and similar methods on which the "best estimate" model was based. Therefore, these additional models do not (and cannot) present any form of validation of his "best estimate" case. Dr. Griffiths' use of these two alternative models is a self-fulfilling, circular argument.

Appendix D of Dr. Griffiths' report presents a basic outline of his method of estimation of the resistances (or discharge coefficients) and flow rate at the time of the capping stack based on:

1. Reservoir pressure (minus a constant gravitational head, as discussed in section 4.3.2 of this report);
2. Bottom of BOP pressure;
3. The capping stack pressure (taken as correct, although we know there to be a small error);
4. Ambient sea pressure (that Dr. Griffiths determines using gauges that are known to be in error – see Appendix F of this report); and
5. Collection flow rates to surface vessels from the BOP.

From these limited data during the capping stack period, Dr. Griffiths arrives at two sets of resistances (or discharge coefficients). On pages 10 and 11 of his report Dr. Griffiths uses the discharge coefficients in various ways (his " δP Best Est", " δP Alternative 1" and " δP Alt 2" in figure 6 on page 11 of his report) to arrive at various estimates of the flow rates at the capping stack time. However, he is making a self-fulfilling circular argument by performing the " δP Best Est", " δP Alternative 1" and " δP Alt 2" calculations and noting the similarity of their results. This argument is circular because the discharge coefficients for the " δP Best Est", " δP Alternative 1" and " δP Alt 2" calculations are all derived from the same set of data and, by definition, have to be internally consistent. Therefore, to use one of these calculations to justify another of them is logically flawed.

Dr. Griffiths then proceeds to apply this same model and the derived flow coefficients throughout the 86 days of the incident, as if the system remains constant. This is done for each of the different versions of his capping stack fits. Dr. Griffiths then compares the results for cumulative discharge over the 86 days for each of the different cases. But this leap of logic is not justified, because, again, these results are ultimately derived from the same set of data, using the same methods, and thus cannot verify each other. So, based on the self-fulfilling circular logic discussed above, Dr. Griffiths applies the same technique over the 86 days, including the incorrect assumption of constant discharge coefficients. Unsurprisingly, this comparison shows a very small difference between the cases because these calculations are all based fixed parameters derived from the one set of data from the capping stack period. This is nothing more than a self-fulfilling prophecy.

Dr. Griffiths' capping stack flow calculation methodology was based on data covering over a few hours. He then applies this methodology over the preceding 86 days and claims that the results show not only that his calculation itself is accurate (which it is not; see Sections 4.1, 4.2

and 4.3 of this report), but also that it yields “significant insight into historical flow rates and potential mechanisms affecting these flow rates.” This insight is, apparently, that “flow rates over the 86-day period were not significantly affected” by any changes in the BOP (see pages 10-11 of Dr. Griffiths’ report). Dr. Griffiths concludes that the geometry of the BOP did not change over time because his analysis predicts that it did not change over time. But, as I demonstrated in Section 4.1 and Section 4.2, Dr. Griffiths’s method of analysis relies on the BOP not changing over time.

Similarly, in Appendix C of Dr. Griffiths’ report he presents an analysis that purports to show that his model’s assumption of constant discharge coefficients is valid. This analysis does not stand up to scrutiny. On page 20, Dr. Griffiths argues that because his “model based on constant discharge coefficients nevertheless reproduces all BOP and capping-stack pressures measured during shut-in,” it must be accurate. However, this is once again a self-fulfilling, circular argument, because the model merely predicts the data on which it was tuned in the first place. Because Dr. Griffiths developed the constants in his model by using the “BOP and capping-stack pressures measured during shut-in,” it is far from surprising that the model then reproduces these data.

In summary, although Dr. Griffiths’ calculations might appear to be internally consistent, that internal consistency proves nothing about the actual cumulative discharge over the 86 days that the well was flowing, nor about the changes that occurred through the system over those 86 days. The conclusions in Dr. Griffiths’ report are predetermined by the flawed logic and assumptions upon which Dr. Griffiths’ model relies.

4.6 The offset that Dr. Griffiths calculated for PT-B is incorrect.

Without accurate BOP pressures, Dr. Griffiths’ model cannot accurately calculate historical flow rates and the cumulative discharge from the well. There are four parameters in Dr. Griffiths’ calculations: reservoir pressure, PI, resistances (*i.e.*, discharge coefficients), and pressure at the bottom of the BOP (from the gauge PT-B). The first of these is reasonably well-known, and Dr. Griffiths assumes the second and third are constant. Thus, the accuracy of the PT-B pressure figures Dr. Griffiths uses in his calculations is important. As a result, any offset in the readings from PT-B must be well understood and quantified.

It is not disputed that the readings from PT-B were in error and a correction was required. This issue with PT-B was most readily demonstrated by comparing the reading of PT-B with the reading of PT-3-K2 (one of the pressure gauges in the body of the capping stack) when the well was finally shut-in on 15th July 2010 (ref. 17). In Appendix E of Dr. Griffiths’ report he discusses which values should be used as the offset in the PT-B pressure readings. His conclusion is that the raw PT-B readings should be corrected by adding 740 psi to all readings prior to 12th July 2010 and by subtracting 620 psi from the readings from 12th July 2010 onwards⁷. The main reasons for these two corrections are that PT-B on 10th March 2010 (ref. 1)

⁷ However, Dr. Griffiths reverts to adding 740 psi to data after 31st July 2010.

was reading 740 psi lower than the PT-A gauge on the LMRP and PT-B was reading about 614 psi higher than the PT-3-K2 gauge on 15th July 2010 respectively.

Appendix E of Dr. Griffiths' report acknowledges the following technical difficulties he encountered with establishing the PT-B correction values:

1. There is wide variation in the apparent offsets in PT-B, as demonstrated in his Table 1 in Appendix E;
2. Uncertainty as to whether the PT-B data from 12th July 2010 onwards had been corrected prior to his receipt of it;
3. The unknown accuracy of the PT-A gauge; and
4. Difficulty measuring the accuracy of the PT-B gauge in a lab environment after it had been removed from the subsea environment.

BP calculated the offset (ref. 19) in PT-B prior to 12th July 2010 as -966 psi (*i.e.*, the correction that needed to be applied was adding 966 psi to the PT-B pressure gauge reading). This calculation was based on comparison of the BOP kill line pressure gauges during a Top Kill attempt. The PT-B data after correction by +966 psi are shown in Figure 11.

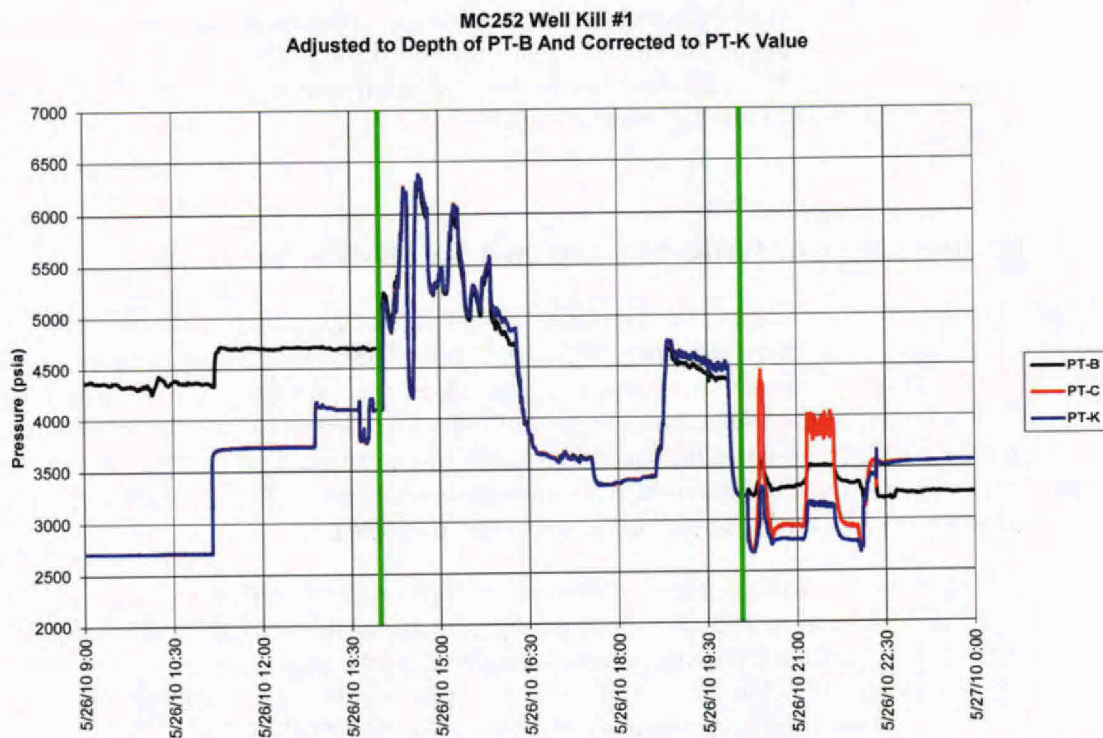


Figure 11. BP Correction of PT-B

Figure 11 is taken directly from (ref. 19) with the addition of the two green vertical lines to denote the main period of interest. During this period of correction, mud was being pumped at various rates between 0 bpm and 70 bpm. If, as argued by Dr. Griffiths in his deposition (ref.

20), the +966 psi correction had been grossly incorrect due to large pressure changes across the Test Ram caused by mud flow across it, then this would have appeared as significant variation in the gap between the blue and the black lines in Figure 11 as the mud flow rates varied resulting in a varying pressure drop across the Test Ram. However, minimal variation is seen. This validates the +966 psi correction.

The discussion in the previous paragraph demonstrates that the flow during the Top Kill attempt shown in Figure 11 was upwards through the Test Ram. When the Test Ram was open, there would have been minimal ΔP across it. In this configuration, a PT-B correction of +740 psi would result in approximately a 200 psi pressure rise upwards across the open Test Ram for the data between Top Kill attempts. This is physically impossible, given that the flow was moving upwards past the Test Ram, because as fluids flow past restrictions, pressure decreases. The pressure measurements between Top Kill attempts are shown in Tables 3a and 3b, using BP's and Dr. Griffiths' corrections respectively:

	BP Offset +966psi			
	25/05 21:00	27/05 09:00	28/05 11:00	28/05 22:00
UAP				
LAP				
Vent Line Pressure	2560	2500	2479	-
ΔP	-60	-120	-108	
BSR				
Upper Kill Line Pressure	2620	2620	2587	2743
CSR				
ΔP	-620	-510	-794	-410
UVBR				
Upper Choke Line Pressure	3240	3130	3381	3153
ΔP	-430	-150	-284	-242
MVBR				
Lower Kill/Choke Line Pressure	3670	3280	3665	3395
ΔP	-730	-40	-32	-101
LVBR				
Bottom of BOP	4400	3320	3697	3496

**Table 3a. Pressures Throughout the BOP Between Top Kill Attempts
BP PT-B Offset**

	Griffiths Offset +740psi			
	25/05 21:00	27/05 09:00	28/05 11:00	28/05 22:00
UAP				
LAP				
Vent Line Pressure	2560	2500	2479	-
ΔP	-60	-120	-108	
BSR				
Upper Kill Line Pressure	2620	2620	2587	2743
CSR				
ΔP	-620	-510	-794	-410
UVBR				
Upper Choke Line Pressure	3240	3130	3381	3153
ΔP	-430	-150	-284	-242
MVBR				
Lower Kill/Choke Line Pressure	3670	3280	3665	3395
ΔP	-504	186	194	125
LVBR				
Bottom of BOP	4174	3094	3471	3270

**Table 3b. Pressures Throughout the BOP Between Top Kill Attempts
Dr. Griffiths' PT-B Offset**

The bottom rows of Tables 1a and 1b show the pressure from PT-B after correction by the addition of 966psi and 740psi respectively. The red and green cells in the tables indicate whether the particular ram is closed or open, respectively. The numbers highlighted in red in table 3b show how Dr. Griffiths' PT-B correction results in a pressure rise upwards across the Test Ram.

Therefore, I strongly disagree with the correction of +740psi applied by Dr. Griffiths to the PT-B reading and there is strong evidence to believe that +966psi is the appropriate correction for this point in time. However, I have no evidence to say that the correction to PT-B is solely an offset. The error in PT-B could also be, or could partially be, a scale error. The correction could also change over time. These caveats do not change my conclusion that Dr. Griffiths' proposed correction is incorrect for the 26th May 2010.

Dr. Griffiths did not adequately account for the uncertainty in the PT-B data in the range of uncertainty for the flow rate estimate. The uncertainty around the corrections to be applied to the PT-B pressure readings is demonstrated in table 1 in Appendix E of Dr. Griffiths' report, which is reproduced here for clarity as Table 4 below:

Near Date	Reference	Offset (psi)	Flow	Comments
3/10/10	LMRP PT-A	-740	No	
5/27/10	PT-C and PT-K	-825 to -860	Yes	Compatt Installed 5/17
5/28/10	PT-C and PT-K	-830 to -866	Yes	
5/30/10	PT-C and PT-K	-852 to -810	Yes	
7/16/10	PT-3K-2	+546 to +576	No	Compatt Change 7/12, 966 Correct
8/2/10	PT-3K-2	-694 to -778	No	Compatt Change ~7/31
6/15/11	DNV Calibration	-622	No	

Table 1. Summary of PT-B offsets determined from various reference pressures.

**Table 4. table 1 from (ref. 1)
PT-B corrections proposed by Dr. Griffiths**

The values in Dr. Griffiths' table show a variation in the possible PT-B offsets he proposes, from -866 psi to +576 psi. If we include in this list the BP calculated offset of -966 psi prior to 12th July 2010 and the maximum offset quoted by Dr. Griffiths from 12th July 2010 onwards of +641 psi (in the penultimate paragraph of page 38 of his report), the range increases such that it is -966 psi to +641 psi – *i.e.*, a spread of 1607 psi. The average PT-B measurement is 4191 psia (using the BP corrections). This significant spread represents a variation of about 40%. This spread of uncertainty is not taken into account in Dr. Griffiths' uncertainty estimation of his flow rate results. Dr. Griffiths only applies a range of +/-130 psi in his uncertainty analysis; this range of +/-130 psi does not even cover the difference between BP's correction to PT-B and Dr. Griffiths' correction.

It has been assumed by some, including Dr. Griffiths, that the errors in the PT-B transmitter are an offset and that that offset undergoes step changes. One such step change is said to have occurred during the battery change-out on 11th July 2010. An earlier battery change-out on 22nd June 2010, at 14:30, does not seem to have resulted in a change of offset, which is inconsistent. Also, there are features in the PT-B profile shown in Figure 10 of this report that are difficult to explain. One such feature is the large increase of about 1200 psi in the PT-B pressure reading over about a day prior to the 2nd battery change-out on 11th July. Dr. Griffiths ignored these data in his report (for example, see figure 3 in Dr. Griffiths' report).

There is no evidence that the error in the PT-B reading is not gradually changing, rather than undergoing step changes. Many other fluctuations in the PT-B data between 8th May 2010 (the first PT-B data point) and the time of shut-in of the well are not obviously associated with a known event (e.g., Top Kill or shut-in). These apparent pressure fluctuations could be due to flow rate fluctuations, brought on by downhole, BOP or riser changes, or they could be fluctuations in the PT-B error.

Dr. Griffiths' report assumes the corrections applied to account for the large and uncertain errors in the PT-B data are correct. However, Dr. Griffiths failed to account for the large uncertainty associated with determining a correction for this PT-B data in the uncertainty ranges of the flow rate and cumulative discharge results.

4.7 Dr. Griffiths reaches incorrect conclusions in his Appendix I regarding changes in the system geometry prior to 8th May 2010.

Appendix I of Dr. Griffiths' report (ref. 1) attempts to estimate the cumulative discharge from the well from the time of the blowout on 20th April 2010 to 8th May 2010 (the time of the first PT-B reading). There are numerous problems with the arguments and statements in Appendix I as follows:

- 1. Dr. Griffiths ignores evidence that the PI was low prior to 8th May 2010** – Dr. Griffiths' conclusions related to the cumulative discharge for the period up to the 8th May 2010 are predicated on a constant PI. Dr. Griffiths argues that this is valid based on the bottom hole having reached a steady state early in the incident, but there is no convincing evidence for this (see the discussion in section 4.2 regarding the infinite number of possible PI paths that could fit available data throughout the incident). In fact, there is evidence that the PI was 9.4stb/d/psi (inferred from the BP report Appendix W (ref. 14)) at the time of the blowout. Dr. Griffiths does not use the low PI evidence other than to say that the PI was rapidly changing at the time of the blowout. Dr. Griffiths extrapolates this change to conclude that the PI would reach the “best estimate value in less than 9 hours.” (see pages 11 and 12 of Dr. Griffiths' report). Not only is extrapolation of the change at the time of the blowout a gross assumption, it is an incorrect calculation, as shown in Section 4.1 of this report.
- 2. Dr. Griffiths fails to account for changes in flow path geometry prior to 8th May 2010** – Dr. Griffiths assumes that all erosion occurred very quickly, but the evidence for this is weak (as discussed in Section 4.4 of this report). This assumption, together with the constant PI assumption, leads to the statement that the flow rate must have been decreasing prior to 8th May 2010. But this would not have been the case, if Dr. Griffiths had correctly taken account of changes in flow path geometry. In fact, it is probable that the flow rate increased for some period prior to 8th May 2010, rather than decreased throughout that entire time (for example see the analysis relating to Dr. Pooladi-Darvish's assumption of pre-8th May 2010 PT-B pressure variation in section 4.3).
- 3. Dr. Griffiths fails to take account of evidence that suggests the resistances in the system continually changed** – Dr. Griffiths totally ignores the effect of materials traveling up from the well and lodging in the BOP and the effect these might have on any already-existing blockages in the BOP. For example, examiners found what appears to be some cement in drill pipe section 148 as shown in Appendix D of this report. This apparent cement probably moved from bottom hole to the drill pipe after the closure of the CSR on 29th April 2010 (because it was found in the drill pipe for which the flow path was restricted by the CSR, although not shut off entirely) suggesting that the bottom hole continued to change, increasing the potential for both greater blockage and more erosion of the BOP as well as changes in the effective PI.
- 4. Dr. Griffiths fails to acknowledge that the final drill pipe location in the well is uncertain and that the restriction from the drill pipe in the well would be very significant** – Dr. Griffiths suggests (page 48) that the drill pipe below the BOP detached prior to the 29th April 2010 and dropped down the well. It is possible that this section of

drill pipe detached before 29th April 2010, but Dr. Griffiths presents no evidence of its final position in the well. Indeed, there is evidence (ref. 35) to show that the bottom of the drill pipe was about 5700 ft above the bottom of the well after shut-in. Figure 12 shows an extract from (ref. 35):

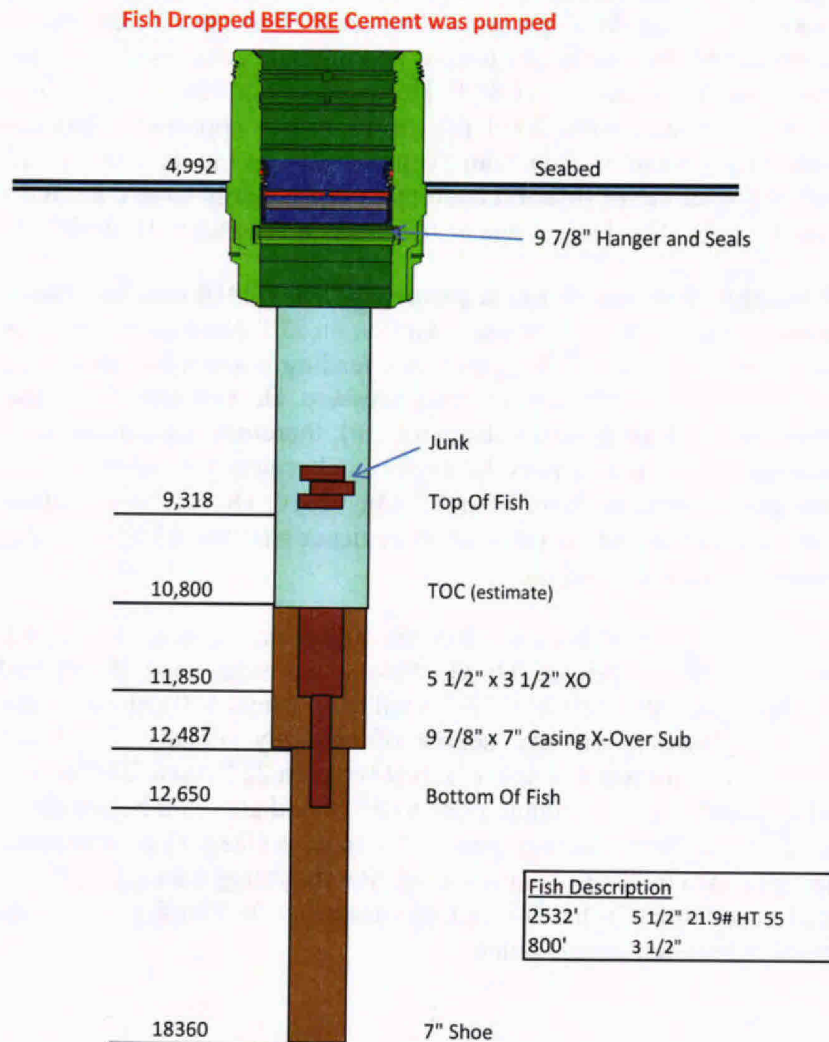


Figure 12. Position of Drill Pipe in the Well After Shut-in

Figure 12 shows the position of the drill pipe after shut-in. There is no evidence indicating that the drill pipe was at a higher position prior to shut-in. These points are discussed more in Appendix C of this report.

Dr. Griffiths asserts that the drill pipe must have detached from the bottom of the BOP prior to 8th May 2010 because there is “no evidence in the BOP pressure history that indicates it failed later.” (see page 48 of Dr. Griffiths’ report). Figure 10 of this report (a graph of the PT-B data) shows numerous changes in the PT-B data that could have been

caused by the detachment of the drill pipe. Dr. Griffiths cannot consistently argue that 1) the corrected PT-B data is accurate and also argue that 2) there is no evidence in the PT-B data that could indicate detachment of the drill pipe.

5. **Dr. Griffiths' presentation of the ae add energy report (ref. 14) flow rates is incorrect** – Dr. Griffiths' presents flow rates from the ae add energy report (ref. 14) (which presents an analysis of the flow and pressure changes in the well leading up to the blowout) based on a net pay of 86 ft. However, ae add energy's conclusion (on page ix of their report) suggests that a net pay of 15 ft was appropriate based on the drill pipe pressure data. As can be seen from the predictions in Figure 2 above (using Dr. Griffiths' method but with the PI inferred from the ae add energy work), large differences in flow rate are possible. This large range of flow rates is ignored in Dr. Griffiths' analysis.
6. **Dr. Griffiths' flow rate estimate prior to 8th May 2010 must be based on conjecture** – From the sinking of the *Deepwater Horizon* on 22nd April 2010 to the first PT-B pressure readings on the 8th May 2010 no pressure reading is available, other than the interpolated reservoir pressure and the ambient sea pressure. Dr. Griffiths' does not make use of the Sperry Sun drill pipe pressure data (ref. 36), therefore, his estimation of flow using his method during this period must be conjecture because it is merely based on extrapolation of available PT-B data from after 8th May 2010. Dr. Griffiths' estimate covering this timeframe is surprising, in the face of evidence that the whole system was in a state of continuous change at this time.

In summary, as discussed above, Dr. Griffiths' arguments in Appendix I of his report are not strongly supported by the evidence. Dr. Griffiths' conclusions about the PI, BSR, drill pipe, and downhole conditions of the well from 20th April to 8th May 2010 require gross assumptions that simply cannot be made with any degree of certainty. Finally, Dr. Griffiths' conclusion regarding cumulative discharge over the period between 22nd April 2010 and 8th May 2010 does not fully reflect the discharge volume prior to 8th May that would be predicted by using one of the better pieces of evidence for that period (the more realistic PI for that period, based on (ref. 14)). Using (ref. 14) could result in a cumulative discharge between 22nd April 2010 and 8th May 2010 of approximately half of that proposed by Dr. Griffiths – see section 4.1 of this report for more discussion on this point.

4.8 Dr. Griffiths' report contains a number of additional technical errors.

1. Dr. Griffiths uses the capping stack gauge (whether PT-3K-2, PT-3C or PT-3K is unspecified) to *measure* the seabed ambient pressure (as given on page 30 of his report). Using the capping stack gauges to measure ambient pressure is inappropriate, given there are accurate Paroscientific pressure measurement data available (ref. 25) for the direct measurement of sea pressure variation with depth.
2. Figure 7 on page 13 of Dr. Griffiths' report compares Dr. Griffiths' frictional pressure drop calculation with some PROSPER simulations performed by Dr. Liao of BP. There Dr. Griffiths states that the BP simulations used the common multiphase correlation by

Beggs & Brill for the well.⁸. This is incorrect. The *Petroleum Experts 2* correlation (a multiphase flow correlation proprietary to Petroleum Experts Ltd) was used. The Beggs & Brill correlation was developed for horizontal and inclined flows. An experienced practitioner of multiphase simulation would know to avoid the use of Beggs & Brill for vertical flows, as much more appropriate correlations exist. Indeed, the *Petroleum Experts 2* correlation was developed specifically for vertical flows. Dr. Liao, in fact, used the Beggs & Brill correlation for the fallen riser, but not for the vertical portions of the well.

3. Appendix A on page 16 of Dr. Griffiths' report states the temperature at the BOP to have been 150 or 180 °F. This is incorrect. The temperature was measured via a probe inserted into the Top Hat (ref. 29) as 220 °F. This temperature error would undoubtedly give Dr. Griffiths significant errors in his oil and gas mixture density (although Dr. Griffiths' report ignored mixture density entirely) and its variation up the well.
4. Dr. Griffiths includes the period prior to the sinking of the *Deepwater Horizon* in his total cumulative oil released from the well even though much of the oil released during this period was consumed in the fire. This is a relatively minor volume (0.1 MMstb by Dr. Griffiths' calculation method) but needs to be removed from the total to accurately determine the oil discharged to sea. Also, Dr. Griffiths does not subtract the volume of oil collected (0.81 MMstb see (ref. 13) by the surface vessels (the *Helix Q4000*, *Helix Producer 1* and *Discoverer Enterprise*) throughout the incident.
5. In his figure 1 on page 42 of his report, Dr. Griffiths reverts to the end of incident reservoir pressure of 10,090 psia that he used in his previous report. This pressure value is the reservoir pressure at the time of shut-in and, therefore, represents the reservoir in a transient state. Using this value is inconsistent with using a steady-state reservoir pressure at the start of the incident.

⁸ The Beggs & Brill correlation is an empirical correlation for predicting, primarily, the pressure drop through a multiphase pipeline.

5 TECHNICAL EVALUATION OF DR. DYKHUIZEN'S REPORT

This section describes the results of my evaluation of Dr. Dykhuizen's Expert Witness Report (ref. 2).

5.1 Dr. Dykhuizen's analyses are based on incorrect or unsupported assumptions in calculating the flow rate from the Top Hat.

In section 5.1, I discuss the errors and uncertainties in Dr. Dykhuizen's calculation of a lower bound flow rate from Top Hat. I have repeated the calculations to establish where the errors were committed.

Dr. Dykhuizen purports to establish a lower bound of the oil flow rate from the well by estimating the flow that could leak out of the Top Hat, under certain assumed conditions, in mid-June 2010. The Top Hat is a very loose fitting vessel placed over the top of the severed riser and riser flange. Figure 13 shows a sketch of the Top Hat and top of the riser and riser flange (taken from the report of Dr. Dykhuizen, page 18):

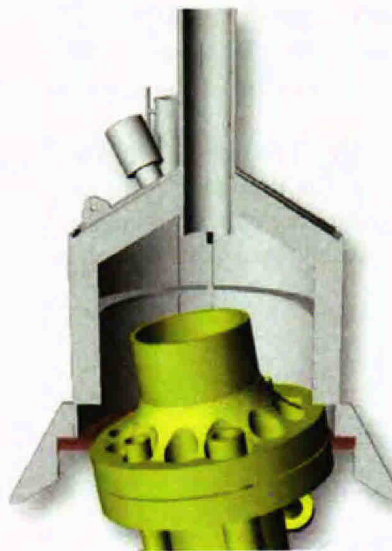


Figure 13. Sketch of the Top Hat and Riser Flange

Dr. Dykhuizen performed two calculations to estimate the flow rate out of the Top Hat (1) the flow from three open vents on the top of the Top Hat and (2) the flow from the skirt at the bottom of the Top Hat.

U.S. scientists such as Dr. Ratzel, who led the DOE-NNSA flow analysis team, (ref. 33) did not believe the Top Hat data could give good flow estimates and neither do I. With respect to the skirt flow rate estimation, Dr. Dykhuizen himself admitted "we could not estimate accurately what was coming out of the skirt." (ref. 39). By repeating the updated calculations of Dr. Dykhuizen, I have identified the following deficiencies in his analysis for the Top Hat:

5.1.1 Dr. Dykhuizen's Top Hat skirt flow estimate is highly inaccurate.

Although Dr. Dykhuizen himself presents no attempt to quantify the uncertainty of the skirt flow calculation, it is subject to large error for the following reasons:

1. The geometry of the Top Hat skirt was very complex.
 - a. The skirt seal was partial damaged / destroyed during installation;
 - b. The Top Hat was tilted at about 5° relative to the riser and riser flange;
 - c. There was the complex geometry of the riser, riser flange, and auxiliaries in the skirt flow area; and
 - d. The Top Hat was not centered on the riser / flange.

For these reasons it is impossible to know the geometry of the skirt flow area well enough to accurately calculate the flow.

2. The Top Hat flow calculation is dependent on very small pressure differences (*i.e.*, less than 2 psi) between the pressure within the Top Hat and ambient sea pressure. Accurately measuring the small pressure difference between the fluids inside the Top Hat and ambient sea pressure was difficult, as recognized by Dr. Dykhuizen himself (page 18 of Appendix A.7 in Dr. Dykhuizen's report). Errors of only a fraction of a psi would lead inevitably to large errors in the skirt flow rate calculation. For example, I calculate that an error of only -0.5 psi would result in approximately *halving* the calculated skirt flow rate.
3. The open area of the skirt would not only affect the area available for flow, but also the pressure loss coefficient (*i.e.*, K value) assumed when calculating the flow rate. To calculate a loss coefficient, one needs to know the area at the base of the skirt through which hydrocarbons flow downwards to the sea, and an area within the Top Hat, above the skirt outlet. Based on the open area of the skirt given in Dr. Dykhuizen's report (page 12 of Appendix A.7 of Dr. Dykhuizen's report) and the area of the inside of the Top Hat (diameter taken from page 12 of Appendix A.7 of Dr. Dykhuizen's report), the open area ratio for the skirt opening is 0.07 (*i.e.*, the ratio of these two areas). Assuming that the skirt outlet acts like an orifice, a loss coefficient can be determined from Figure 3 above. This resulting loss coefficient is at least 2, but possibly 3, orders of magnitude greater than Dr. Dykhuizen's work assumed. That is to say, the loss coefficient should be at least 100 times larger (a three-figure loss coefficient), and possibly 1000 times larger (a four-figure loss coefficient) than assumed by Dr. Dykhuizen. A loss coefficient of 700, for example (consistent with an open area ratio of 0.07 from Figure 3 above), would reduce the calculated skirt flow to about 1,800 stb/d, down from Dr. Dykhuizen's June 2010 estimate of 45,000 stb/d (page 17 of Dr. Dykhuizen's report).

It is possible that the area leading into the skirt could be considered smaller than that of the inside of the Top Hat due to the presence of the riser and flange. This would result in a loss coefficient for the skirt of less than 700. For example, accounting for the riser cross-sectional area reduces the skirt loss coefficient to about 450 resulting in a skirt flow rate of 2,300 stb/d. It is possible that other calculations of the loss

coefficient could be performed (e.g., it could be argued that the skirt consists of part contraction, due to the riser and flange, and part orifice, due to the presence of some of the seal), but any calculated loss coefficient will be much greater than the value of 2 used by Dr. Dykhuizen. Therefore, I believe that Dr. Dykhuizen's June 2010 flow estimation from the Top Hat skirt is over estimated by at least an order of magnitude.

5.1.2 Dr. Dykhuizen misrepresents his well flow rate estimate, based on the Top Hat vent flow calculation, as a lower bound.

Dr. Dykhuizen adds the highest maximum collection rate (25,000 stb/d) to a calculated vent flow rate (18,000 stb/d) to generate another purported lower bound estimate of the flow rate. This approach is incorrect and assumes that the collection flow rate of 25,000 stb/d applies for the whole of the Top Hat collection period. Claiming that this is a lower bound flow rate for the whole of that period is incorrect. The collection flow rates from the *Helix Q4000* (collection from the BOP) and *Discoverer Enterprise* (collection from the top of the Top Hat) (ref. 33) are shown in Figure 14:

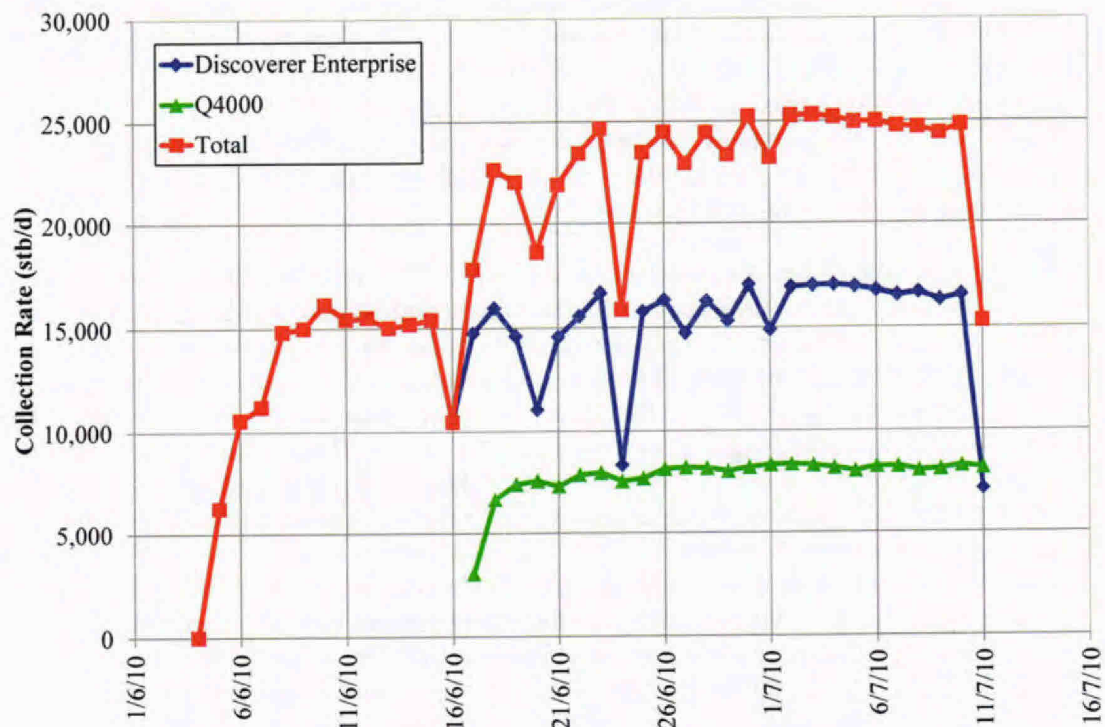


Figure 14. Collection Flow Rates During the Top Hat Period

In Figure 14, the collection flow rate from both vessels reaches 25,000 stb/d only for approximately the last 2 weeks of the Top Hat being in place – i.e., approaching the capping stack period. But simply assuming that the maximum observed collection rate would have also occurred at all times earlier, when in fact such collection rates were not achieved, is not a consistent methodology for estimating a *lower bound* for the flow rate.

Prior to the final two weeks of the Top Hat period the actual, recorded, lower collection rates should be added to generate true *lower bound* flow rates, as shown in Figure 15.

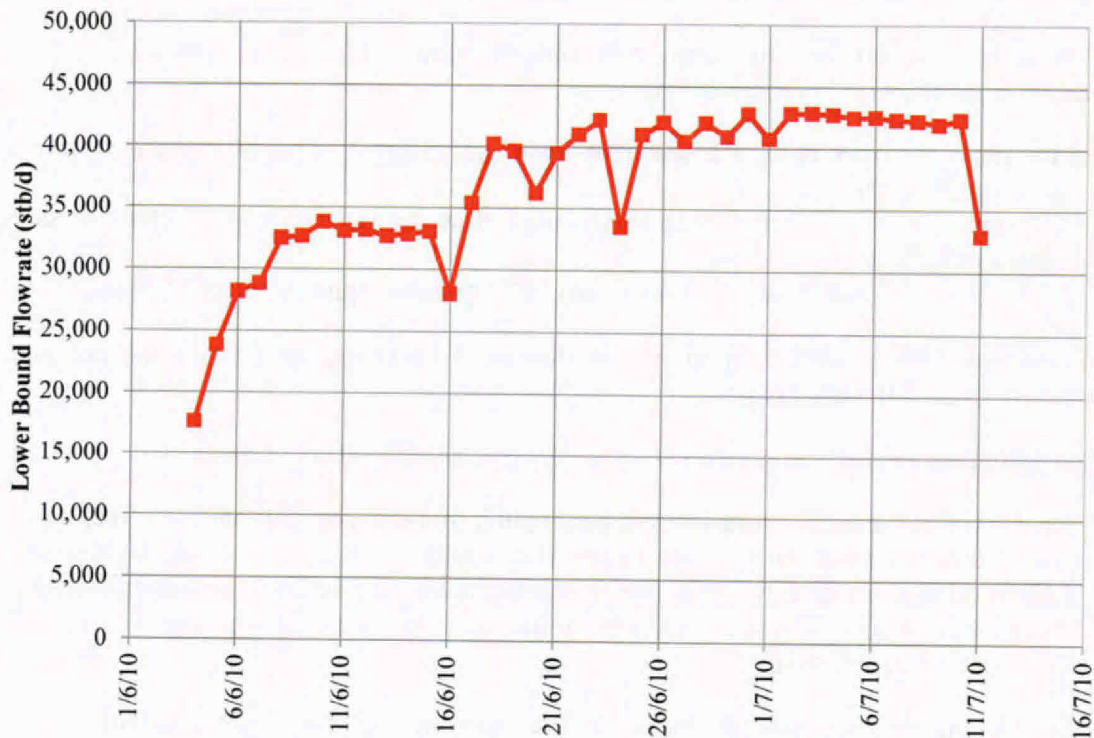


Figure 15. Revised *Lower Bound* Flow Rate Profile

The analysis for the vent, skirt, and riser flows were separately performed (“decoupled”) in Dr. Dykhuizen’s work. However, the various flow paths are interrelated, and the changes in flow rate for each path affect the flow rates in the other flow path. An accurate analysis of these interactive flow rates must therefore be performed as one analysis in an integrated model that would then account for these interactions.

5.2 Dr. Dykhuizen’s Top Kill analysis has serious technical errors that affect the validity of his flow rate calculations.

In section 5.2, I present the examination of the errors Dr. Dykhuizen committed in his calculation of a lower bound flow rate from data at the time of the final Top Kill attempt. I present a calculation, using Dr. Dykhuizen’s own spreadsheet, that produces a significantly lower flow rate result for the data available from the first Top Kill attempt.

Dr. Dykhuizen’s method of analysis posits a relationship between pressure drop and flow rate for flow through the BOP during Top Kill on 28th May 2010, and then applies this relationship

to data from after the Top Kill event. This approach is technically incorrect, because it assumes that the Top Kill had no effect on the flow restriction in the BOP and fallen riser. This technically incorrect assumption is then used to arrive at an incorrect oil flow rate result that is asserted to be a *lower bound* estimate of the flow rate through the well.

Dr. Dykhuizen's report uses the terms *Idle Time*, *Normal Time*, and *Kill Time*. These are defined on page 11 of Dr. Dykhuizen's report as:

1. Idle time: no mud flow, the test ram open and a BOP pressure measurement was approximately 3500 psi.
2. Kill time: 78 barrels per minute (bpm) mud flow, the test ram open, BOP pressure approximately 5500 psi.
3. Normal time: no mud flow, test ram closed, BOP pressure approximately 4350 psi.

The discussion below includes an analysis performed for different mud flows and pressures from the 26th May 2010 kill attempt.

I have highlighted the following deficiencies in Dr. Dykhuizen's Top Kill analysis:

1. Dr. Dykhuizen makes a fundamental assumption that the Top Kill had no effect on the flow restriction in the BOP or the kinked riser (point 2. on page 13 of Dr. Dykhuizen's report). This constant flow resistance is represented by the constant loss coefficient (K) throughout the analysis (as represented by the ratio of loss coefficients equal to 1 in Dr. Dykhuizen's equation 6).

Dr. Dykhuizen's analysis was based on data from the 28th May 2010 Top Kill attempt, and the period after that Top Kill attempt ceased but while the Test Ram remained open. This Top Kill attempt included the use of junk shot (bridging) material (ref. 5) – material deliberately injected into the well in an attempt to block the flow of oil and gas. The effect of these junk shot materials on subsequent flow rates is not accounted for in Dr. Dykhuizen's analysis either as a change in the loss coefficient or as a change in the density (reflecting the wide variety of solid materials used in the junk shot) assumed in Dr. Dykhuizen's equation 5 (page 12). However, observation of the BOP after it was recovered revealed junk shot materials (ref. 30) and it is my opinion that it is improbable that these materials did not change the effective size of the restrictions in the BOP and riser kink at all. While not all of the junk shot materials that were injected remained in the BOP, the examination of the BOP after it was recovered revealed significant amounts of material in the drill pipe and the BOP suggesting that there had to have been some additional flow restriction due to junk shot. Indeed, the purpose of the junk shot was to introduce materials that would block the flow paths and restrict flow. Even Dr. Dykhuizen himself (ref. 38) recognized how the restriction in the BOP changed during the 28th May 2010 Top Kill attempt. The plot taken from (ref. 38) is shown in Figure 16 and demonstrates that the pressure drop across the BOP was different before and after Top Kill (shown by the hysteresis in the plot as the mud flow rate is increased versus when it is decreased). If the pressure drop was different before and after Top Kill then the loss coefficient in the BOP must also have been different to cause this change.

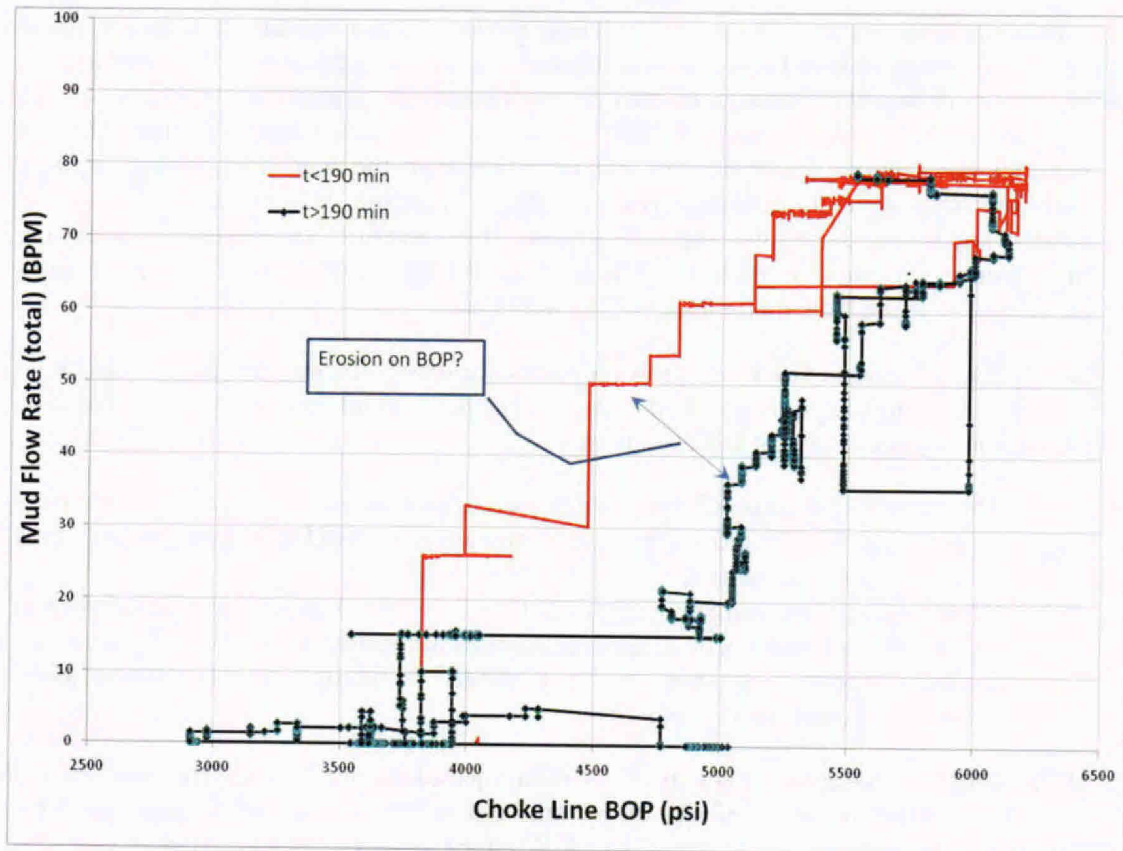


Figure 16. Dr. Dykhuizen's Demonstration that Top Kill Affects BOP ΔP (ref. 38)

The amount of Top Kill material in the BOP did not remain constant before and after Top Kill, but rather varied during the time period being analyzed. As a result, Dr. Dykhuizen's analysis should not have assumed the loss coefficients (K factors, *i.e.*, resistance to flow) during and after the Top Kill attempt (see note 2 on page 13 of Dr. Dykhuizen's report). As demonstrated by Figure 3, above, a small change in the effective open area of the BOP and riser kink can easily lead to an order of magnitude change in the loss coefficients (K factors).

Regarding the effect of the junk shot material on the loss coefficients, there are two possibilities:

- a. The loss coefficient (resistance to flow) could have been greater during the junk shot process – *i.e.*, when the junk shot was being pumped into the BOP, potentially blocking flow paths – and decreased again after, or
- b. Loss coefficient (resistance to flow) increased as junk shot materials found their way into openings in the flow paths after the junk shot.

Either of these possibilities could cause at least an order of magnitude (factor of 10) change, and potentially a two order of magnitude (factor of 100) change, in the ratio of loss coefficients. This results in Dr. Dykhuizen's *lower bound* flow rate of 43,000 stb/d

calculated from equation 6 (page 13) being between about 13,000 stb/d and 130,000 stb/d, depending on whether the loss coefficient was greater after Top Kill or during it. A two order of magnitude change in the loss coefficient would greatly increase this range. This demonstrates that if Dr. Dykhuizen had correctly accounted for the junk shot material, the analysis would be very different. However, the conditions during Top Kill with junk shot are extremely dynamic and rapidly changing. It is not possible to know what is happening during the Top Kill process. It is therefore not possible to determine the effect of junk shot on the loss coefficients for the BOP, and therefore not possible to accurately estimate flow on the basis of Top Kill data.

Dr. Dykhuizen asserts that PT-B shows no evidence of significant changes in flow rate – and, therefore, blockage in the BOP – due to Top Kill (point 2. on page 13). However, two major points cut against this argument:

- a. That the PT-B reading did not change before and after Top Kill can only be used to show that $K \times Q^2$ did not change. A change in K could have been counteracted by an opposite change in Q^2 .
 - b. PT-B readings have large uncertainties (see 2. below). Lack of observed change in PT-B readings could reflect the uncertainties associated with the PT-B gauge, as discussed above in Section 4.6. Dr. Griffiths' report (ref. 1) also acknowledges these uncertainties in its table 1.
2. Dr. Dykhuizen's assumption is that all the mud injected during Top Kill traveled upward through the BOP. However, if any of the mud did not travel upward through the BOP, this would proportionally decrease Dr. Dykhuizen's lower bound estimate (see Dr. Dykhuizen's equation 6 on page 13 of his report). This assumption is also reflected on page 12 of Dr. Dykhuizen's report, where the mud flow through the BOP is assumed to be the same as that injected by the ship. For example, a flow rate of 40 bpm of mud through the BOP (instead of the 78 bpm injected) would have resulted in Dr. Dykhuizen's 48,000 stb/d being 24,000 stb/d. Given that it cannot be known where the mud traveled during the Top Kill event (especially given the presence of junk shot material) a lower bound flow rate cannot be established by this method.
 3. Dr. Dykhuizen failed to use the most appropriate data for the Top Kill lower bound calculations. Dr. Dykhuizen uses data from the Top Kill event on 28th May 2010. As described above, this attempt included the injection of large amounts of junk shot material, making it unsuitable for flow rate calculation, for reasons outlined in point 1. above. Data also exists for the Top Kill attempt on 26th May 2010, an attempt that did not involve the use of junk shot material. This set of data is more suitable for flow rate estimation, because the uncertainty surrounding the presence of the junk shot material does not apply to it. Why Dr. Dykhuizen chose the data from 28th May 2010 is unclear, but repeating his calculations (using his spreadsheet (ref. 32)) for the data of 26th May 2010 19:22 results in a lower bound flow rate of 32,700 stb/d (see Appendix E for details of this calculation). Dr. Dykhuizen's stated lower bound flow rate estimate for this period is 43,000 stb/d, which is 31% higher than the above result. This further demonstrates that Dr. Dykhuizen's lower bound result is inaccurate.

4. Dr. Dykhuizen commits the same error as Dr. Griffiths in assuming the frictional pressure drop in the Macondo well is proportional to stock tank oil flow rate squared. Dr. Dykhuizen does this in the calculation to adjust the flow rate for a higher PT-B pressure (e.g., the adjustment of 48,000 stb/d to 43,000 stb/d on page 13). As shown in Section 4.3 of this report, the presence of the drill pipe in the well results in frictional pressure drop not being proportional to stock tank oil flow rate squared. Therefore, this oversimplification cannot be made.

Additional points of concern and error in Dr. Dykhuizen's Top Kill calculation are as follows:

1. There is confusion in the terminology throughout Dr. Dykhuizen's calculation regarding barrels of oil flow and barrels of hydrocarbon flow. For example, the result in equation 6 (page 13) shows "158,000 bopd", whereas this should be 158,000 bpd of oil and gas. A similar confusion is prevalent between bpd and stb/d – for example, the "48,000 bopd" on page 13 of Dr. Dykhuizen's report is, in fact, 48,000 stb/d of oil.
2. Dr. Dykhuizen's analysis gives no reference for the mud observed exiting the riser (page 12).
3. Dr. Dykhuizen's calculation cites Dr. Griffiths' method as representing the system (page 10) but as discussed in Section 4.3 above, this method has been shown to be inaccurate for a complex system such as the Macondo well.
4. Dr. Dykhuizen uses an ambient sea pressure for his calculations of 2200 psi. It is not stated what location on the system this is for, or whether it is absolute or gauge pressure.

Appendix F of this report presents the sea pressures for the system, and 2200 psia can be seen to be consistent with the kink leak. Based on the difference in elevation between the kink leak location and the end of the riser, a more accurate pressure at the riser exit would be 2220 psia. This higher ambient sea pressure lowers the flow calculated by Dr. Dykhuizen's model by 120 stb/d.

5. In his equation 6 for calculation of the *Idle Time* flow rate, Dr. Dykhuizen uses the mixture density for *Normal Time* (i.e., 388 kg/m³) from his table 1 but he should have used the density for the *Idle Time* (i.e., 411 kg/m³). I suspect this is an error in Dr. Dykhuizen's table 1, however, because he appears to use 388 kg/m³ as the *Idle Time* flow rate in his spreadsheet (ref. 32).
6. Dr. Dykhuizen's assumptions regarding zero oil flow are inconsistent with the measured PT-B pressure during Top Kill. In equation 6, Dr. Dykhuizen assumes zero oil flow and uses the measured kill time PT-B pressure of 5500 psia. This pressure is considerably below the PT-B pressure if the flow was zero (i.e., when the well is effectively shut-in), a point that Dr. Dykhuizen recognizes (in point 1. on page 13) but does not address the issue further. From the final shut-in on 15th July 2010, the shut-in PT-B pressure was about 6500 psia. Purely based on the reservoir pressure decline, the shut-in PT-B pressure would be expected to be about 7200 psia on 28th May 2010. With a higher PT-B pressure for zero well flow, the resulting *Idle Time* flow rate would be lower by about 19%. Dr. Dykhuizen's use of these data and assumptions is internally inconsistent.

7. The combined effect of the errors in 4. & 6. above this would reduce Dr. Dykhuizen's resulting flow rate by about 19%. Combined with the reductions suggested by Dr. Dykhuizen on page 10 (due to reservoir pressure and flowing temperature), this would reduce the lower bound estimate by a total of 25%. This would make Dr. Dykhuizen's lower bound oil flow rate about 32,300 stb/d.

5.3 Dr. Dykhuizen made incorrect assumptions in calculating the flow rate from the well through time and the cumulative discharge.

Dr. Dykhuizen refers back to his earlier work in the DOE-NNSA Flow Analysis report (ref. 31) for his estimate of cumulative discharge from the well over the 86 days of the incident. He does not present a new calculation, but simply presents adjustments to the result from (ref. 31): a 3% decrease in volume due to the increased reservoir pressure at the end of the incident and a 4% decrease for the higher fluid temperature. These adjustments would reduce the cumulative discharge result of Dr. Dykhuizen's calculation. Subtraction of the oil volume collected and the volume consumed in the *Deepwater Horizon* fire would further reduce Dr. Dykhuizen's estimate of the oil volume leaked to sea.

I have the following concerns with Dr. Dykhuizen's cumulative discharge calculation:

1. Dr. Dykhuizen commits very similar errors to Dr. Griffiths in calculation of the flow rate throughout the 86 days of the incident. Indeed, Dr. Dykhuizen relies on Dr. Griffiths' work to support his results and conclusions (see page 9 and 10 of Dr. Dykhuizen's report). The incorrect assumptions made by Dr. Dykhuizen in calculating the flow rate with time and cumulative discharge estimate are listed briefly below. The problems with these assumptions were discussed in detail in Section 4 of this report.
 - a. Dr. Dykhuizen's principal error is to assume that the flow rate decreases with time purely based on the decrease in pressure difference between the reservoir and PT-B.
 - b. Dr. Dykhuizen does not take account of presence of the second flow path through the drill pipe in the well.
 - c. Dr. Dykhuizen assumes that the resistances through the system remain constant with time.
 - d. Dr. Dykhuizen decouples the frictional and gravitational pressure drops in the same way that Dr. Griffiths did.

Dr. Dykhuizen states on page 10 that erosion did not have a significant effect on the overall flow after the first 2 days, but does not state why. It has been shown through Section 4 of this report that there are many changes occurring in the system (erosion being only one of them) throughout the incident. Assuming that the flow path did not change is a fundamental assumption of Dr. Dykhuizen's method of analyzing historical flow by backwards extrapolation. But based on the numerous changes that occurred to the flow path during the incident, this assumption does not accurately reflect the actual physical conditions that existed during this period.

6 CONCLUSIONS

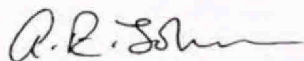
Dr. Griffiths' Report

1. Dr. Griffiths' assumption that the productivity index ("PI") increased to 43.8 stock tank barrels per day per psi (stb/d/psi) during the first 8.6 hours following the blowout is a misinterpretation of available data and is incorrect. Dr. Griffiths' assumption that the PI then remained constant throughout the 86 days is unfounded. The constant PI Dr. Griffiths assumed is only one of many scenarios of how the PI may have changed over time. In the absence of an assumed constant PI, Dr. Griffiths' own methods generate a much wider uncertainty range than he claims.
2. Dr. Griffiths makes incorrect assumptions about the bottom of BOP pressure ("PT-B") prior to the first available data on 8th May 2010. Application of Dr. Pooladi-Darvish's (a US Government expert witness) PT-B methodology prior to 8th May 2010 further increases the uncertainty around Dr. Griffiths' estimate by reducing Dr. Griffiths' "best estimate" by 10%. Combining Dr. Pooladi-Darvish's PT-B methodology with a non-constant PI in Dr. Griffiths' method further increases this uncertainty range of Dr. Griffiths' results, reducing his "best estimate" by more than 30%.
3. Dr. Griffiths' calculation methods are overly simplistic. They do not represent two critical features of the system that affected the flow rate (multiphase flow and the presence of two flow paths in the well caused by the drill pipe in the well) sufficiently to calculate the flow rate accurately. Comparison to an industry-standard multiphase simulator demonstrates the errors in Dr. Griffiths' calculations.
4. Dr. Griffiths' model determines the well and BOP discharge coefficients using only a few hours of capping stack data from the end of the flowing period. Dr. Griffiths then assumes that this model (with constant well and BOP discharge coefficients) based on a few hours at the end of the incident can be applied to the prior 86 days of the incident. This is contrary to the physical evidence which indicates that numerous changes in the flow path occurred throughout the incident.
5. The two alternative methods that Dr. Griffiths used to "validate" his model were derived from the same set of data from which his initial model was based. Therefore, they do not (and cannot) present any form of validation of his "best estimate" case. Dr. Griffiths' use of these two alternative models is a self-fulfilling circular argument. Furthermore, the application of these "validation" methods to the entire 86 day flow period offers no validation of Dr. Griffiths' cumulative discharge results.
6. Dr. Griffiths has not demonstrated that his adjustments of the PT-B readings are correct. The uncertainty surrounding the proper correction (or corrections) to be applied to PT-B indicates that the overall uncertainty of Dr. Griffiths' flow estimates is much greater than he acknowledges.

7. Dr. Griffiths' analysis of the flow rates and cumulative discharge prior to 8th May 2010 is mainly conjecture and the estimates for this period could be incorrect by a factor of approximately 2.

Dr. Dykhuizen's Report

1. Dr. Dykhuizen's calculation of a lower bound flow rate, based on the flow from the vents on the Top Hat, was incorrect outside of a narrow time frame. Dr. Dykhuizen added the result of the calculation to the collection flow rate just prior to the installation of the capping stack, when the collection rate from the Top Hat was higher than it had been at earlier times. At earlier times in the Top Hat period this lower bound flow rate would have been about 20,000 stb/d. Dr. Dykhuizen's lower bound estimate is, therefore, only a lower bound near the capping stack period.
2. Dr. Dykhuizen's June 2010 calculation of flow from the skirt at the base of the Top Hat is subject to large uncertainties in two key parameters used in the analysis: the skirt geometry and pressure data. Dr. Dykhuizen's flow rate estimate for the flow from the skirt at the base of the Top Hat is a gross overestimate, by a factor of at least 10.
3. Dr. Dykhuizen's calculation of a lower bound flow rate based on the Top Kill period is incorrect. When I performed a calculation using Dr. Dykhuizen's own method for an earlier Top Kill attempt, it yielded a result of 32,700 stb/d. Other uncertainties in the calculation could result in an even lower flow rate than 32,700 stb/d. Given the uncertainties of mud flow direction and presence of junk shot materials during the Top Kill attempt on 28th May 2010, I do not believe that subset of later Top Kill data can be used for accurate flow rate estimation.
4. My analyses as to why Dr. Griffiths' calculation of flow rate over the 86 days is incorrect equally apply to Dr. Dykhuizen's estimate (*i.e.* Dr. Dykhuizen, like Dr. Griffiths, incorrectly assumes that restriction and PI were constant over time, and fails to account for the drill pipe in the well). Had Dr. Dykhuizen performed this calculation correctly (taking account of changing restrictions in the system, the drill pipe in the well, and multiphase effects) the results would not have indicated a decreasing flow rate with time.
5. Also, as in the case of Dr. Griffiths' calculation of the volume of oil leaked from the well, Dr. Dykhuizen's estimate is (at best) an order of magnitude estimate. And (although Dr. Dykhuizen does not quantify them) the uncertainty bands around the cumulative flow estimates are large.



Adrian E. Johnson PhD CEng MIMechE

1st May 2013

Date



7 FEDERAL RULES OF CIVIL PROCEDURE

1. This report contains my opinions, conclusions and reasons therefore.
2. A statement of my qualifications is contained in section 2.
3. My employer, FEESA Ltd., is compensated for my time, and my assistants' time, at a rate of £300 per hour. Neither I nor my assistants have received any compensation as an individual apart from remuneration as an employee of FEESA Ltd. This compensation is not contingent upon the outcome of the litigation.
4. I have not previously testified as an expert witness, although I have performed work on behalf of an expert witness.
5. The references are listed in section 8.

8 REFERENCES

- (1) Griffiths, Stewart. K., Dr. - *Oil Release from the MC252 Macondo Well* (22nd March 2013).
- (2) Dykhuizen, Ron. C., Dr. - *Flow Rates from the Macondo MC252 Well* (22nd March 2013).
- (3) Spreadsheet – *Flow Status Log rev2 (BP-HZN-2179MDL06393411) (native)*
- (4) Spreadsheet – *BP-HZN-2179MDL01608483 (native)*
- (5) Spreadsheet *5.8 Pump Volume and Rates - BP Summary (BP-HZN-2179MDL05048308) (native)*
- (6) *List of Items Pumped in Order of Discharge (BP-HZN-2179MDL05497214)*
- (7) Spreadsheet *MC252_PT_B_301_1 (BP-HZN-2179MDL06743478) (native)*
- (8) Spreadsheet *MC252_PT_B_301_2 (BP-HZN-2179MDL06744885) (native)*
- (9) Spreadsheet *Q4000_MC252_PT_B_301 (BP-HZN-2179MDL06742613) (native)*
- (10) Spreadsheet *Skandi_MC252_PT_B_301_1 (BP-HZN-2179MDL06742965) (native)*
- (11) Spreadsheet *Skandi_MC252_PT_B_301_2 (BP-HZN-2179MDL06744773) (native)*
- (12) *Stipulation Mooting BP's Motion for Partial Summary Judgment Against the United States*, Document 8620, Filed Feb. 19, 2013
- (13) Ratzel, Arthur C., III, *DOE-NNSA Flow Analysis Studies Associated with the Oil Release following the Deepwater Horizon Accident*" (September 2011 page 45, footnote 18)
- (14) *Dynamic Simulations Deep Water Horizon Incident BP (from ae add energy)*, Appendix W. (29th August 2010), BP-HZN-BLY00000526
- (16) Miller D. S., *Internal Flow Systems* ISBN 0-947711-77-5 1990
- (17) BP-HZN-2179MDL06743478, *MC252_PT_B_301_1* and
BP-HZN-2179MDL06743284, *MC252_PT_3K_2_1*
- (19) Spreadsheet - *Tranmitter Calibration (native)*, BP-HZN-2179MDL05187232
- (20) Deposition transcript of Dr. Stewart K. Griffiths 13th to 14th November 2012
- (21) Moody L. F., *Friction Factors for Pipe Flow*, 66 Transactions of ASME pp. 671 – 684 (Nov 1944).



- (22) Spreadsheet – DNV2011061504 - P-T Sensor Test Data
- (23) *Forensic Examination of Deepwater Horizon Blowout Preventer*, (20th March 2011) (DNV BOP Report Vol. I).
- (24) ROV footage BOS-7677 - OI3_Millennium42_DVD20_BOS-007677a
- (25) Gochmour, M., Deposition Exhibit 8682 – Paroscientific pressure and depth data (21st August 2010).
- (26) Hewitt, G.F., and Roberts, D.N., *Studies of Two-Phase Flow Patterns by Simultaneous X-ray and Flash Photography*” AERE-M 2159, (1969).
- (27) R.W. Lockhart and R.C. Martinelli, *Proposed correlation of Data for Isothermal, Two Phase, Two Component Flow in Pipes*, Chem. Eng. Prog., pp. 39–48 (1949).
- (28) P.B. Whalley, *Boiling, Condensation and Gas-Liquid Flow*, pp 52 – 59, (Oxford University Press, 1987)
- (29) Camilli, Deposition Exhibit 9012
- (30) BP-HZN-2179MDL06475244 and *Forensic Examination of Deepwater Horizon Blowout Preventer*, (20th March 2011) (DNV BOP Report Vol. I).
- (31) Dykhuizen, R., Dep. Ex. 9361
- (32) Spreadsheet – *Topkill#3 (Autosaved).xls*m – Dr. Dykhuizen’s Top Kill flow rate calculations
- (33) BP-HZN-2179MDL07266154 (14 June 2012 email from S. Carmichael to B. Carlson & N. McCasin re Q4000 collection spreadsheet update); spreadsheet - BP-HZN-2179MDL07266193 (native) - flow rate values; spreadsheet - BP-HZN-2179MDL07266256 (native) - Flow recovery data
- (34) Dep. Transcript of Dr. A. Liao (10th to 11th November 2010).
- (35) *BP-HZN-2179MDL01088589 native*, PowerPoint slides of the results of a fish drop prior to cementing the well.
- (36) *TREX-63059* – Sperry Sun drill pipe pressure data
- (37) Pooladi-Darvish, M., Dr., *Estimate of Cumulative Volume of Oil Released from the MC252 Macondo Well* (22nd March 2013).
- (38) Ron Dykhuizen & Charlie Morrow, *Mud Flow during Kill*, (1st June 2010), SNL075-004401.
- (39) Dep. Transcript of Dr. R. C. Dykhuizen, (31st January 2010)



9 APPENDICES

The following is a list of Appendices:

- Appendix A - Glossary
- Appendix B - Dr. Griffiths' Method with Alternative PI Profiles
- Appendix C - Comparison of Griffiths Approach With Industry Standard Model
- Appendix D - Physical Evidence Examination
- Appendix E - Top Kill Evaluation
- Appendix F - Sea Pressures
- Appendix G - Bottom Hole Pressure Calculation
- Appendix H - Materials Considered

Appendix A

Glossary

A_o	Area of an orifice.
Absolute pressure	The measurement of pressure relative to zero pressure (<i>i.e.</i> zero pressure occurs in a vacuum). Equal to the sum of the pressure shown on a pressure gauge and atmospheric pressure.
Accelerational pressure drop	Pressure drop due to changes in volume flowrate caused by spatial acceleration which occurs when the fluid undergoes a change in fluid density.
Ambient sea pressure	The pressure at a point in the sea dependant on the sea depth, density and atmospheric pressure at the sea surface.
Ambient sea temperature	The temperature at a point in the sea.
Annular flow	A multiphase flow regime in which the lighter fluid flows in the centre of the pipe, and the heavier fluid is concentrated in a thin film on the pipe wall.
Aspect ratio	The ratio of the width of a component, or shape, to its length.
A_{tot}	Total cross-sectional area.
β	Constant of proportionality.
Beggs & Brill correlation	An empirical correlation for predicting, primarily, the pressure drop through a multiphase pipeline.
BOP	Blow Out Preventer: A piece of equipment on the top of the well that has a number of mechanisms which can be used to shut off or restrict flow from the well (<i>e.g.</i> , CSR, BSR, VBR, etc.).
bopd	Barrels of oil per day. Generally used for actual barrels of oil per day at the local conditions, not stock tank barrels of oil (<i>i.e.</i> , at standard conditions).
Bottom Hole	Bottom of the well bore.
Bottom Hole pressure (BHP)	The pressure measured in a well at the depth of the producing formation.
bpm	Barrels per minute.

BSR	Blind Shear Ram: A pair of rams designed to cut and crimp or seal the drill pipe. These rams have a latch which, once fully closed, prevents reopening.
Coffer dam	A large, steel, box-like construction used in an attempt to capture (and funnel upwards via a riser) hydrocarbons escaping from the fallen riser.
Completion (of a well)	The completion of an oil or gas well is the finishing of the well so that it is ready for production. The completion comprises perforation through the tubing (the tube lowered down into a well through which the production fluids travel) wall so that the reservoir can flow into the well and any screen to prevent sand from the reservoir escaping into the tubing. The Macondo well did not have a completion.
CS	Capping Stack: Equipment containing three rams which can be shut to stop flow through the stack. The capping stack was installed at the top of the LMRP.
CSR	Casing Shear Ram: A pair of rams in the BOP that when activated cut the casing and drill pipe (with a scissor action) and practically shut off the flow from the well, although the CSR is not designed to seal the well. There is no latch on the CSR, so it may reopen once hydraulic pressure is removed.
Cumulative Oil	The total amount of oil collected up to a point in time.
D	Pipe diameter (upper case D generally denotes outside diameter).
δP_{BOP}	Pressure drop across the BOP (as used originally in Dr. Griffiths' report).
ΔP	Pressure change across an item or over a distance.
ΔP_f	See "Frictional pressure drop".
DE	Drilling vessel <i>Discoverer Enterprise</i> used to collect flow from the Macondo well.
Density (ρ)	Mass per unit of volume.
Discontinuity	A boundary or interface at which a physical quantity, such as viscosity, density, or velocity, etc., changes abruptly.
Drag	Force which acts on a solid object in the direction of the relative fluid flow velocity.

DWH	Deepwater Horizon.
e	Pipe wall roughness.
Effective diameter	The diameter of a circle with the same cross-sectional area as a non-circular opening or hole.
Elevational pressure drop	Drop in pressure between two points as a result of the difference in elevation and fluid density between the two points.
Erosion	The wearing away of a surface by a flow. Erosion increases as the solids content in the flow increases.
Friction factor	A factor dependent on surface roughness which dictates the frictional pressure drop over a surface.
Frictional pressure drop (δP_f)	Loss of pressure that occurs in pipe flow due to viscous effects and turbulent energy losses to heat in the fluid. The loss generally increases with increasing surface roughness of the pipe.
Gauge pressure	A measurement of pressure which is referenced to ambient pressure. The gauge pressure equals absolute pressure minus local ambient pressure.
GoM	Gulf of Mexico.
Gravitational pressure drop	See "Elevation pressure drop". Also called gravitational head.
Homogeneous flow	An oil and gas flow that is thoroughly mixed such that both phases move together and act as a single phase.
HP1	Drilling vessel <i>Helix Producer 1</i> used to collect flow from the Macondo well.
InfoChem	The company that owns the software Multiflash.
Junk Shot Material	Material (of various hardnesses and shapes) deliberately injected into the well in an attempt to block the flow of oil and gas. Also known as Bridging Material.
k_{BOP}	BOP discharge coefficient as defined by Dr. Griffiths.
k_{eff}	Effective discharge coefficient as defined by Dr. Griffiths.
k_{well}	Wellbore discharge coefficient as defined by Dr. Griffiths.



K value (Loss coefficient)	Loss coefficient refers to the constant of proportionality between the pressure drop across the BOP and the flow rate squared through the BOP.
Kink	The sharp bend in the DWH riser after it fell. The kink also contained two sections of kinked drill pipe.
LAP	Lower Annular Preventer: A large multi-element ram encased in a polymeric donut which can close around a tube and restrict the flow past the outside of the tube.
Least-squares fit	A mathematical procedure for finding the best-fitting curve to a given set of points by minimizing the sum of the squares of the offsets of the points from the curve.
LIB	Lead Impression Block: A steel cylinder housing with soft lead molded at the bottom, which is pressed into the top of a blockage in a well in order to gain some information about its location and shape.
LMRP	Lower Marine Riser Package: Connects the riser to the BOP and incorporates annular preventers which can be closed round the drill pipe to restrict flow.
Test Ram	A multi-element ram in a steel housing, with separate "elements" around a polymeric ring. This ram can close around a drill pipe and restrict the flow past the outside of the pipe.
MAF	NASA Michoud Assembly Facility: This is where the physical evidence from the well is stored.
Maximus	Industry-standard multiphase, life of field, network simulations software; used primarily to simulate oil and gas production systems.
Mixture density	Density of an oil and gas mixture.
MMstb	Millions of stock tank barrels.
Mstb	Thousands of stock tank barrels.
Moody friction factor	Correlation developed by Moody in the 1940's to calculate frictional pressure drops for single phase flows.
Multiflash	Software that models fluid properties based on the user specification of the components of the fluid in the mixture.



Multiphase	A flow with more than one phase (e.g., oil, water, solids and gas). In the case of Macondo, the multiphase flow is comprised of oil and gas (and most likely some solids), as no water is present.
MVBR	Middle Variable Bore Ram: This ram is designed to shut off flow when closed around the drill pipe.
MW	Molecular weight.
Net pay	The thickness of reservoir that can deliver hydrocarbons to the well bore.
OEM	Original Equipment Manufacturer: OEM samples are new parts (in this case for the Macondo BOP), direct from the manufacturer. These parts are used for comparison with the equivalent damaged parts recovered from the Macondo BOP.
OLGAS	A multiphase flow correlation proprietary to SPT – Schlumberger.
Open area ratio	The ratio of an upstream and an orifice area through which flow travels.
Overall heat transfer coefficient	A measure of the overall ability of a series of conductive and convective barriers to transfer heat.
Petroleum Experts 2 correlation	A multiphase flow correlation proprietary to Petroleum Experts Ltd.
Pressure (P)	Force per unit area exerted by the fluid.
Productivity index (PI) (κ)	The number of stock tank barrels produced from the reservoir per day per psi of pressure drop across the near well bore reservoir and any bottom hole restrictions. In a normal well this would be based on the pressure drop across the completion, but the Macondo well didn't have a completion.
PROSPER	Multiphase flow simulations software, primarily for wells. The software is written and owned by Petroleum Experts Ltd.
psi	Pounds per square inch (of pressure, in this case).
PT-3C	The pressure transmitter positioned on the choke line side of the capping stack.
PT-3K-1	The pressure transmitter on the kill side of the main body of the capping stack.

PT-3K-2	The pressure transmitter on the kill side of the main body of the capping stack. This is the key transmitter used for capping stack body pressure readings.
PT-A	The pressure transmitter positioned at the LMRP.
PT-B	The pressure transmitter positioned at the bottom of the BOP.
PT-C	The pressure transmitter positioned on the choke line of the BOP.
PT-K	The pressure transmitter positioned on the kill line of the BOP.
ρ_g	Gas density.
ρ_l	Liquid density.
Q	Volumetric flow rate.
Q4000	Drilling vessel <i>Helix Q4000</i> used to collect flow from the Macondo well.
Q_{BOP}	Volumetric flow rate through the BOP.
Q_{st}	Volumetric flow rate stock tank conditions.
Regression analysis	A statistical method for the investigation of relationships between variables.
Reservoir	A subsurface body of rock having sufficient porosity and permeability to store and transmit fluids.
Reynolds number	A dimensionless number that gives a measure of the ratio of inertial forces to viscous forces and consequently quantifies the relative importance of these two types of forces for given flow conditions.
RITT	Riser insertion tube tool: A tool inserted into the end of the fallen riser to collect flow to the <i>Discoverer Enterprise</i> .
ROV	Remotely operated vehicle: An unmanned submersible vehicle controlled from the surface.
Sand face	The physical interface between the formation and the wellbore. The diameter of the wellbore at the sand face is one of the dimensions used in production models to assess potential productivity of the well.



SG	Specific gravity: Density of the fluids relative to that of a reference substance (air or water).
Shoe track	Another term for float joint; a full-sized length of casing placed at the bottom of the casing string that is usually left full of cement on the inside. Together with cement in the annulus, the shoe track serves as the primary barrier preventing the hydrocarbons in the reservoir from flowing up the well. In this way, the shoe track acts as a plug between the inside of the casing and the formation.
Slip	The difference in velocity between phases in a multiphase flow. For example, the difference in the velocity of the gas versus oil in a flowing mixture.
SPT	Formerly Scanpower Technology: The company that produced and owns OLGA. SPT was recently purchased by Schlumberger.
ST latch	A mechanical latch which prevents the opening of the BSR or VBRs once fully closed.
stb/d	Stock tank barrels per day: A measure of the volume of oil flowing per day at stock tank conditions.
Steady state	A system that has reached equilibrium for the measurement or phenomenon concerned. For example, a steady state is reached when the flow rate, upstream and downstream pressures no longer change with time.
Stock tank conditions	Conditions of 60 °F and 14.7 psia.
Superficial gas velocity (U_g)	The velocity of gas moving through a pipe, assuming the gas fills the cross-sectional area of the pipe. Defined as the volumetric flow rate of gas divided by the cross-sectional area.
Superficial liquid velocity (U_l)	The velocity of liquid moving through a pipe, assuming the liquid fills the cross-sectional area of the pipe. Defined as the volumetric flow rate of liquid divided by the cross-sectional area.
Superficial velocity	The velocity of fluid moving through a pipe, assuming the fluid fills the cross sectional area of the pipe. Defined as the volumetric flow rate of fluid divided by the cross-sectional area.



Top Hat	A steel vessel placed over the top of the severed riser and flange to enable collection of the fluids escaping from the Macondo well.
Top Kill	A procedure used as a means of regaining control over an oil well that is experiencing an uncontrolled eruption of crude oil or natural gas (blowout). The process involves pumping heavy drilling mud into the well. This procedure is expected to stop the flow of oil and gas from the well.
Transient flow	A flow where the velocity and pressure of the flow are changing with time.
Trapezoidal rule	Numerical method used to measuring the area under a function (<i>i.e.</i> , the area under a line or curve).
TVD	True vertical depth: The vertical depth from the wellhead (the seabed in this case).
TVDss	TVD minus the elevation above mean sea level of the depth reference point of the well.
U	Overall heat transfer coefficient. A measure of how efficiently heat is transferred.
UAP	Upper Annular Preventer: A large multi-element ram encased in a polymeric donut which can close around a tube and restrict the flow past the outside of the tube.
UVBR	Upper Variable Bore Ram (see MVBR).
VBR	Variable Bore Ram: A multi-element ram which can close around a tube and restrict the flow past the outside of the tube.
Velocity (v)	The speed of the fluid or a particle in a particular direction.
VLE	Vapour-Liquid Equilibrium: The condition where the liquid and vapor in the production fluids are at equilibrium at a given temperature and pressure (<i>i.e.</i> , no more vapor can be released from, or dissolved back into, the liquid).

Appendix B

Alternative PI Profiles Using the Dr. Griffiths Method

The model Dr. Griffiths proposes for the Macondo system has been reproduced in an Excel spreadsheet, using the same parameters and assumptions as his "best-estimate" model, as far as we were able to determine from his report. The purpose of this exercise is to use Dr. Griffiths' methods to demonstrate that the Productivity Index and k_{BOP} (the flow resistance, or discharge coefficient, of the BOP) could have changed through time while still exhibiting the PT-B pressure values recorded.

In order to do this, I had to make certain assumptions in this spreadsheet that I do not consider correct, but rather to be consistent with those assumptions that Dr. Griffiths made.

BOP Pressure History (PT-B)

The first step is to compile the available bottom of pressure data (PT-B), using the same offsets that Dr. Griffiths assumed. The sources of PT-B data were:

- MC252_PT_B_301¹
- Skandi_MC252_PT_B_301²
- Q4000_MC252_PT_B_301³

These three data sets were combined to produce a complete profile of PT-B data through time from 8th May 2010 (the first PT-B reading) to 15th July 2010. The combined PT-B data set contained over 220,000 data points. To make these more manageable, the volume of data was reduced, removing superfluous data whilst retaining all the details of the original PT-B profile. The volume of PT-B data was reduced using the following steps:

1. Remove data points that were superfluous for this analysis (*i.e.*, pressure data after the well was shut-in),
2. Remove obviously wrong data (all pressure readings below the ambient sea pressure were assumed to be erroneous and were deleted),
3. Reduce the volume of data (any data point that could be interpolated from the points either side of it, without loss of detail, was removed), and
4. To be consistent with Dr. Griffiths, the data during the top kill attempts (between 13:59 on 26th May 2010 and noon on 30th May 2010) was removed.

This reduced the PT-B data set to 6680 points. To be consistent with Dr. Griffiths' approach only, I adopted his assumption that the PT-B values before 11th July 2010 were under-reading the actual PT-B pressure by 740 psi and over-reading by 620 psi after that date. The data were

¹ MC252_PT_B_301_1 (BP-HZN-2179MDL06743478) (native) and MC252_PT_B_301_2 (BP-HZN-2179MDL06744885) (native).

² Skandi_MC252_PT_B_301_1 (BP-HZN-2179MDL06742965) (native) and Skandi_MC252_PT_B_301_2 (BP-HZN-2179MDL06744773) (native).

³ Q4000_MC252_PT_B_301 (BP-HZN-2179MDL06742613) (native).

modified accordingly to reflect Dr. Griffiths' assumptions. I do not agree with Dr. Griffiths that these offsets are correct.

No PT-B data exists before 8th May 2010. As PT-B is required to calculate flowrate via this method, I assumed that PT-B was reading the value that Dr. Griffiths created for his time zero (reproduced below in Figure B-2), which was 4300 psia at the start of the incident (20th April 2010). The resultant set of assumed PT-B points through time are plotted in Figure B-1.

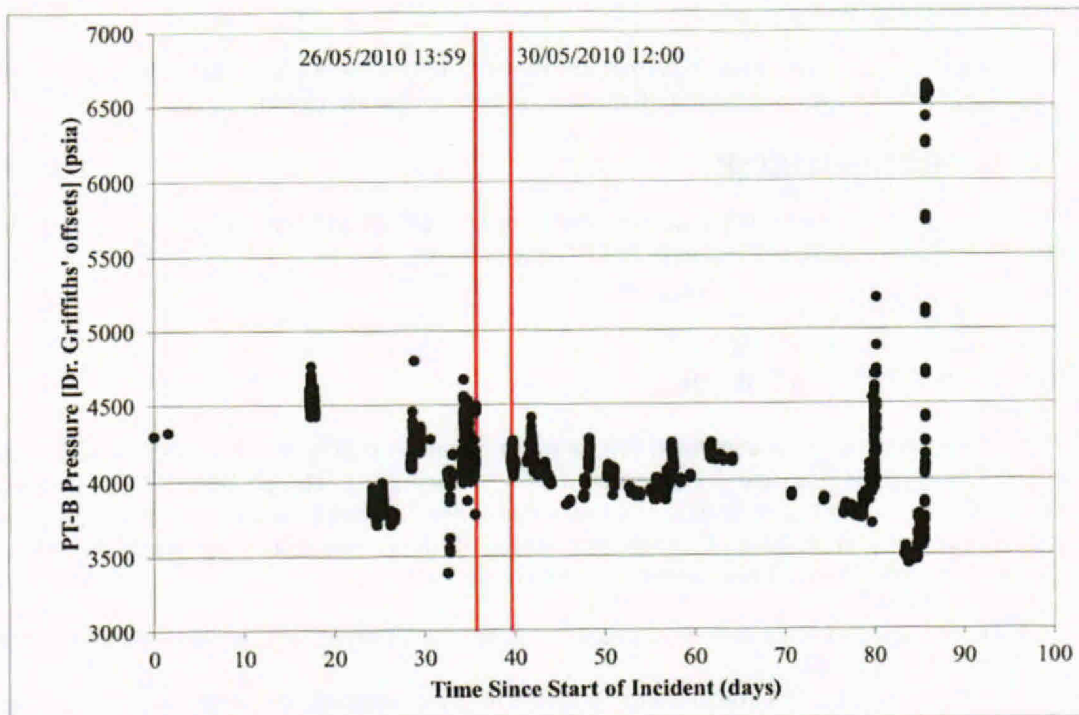


Figure B-1. BOP Inlet Profile using Dr. Griffiths' Offset Assumptions
(the red lines show the start and end of the Top Kill attempts)

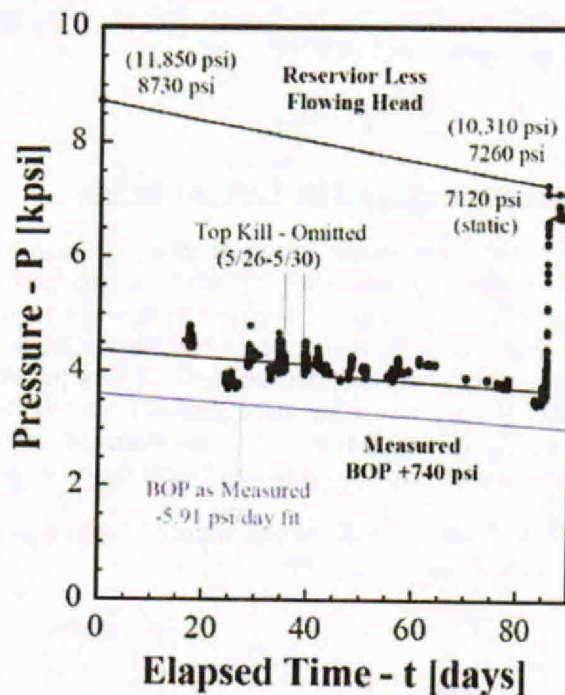


Figure B-2. Dr. Griffiths' "Best Estimate" BOP Inlet Pressure Histories

Comparing the PT-B profile I created using Dr. Griffiths' assumptions (Figure B-1) with the one presented by Dr. Griffiths (Figure B-2) shows that the data sets are very similar, though Dr. Griffiths seems to have omitted the ~3500 psia data on 23rd May 2010 (day ~33). Dr. Griffiths also omitted data between 8th and 10th July 2010 (days 78.6 to 80.2) where PT-B readings increased significantly before and during the removal of the Top Hat.

Predicting the Flow Rate Profile Through Time

With an assumed profile for the pressure below the BOP (*i.e.*, PT-B) and an assumed reservoir pressure profile (assuming it varies linearly between 11,850 and 10,310 psia throughout the event, as assumed by Dr. Griffiths), I can calculate the pressure drop up the well. The pressure drop up the well consists of an elevational term, a frictional term and an acceleration term. Assuming the accelerational term is negligible compared to the others (as I have observed it to be in all oil and gas wells I have studied) and that the elevational term is constant (Dr. Griffiths assumed a constant 3100 psi elevational term), the frictional pressure drop term can be deduced. This frictional pressure drop can be converted to a flow rate using the following equation as given by Dr. Griffiths (equation (1) on page 45 of his report):

$$Q_{st} = \frac{\theta}{2} \left(\sqrt{1 + \frac{4\kappa\delta P}{\theta}} - 1 \right) \quad (B1)$$

Where Q_{st} is the stock-tank flow rate, κ is the productivity index (PI), and if δP is the frictional pressure drop between the reservoir and BOP inlet, and

$$\theta = \frac{k_{well}^2}{\kappa} \quad (B2)$$

Check of the Spreadsheet Model Against Dr. Griffiths' Results

Using Equation B1, the BOP inlet pressure history (Figure B-1) and the values for PI and k_{well} proposed by Dr. Griffiths (43.8 stb/d/psi and 1152 stb/d/psi^{1/2}, respectively), the well flow rate profile presented in Figure B-3 is calculated. As can be seen by comparison to Dr. Griffiths' own plot (reproduced in Figure B-4), aside from a few short term deviations (caused by my inclusion of more PT-B data than Dr. Griffiths), the predicted flow profiles are the same. Indeed, if the path of Figure B-3 is integrated using the trapezoidal rule (as Dr. Griffiths did with his model), this generates a value of 5.0 MMstb of oil being produced from the well throughout the whole incident, the same value Dr. Griffiths proposes for his "best estimate."

Therefore, the spreadsheet model is a sufficiently accurate reproduction of Dr. Griffiths' best estimate model for the purposes of this Appendix.

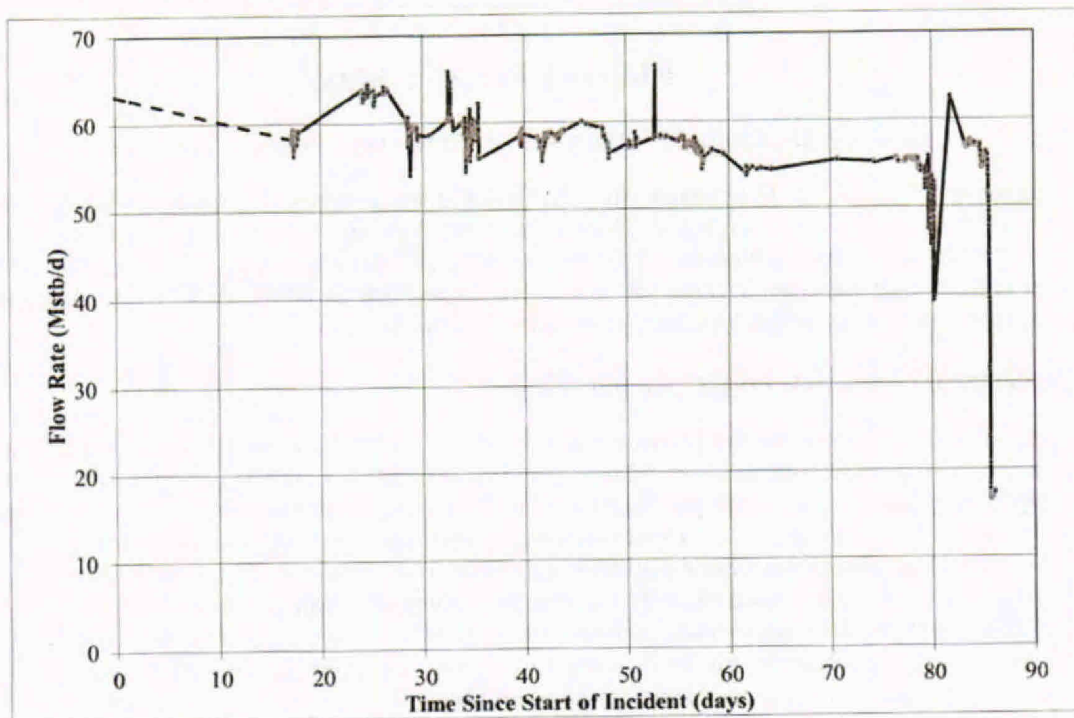


Figure B-3. Well Flow Rate Profile Through Time using Dr. Griffiths' Method

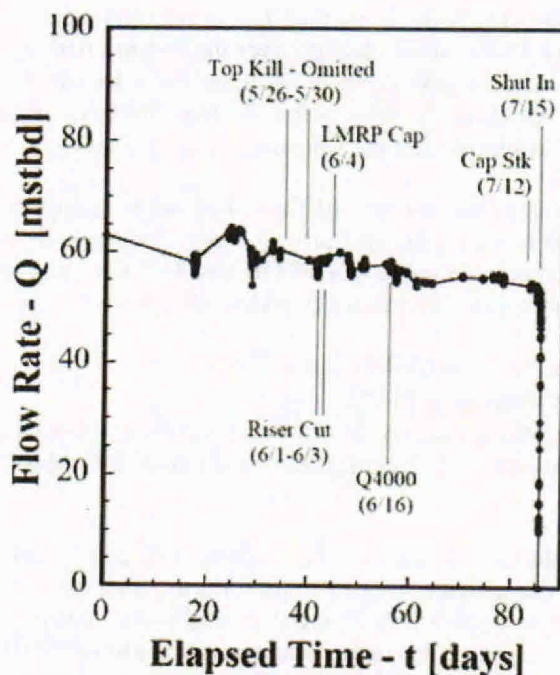


Figure B-4. Dr. Griffiths' "Best Estimate" Well Flowrate Profile

Alternative Well PI profiles

Appendix W⁴ of the BP report presents values of net pay of the reservoir that are consistent with a PI at the start of the incident of approximately 10 stb/d/psi.

From the capping stack analysis (pressure drop across a known geometry), it is possible to estimate the flowrate. Hence, with a known reservoir pressure and BOP inlet pressure, as well as assumed well hydraulics (*i.e.*, k_{well} and elevational pressure drop in Dr. Griffiths' method), it is possible to deduce the well PI that matches the capping stack flow rate estimate. Using Dr. Griffiths' hydraulic model, it is possible to say that the PI was approximately 43.8 stb/d/psi during the capping stack period.

Apart from the PI at the start and end of the incident, there is insufficient flow rate or pressure data to estimate the well PI at other times in the incident. As a result, how the PI changed from ~10 to ~40 stb/d/psi during the incident is a matter of engineering judgement.

Dr. Griffiths assumed that the PI reached the value of 43.8 stb/d/psi so early in the incident (within 9 hours) that the model could assume the PI remained constant throughout the incident. Dr. Griffiths avoided analysis of any other potential PI values and therefore there is no

⁴ Document number BP-HZN-BLY00000526 - Appendix W - "Dynamic Simulations Deep Water Horizon Incident BP (from ae add energy)" - 29th August 2010.

discussion of alternative PI paths as part of his uncertainty analysis. However, there is no evidence that proves the PI remained constant over the flowing period, as Dr. Griffiths assumed. Indeed, as discussed in my report there is no basis for selecting a constant PI versus other plausible assumptions about the PI value before 8th May 2010 (the date at which the first PT-B pressure data becomes available after the *Deepwater Horizon* sank).

To illustrate the potential effects on Dr. Griffiths' decision to assume a constant PI value versus assuming alternative PI histories, the spreadsheet model described above has been used on three paths between the start and end values for PI (10 and 43.8 stb/d/psi, respectively). Figure B-5 shows the three arbitrary paths between the two known values:

- Constant PI: *i.e.*, that assumed by Dr Griffiths
- Path A: a linear increase in PI from start to end
- Paths B: a path with a constant PI of 10 stb/d/psi from the start of the incident to the 20th May 2010 followed by a linear increase in PI from 20th May 2010 to the end value of 43.8 stb/d/psi.

Any number of PI paths can be drawn between these two points and it is possible that the PI could have changed dramatically several times during the incident as the flow path and restrictions in the well or bottom hole changed through time. Such changes in flow paths and restrictions may be the cause of the sudden changes in measured PT-B observed in Figure B-1. Nevertheless, these three paths are sufficient to illustrate the point.

Figure B-6 plots the well flow rate profiles for each of these possible PI paths, all of which fit the PT-B pressure profile perfectly.

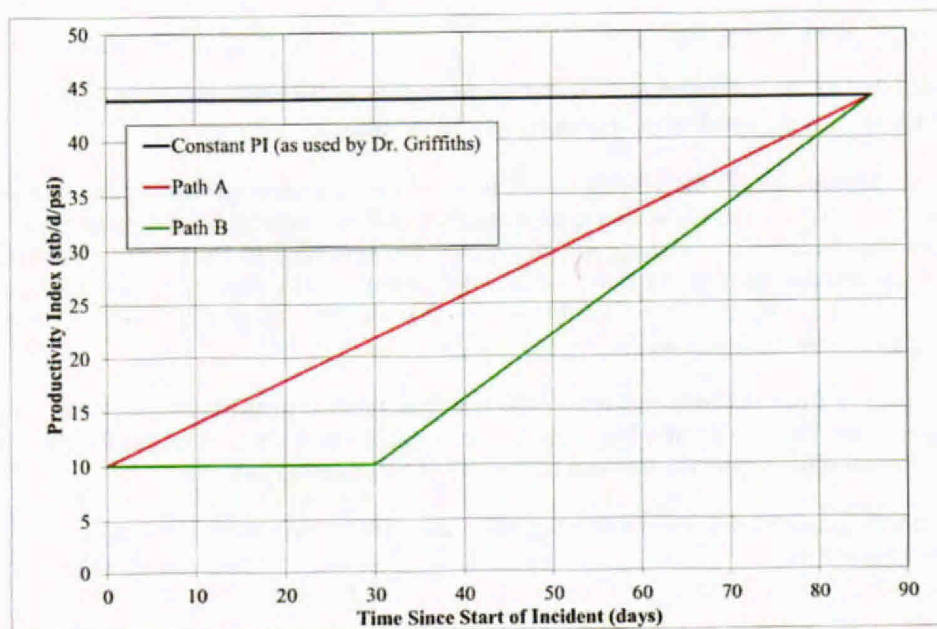


Figure B-5. Alternative PI Paths Through Time

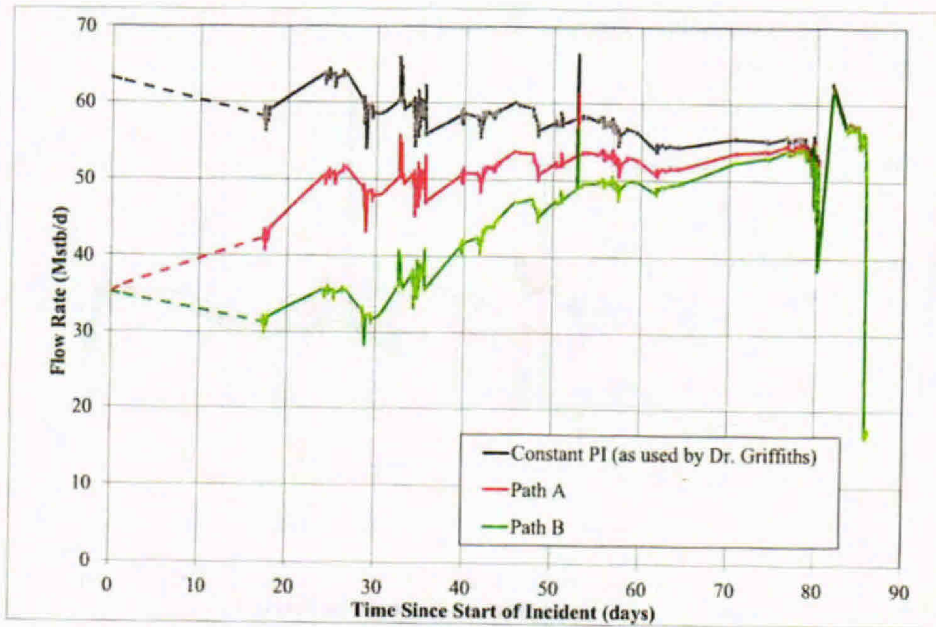


Figure B-6. Well Flow Rate Profiles for Alternative PI Paths

One can continue the analysis by calculating what Dr. Griffiths calls the BOP restriction (k_{BOP}) through time for each of these cases, knowing the pressure drop across the BOP (δP_{BOP}) and the stock tank flowrate through the BOP (Q_{BOP}), using the following:

$$k_{BOP} = \frac{Q_{BOP}}{\sqrt{\delta P_{BOP}}} \quad (B3)$$

Figure B-7 plots the result of this calculation.

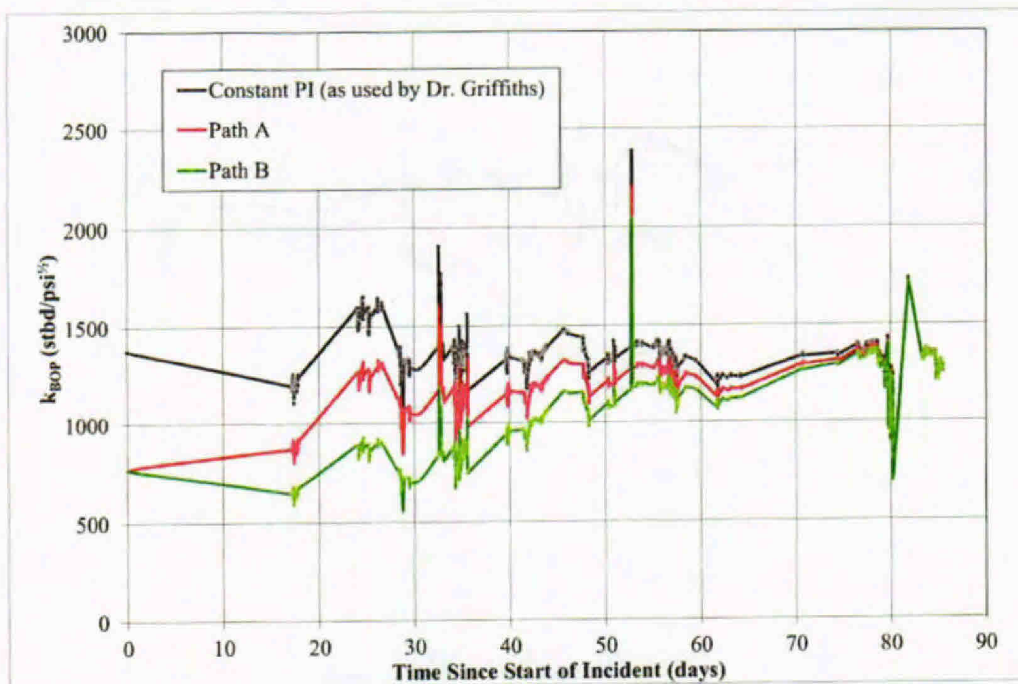


Figure B-7. BOP Discharge Coefficients through time for Each PI Path Scenario

The variation in k_{BOP} in the black line in Figure B-7 shows that k_{BOP} is not constant for Dr. Griffiths' constant PI assumption when the PT-B data is matched (as done in this calculation). Ignoring large spikes in k_{BOP} (corresponding to spikes in the PT-B data) the values of k_{BOP} shown on the black line in Figure B-7 still vary by ~40% during the incident. The other PI scenarios require k_{BOP} to generally increase over time from 8th May 2010 (day 17) onwards. The next step was to investigate how plausible an increasing k_{BOP} is.

Though Dr. Griffiths used a stock tank version of a discharge coefficient to represent the BOP in his hydraulic model (*i.e.*, k_{BOP}), this is not a familiar parameter to most engineers. It is more typical to represent the pressure drops of such discontinuities as loss coefficients. Engineers generally call these "K factors", but as Dr. Griffiths has already used "k" to represent his stock tank discharge coefficients, to avoid confusion we shall use L_{BOP} to represent the loss coefficient of the BOP. Loss coefficients are commonly defined by the following formula:

$$L_{BOP} = \frac{\Delta P}{\frac{1}{2}\rho v^2} \quad (B4)$$

Where ΔP is the pressure drop in Pascals, ρ is the density in kg/m^3 , and v is the velocity in m/s . Using these units, the loss coefficient is dimensionless.

The profile of the equivalent loss coefficient of the BOP for each of the PI path scenarios has been calculated assuming that the relevant density and velocity are those in the 18.75 inch inner

diameter of the BOP immediately upstream of the Test Ram. These profiles are plotted in Figure B-8.

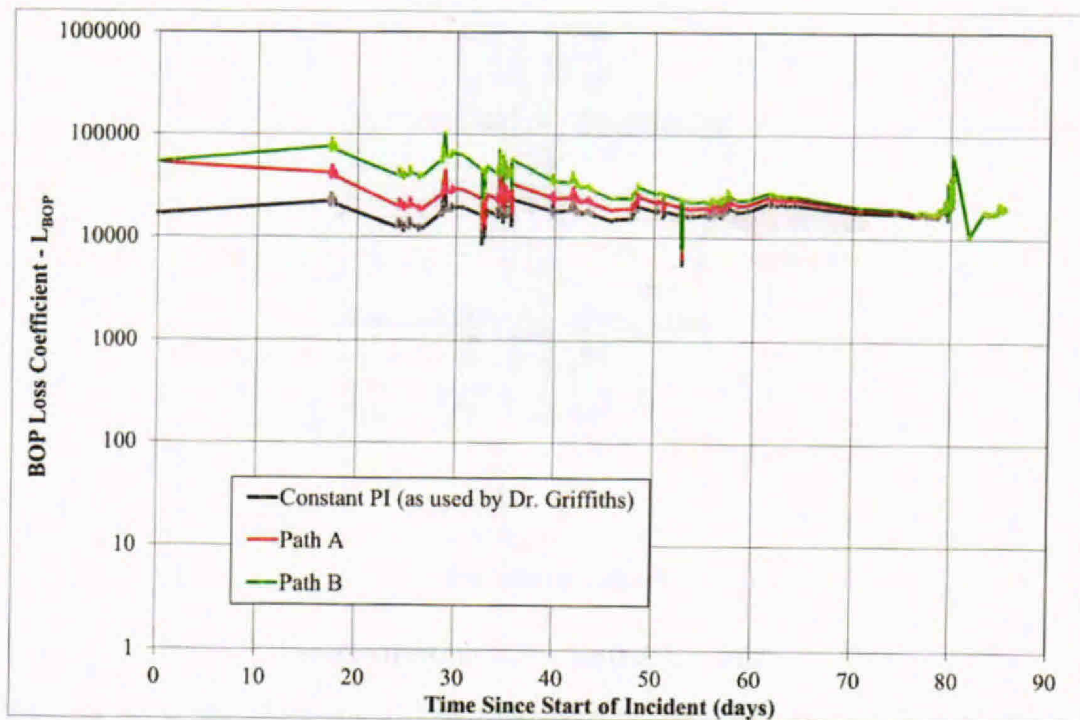


Figure B-8. BOP Loss Coefficients Through Time for Each PI Path Scenario

As can be seen, under some of the PI path scenarios, the loss coefficient must have changed by a factor of more than ten. We can get an idea for how realistic this might be by inspecting standard loss coefficient charts.

Loss coefficient charts are compilations of lab data for particular geometries, such as bends and junctions, etc. Typically they are in the form of loss coefficient versus some parameter of that geometry, such as bend radius or angle, for example. Engineers use such charts to predict the loss coefficient of a particular geometry and therefore calculate the relationship between flow rate and pressure drop to solve a particular problem. A well-used reference for loss coefficient charts is "Internal Flow Systems" by D.S. Miller,⁵ henceforth referred to as "Miller".

No loss coefficient chart exists for the specific complex geometry of the Macondo BOP during the incident. The pressure drop across the rams in the BOP has been approximated here by an orifice plate. An orifice plate is a thin plate perpendicular to the flow with a circular hole in the middle (see Figure B-9). The loss coefficient chart for such a device from Miller is reproduced in Figure B-10. As can be seen, it is in the form of loss coefficient versus the ratio of orifice area to

⁵ ISBN 0947711775.

upstream area. Miller states that this chart is applicable to both round and square holes and so is presumably applicable for a range of other shaped holes.

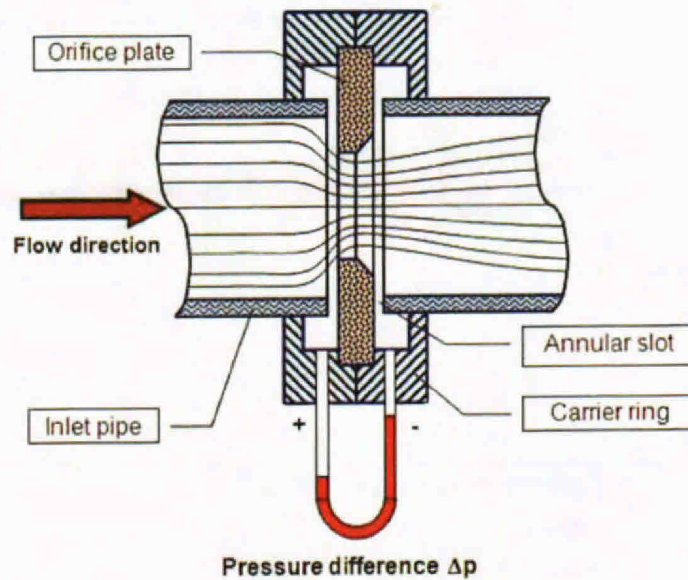


Figure B-9. Diagram of an Orifice Plate

As can be seen in Figure B-10, the chart only goes up to a loss coefficient of one thousand, whereas our L_{BOP} could be in the hundreds of thousands (Figure B-8). However, it is logical to assume that the loss coefficient will continue to climb sharply with reducing orifice area; ultimately the loss coefficient is infinite when the orifice area is zero. Hence, in order to convert the loss coefficients into an effective orifice area and ultimately an orifice diameter, the following correlation was fitted to the data in Figure B-10 to allow extrapolation to the large L_{BOP} values shown in Figure B-8:

$$\frac{A_o}{A_{tot}} = 0.6(\log(L_{BOP}))^{-0.2} \quad (B4)$$

Where A_o is the area of the orifice and A_{tot} is the total cross-sectional area.

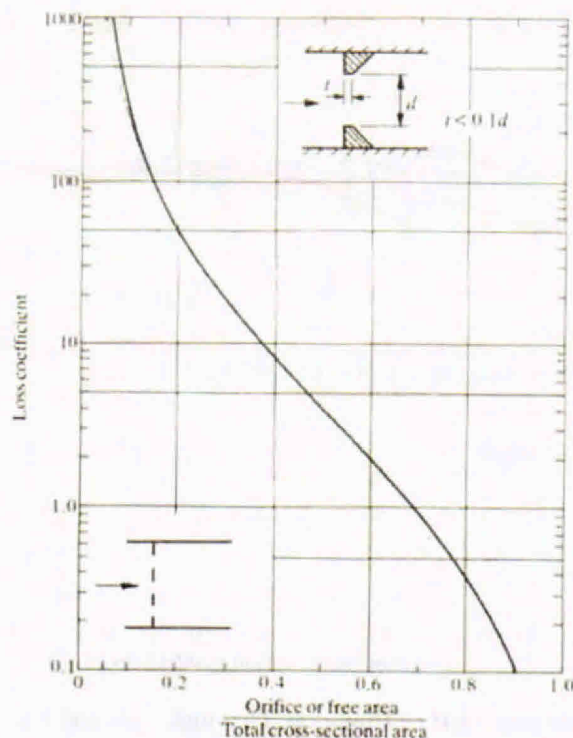


Figure B-10. Miller Loss Coefficient Chart for Sharp Edge Thin Orifices

Figure B-11 plots the results of this calculation of equivalent orifice diameter through time for each of the PI path scenarios.

As can be seen, even if we are to use the same hydraulic model and PT-B offset assumptions as Dr. Griffiths, the alternative PI paths do not require a massive change to the geometry of the BOP between 8th May 2010 and the capping stack period. Even if most of the damage to the BOP occurred in the first 9 hours, as Dr. Griffiths claimed,⁶ the PT-B variations observed after that time can be caused, and explained, by small changes in the effective opening of the BOP. Indeed, even a gradual increase in the effective flow path diameter of less than an inch, occurring over the following 84 days, would be sufficient to explain the PT-B variation through this period. Based on evidence of significant changes in the BOP (e.g., activation of rams, erosion, junk shot) it is unreasonable for Dr. Griffiths to assume, as he did, that such a small change to the BOP flow path could not occur.

⁶ See footnote 11 on page 12 of Dr. Griffiths' report.

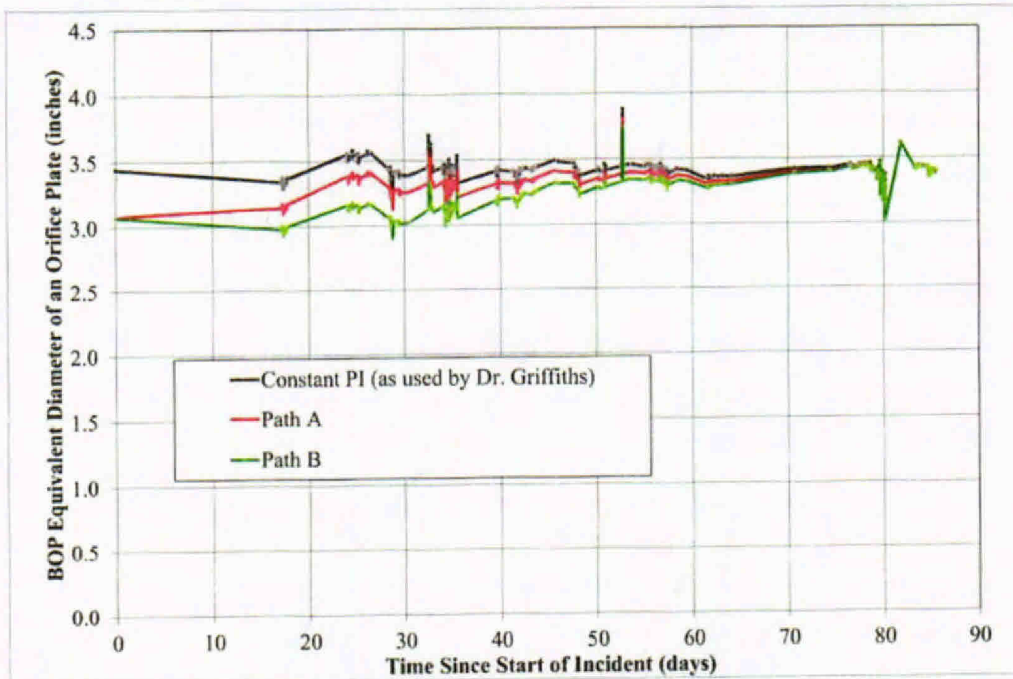


Figure B-11. Equivalent Orifice Diameter Through Time for Each PI Path Scenario

Thus, using Dr. Griffiths' own methods, data, and assumptions, there are many alternative flow rate paths that fit the available data. Therefore, the error bands for Dr. Griffiths' analysis should be much wider than he asserts. For example, the cumulative volume from the well for the "Path B" scenario is 3.7 MMstb, which results in an estimate of oil volume leaked to the sea of approximately 70% of Dr. Griffiths' best estimate, and far below the lower band of error of -13.9% proposed in his report. Other paths of the PI profile are possible which would yield even lower estimates of the oil released from the well.

Appendix C

Alternative Hydraulic Model for the Flow in the Well

Only when the capping stack is installed is there sufficient data (*i.e.*, a measured pressure drop across a well-defined geometry with a known relationship between flow rate and pressure drop) to back-calculate the flow rate from the well. Though some pressure drops may be known before the capping stack was installed, the detailed geometries of the flow path, including any restrictions, are unknown making a flow rate estimate prior to the capping stack's installation highly uncertain.

Dr. Griffiths contends that if the well productivity index (PI) is known, then the relationship between flow rate and pressure drop between the reservoir and the BOP inlet pressure can be determined. Pressure measurements are available at the BOP inlet for most of the event and a reasonable assumption can be made about how the reservoir pressure changed through time. Therefore, since the pressure drop is known, Dr. Griffiths asserts that the flow rate can be predicted to a significant degree of accuracy (error bands of -13.9% to +9.7%).

In general, the problem Dr. Griffiths faced is a common situation in the oil and gas industry: tuning a model to available data (usually called "history matching" by Petroleum Engineers), and using this model to predict results for times where there is less data. The quality of the predicted results relies on the quality of the model and the assumption of changes in the system data between the time of the tuning and the time of the predictions.

Appendix B describes the error in Dr. Griffiths' assertion that the only assumption about the well's PI that fits the data is to hold the well PI constant over the entire 86 days when the well flowed. In this Appendix, I show that Dr. Griffiths' model of the flow in the casing is not as accurate as asserted by comparing it to industry-standard methods of calculating the hydraulics of wells.

In order to avoid confusion and to distinguish the effects of Dr. Griffiths' assumed model from the effects of his assumptions about PI and PT-B offset, the work in this Appendix shall make the same constant PI and +740 psia PT-B offset assumption as Dr. Griffiths made. However, I do not agree with these assumptions, for the reasons discussed in my report.

The Geometry of the Casing

In the early days of the incident, 2513 feet of 5.5 inch drill pipe hung from the bottom of the BOP and the 5.5 inch drill pipe was connected to 800 feet of 3.5 inch drill pipe.¹ A simplified drawing of this configuration is shown in Figure C-1 and is described as the "Drill Pipe High" Case.

Results from a Lead Impression Block (LIB) study after the well was shut-in are also available.² An LIB is a steel cylinder housing with soft lead molded at the bottom which is pressed into the top of a blockage in a well in order to gain some information about its location and shape. From

¹ BP-HZN-2179MDL00477088.

² BP-HZN-2179MDL01088589.



the results of the LIB study, the top of the drill pipe was at a depth of 9318 ft TVDss, hence knowing the lengths of the sections of drill pipe, it can be concluded that 163 ft of the 3.5 inch drill pipe was in the 7 inch Casing³; Figure C-1 shows a sketch of this final geometry, called the "Drill Pipe Low" case.

Though it is not possible to determine precisely when or how quickly the drill pipe fell from the "High" to the "Low" position, the results of the LIB study allow us to determine the lowest position of the drill pipe. At any point in time the drill pipe must have been between the top of the well and the LIB measured position and thus its resistance to flow must be between that exhibited at each of these two positions.

Thermal Hydraulic Model

Models of both the Drill Pipe High and Drill Pipe Low geometries were built in FEESA's industry standard thermal hydraulic simulator, Maximus.

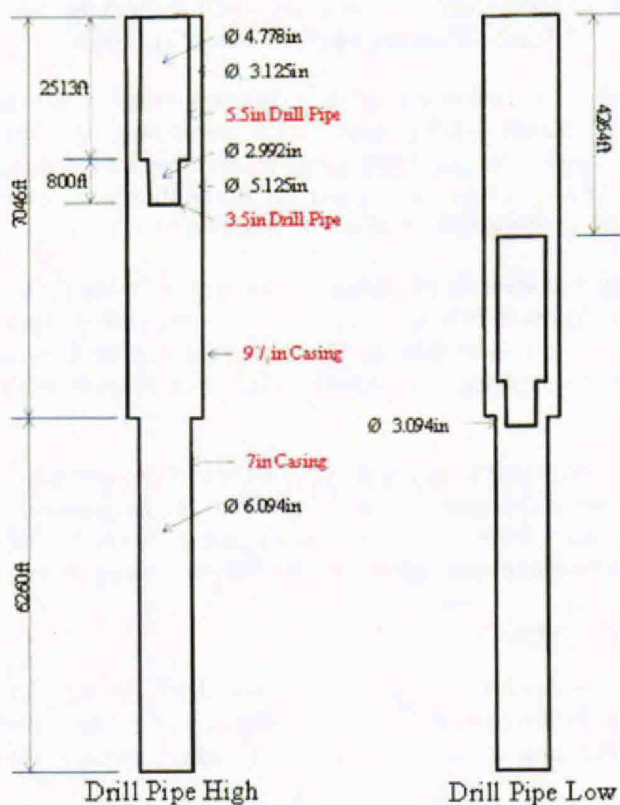


Figure C-1. Extremes of possible Drill Pipe Positions

³ BP-HZN-2179MDL01088589 native.

Maximus has been used on dozens of projects around the world to investigate the thermal hydraulic behaviour of complex networks of wells and pipelines, including several multibillion dollar deepwater developments in Angola, Ghana, and Western Australia and has been benchmarked against field data. The Maximus models for the deep-water wells listed above used the industry-standard multiphase flow model (SPT's OLGA-S) and one of the industry-standard thermo-physical properties package (InfoChem's Multiflash) to carry out a compositional simulation of the flow in the well.

Maximus is therefore the type of model that Dr. Griffiths referred to as a "general purpose" simulator. "General purpose" simulators (to use Dr. Griffiths' terminology) take into account the change in flow cross-sectional area, physical properties of the oil, gas and flow path, and multiphase flow behaviour of the fluids along the length of the well. Over the last thirty years, the predictions of such models have proved to be so accurate that they have become the industry-standard way to predict fluid flow behaviour in systems such as this one. These simulation models have displaced the less accurate correlation-based methods that preceded them, such as the model proposed by Dr. Griffiths.

In addition to the geometry assumptions noted in Figure C-1, the following modeling assumptions were made:

- The Macondo fluid composition⁴ was characterised as shown in Table C-1. A routine in Multiflash was used to reduce the number of components in the fluid whilst still maintaining a good match to gas/liquid ratios at stock tank and bubble point.
- The roughness of the drill pipe and casing was 5 microns (5×10^{-6} m or 0.0002 inches). This represents a very smooth pipe and would result in higher estimated flow rates.
- The ambient temperature varied linearly between 262 °F at 18,360 ft TVDss and 39.4 °F at mud level.⁵
- Based on FEESA's past experience with the thermal hydraulics of deepwater oil wells when they start to produce and warm-up, the overall heat transfer coefficient of the casing (U) in BTU/hr/ft²/°F was varied with time in accordance with the following relationship of U versus time since the beginning of the incident (t) in days:

$$U = 2.9t^{-0.2} \quad (C1)$$

Hence the overall heat transfer coefficient is ~1.6 BTU/hr/ft²/°F on 8th May 2010, and ~1.2 BTU/hr/ft²/°F on 15th July 2010.

⁴ Sample 1.06 from BP-HZN-2179MDL01608973.

⁵ BP-HZN-2179MDL00477088 (Native)



Name	Moles	Boiling	Molecular	Specific	Critical	Critical	Critical	Acentric
		Point	Weight	Gravity	Pressure	Temperature	Volume	Factor A
	%	*F	lb/mol	-/-	psia	*F	m3/mol	--
Methane	66.2451	-258.736	0.0353683	0.146044	667.059	-116.655	9.86E-05	0.0104
Water	0.665541	212	0.0397167	0.999931	3208.24	705.47	5.59E-05	0.344
Nitrogen	0.312278	-320.444	0.0617591	0.281301	492.52	-232.524	8.94E-05	0.0372
Ethane	6.45655	-127.48	0.066293	0.366448	706.596	89.924	0.0001456	0.0991
Carbon Dioxide	0.919953	-63.67	0.097025	0.836556	1069.99	87.7608	9.41E-05	0.223
Propane	4.54769	-43.78	0.0972142	0.515928	616.072	206.06	0.0002	0.152
I-Butane	0.918773	10.886	0.128138	0.56218	527.938	274.46	0.0002591	0.1844
N-Butane	2.09199	31.1	0.128138	0.583715	550.564	305.618	0.0002551	0.1985
I-Pentane	0.818164	82.184	0.159061	0.624246	489.793	369.14	0.000306	0.227
N-Pentane	1.02505	96.908	0.159061	0.630049	488.27	385.79	0.000311	0.2513
Benzene	0.116123	176.162	0.172212	0.886078	710.396	552.218	0.000259	0.208
Methylcyclopentane	0.391587	161.258	0.185544	0.753947	548.969	499.352	0.000319	0.230249
Cyclohexane	0.358585	177.314	0.185544	0.782854	590.305	536.738	0.000308	0.209
N-Hexane	1.35481	155.714	0.189984	0.662755	437.739	454.406	0.0003696	0.2979
Toluene	0.265463	231.134	0.203136	0.870915	595.236	605.552	0.000316	0.263
Methylcyclohexane	0.509207	213.681	0.216468	0.774775	503.427	570.272	0.000368	0.234982
N-Heptane	1.07191	209.174	0.220908	0.687561	395.519	512.564	0.0004319	0.3498
Ethylbenzene	0.051303	277.16	0.23406	0.873725	523.007	651.29	0.000374	0.302604
P-Xylene	0.279969	281.066	0.23406	0.864704	509.228	649.49	0.000379	0.318
O-Xylene	0.101078	291.974	0.23406	0.883656	540.992	674.87	0.000369	0.308
N-Octane	1.22757	258.206	0.251836	0.706621	362.16	565.106	0.0004863	0.396
C9-38	9.39828	564.551	0.483028	0.857005	258.408	856.232	0.0008674	0.924249
C38+	0.873065	1119.94	1.7034	0.969092	96.4218	1329.06	0.0033521	1.47415

Table C-1. Characterized Composition

Preliminary calculations⁶⁷ concluded that flow must be occurring through both the casing and the drill pipe. This is because even if the near-wellbore region offered no resistance to flow (an infinite PI), the maximum flow rate achievable on 15th May 2010 was 31 Mstb/d for the High Drill Pipe scenario (or 28 Mstb/d for Low Drill Pipe) if flow was only on the outside of the drill pipe.

Thus, it is likely that the flow traveled up the well through two flow paths: some going up the drill pipe, some flowing up the annulus between the drill pipe and the casing. The ratio of how much flow went up the annulus and how much went up the drill pipe is calculated as part of the network solution in Maximus from the boundary conditions (reservoir pressure and inlet to BOP pressure) specified by the user.

Comparison with Dr. Liao's Model

Figure C-2 reproduces Dr. Griffiths' plot of Dr. Liao's frictional pressure drop data versus flow rate, including a curve of the fit that Dr. Griffiths did of his frictional pressure drop correlation. This plot is Dr. Griffiths' main justification for the functional form of his correlation for the elevational pressure drop in the well.

⁶ BP-HZN-BLY00000526 – Appendix W of the BP report.

⁷ The ae add energy appendix W to the BP report.



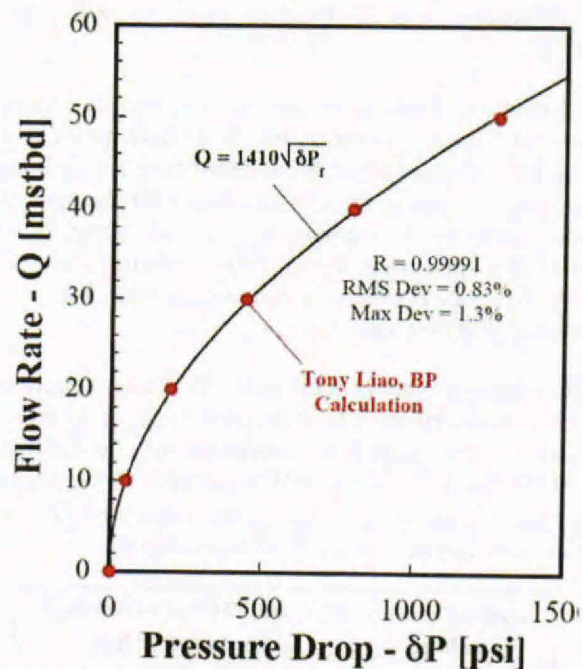


Figure C- 2. Dr. Griffiths' Correlation Fit to Dr. Liao's PROSPER Frictional Pressure Drop Results

Dr. Liao's model clearly assumes that the drill pipe is not present in the casing.⁸ This might be a perfectly reasonable assumption for Dr. Liao to make to obtain conservative estimates for the parameters he was interested in (*e.g.*, shut-in pressures), although as stated earlier in my report, Dr. Liao himself could not remember exactly the purpose of this PROSPER modelling. However, I do not believe this to be a reasonable assumption to make to generate a hydraulic model for calculating flow rates before the capping stack period because of the absence of the vitally important second flowpath (drill pipe) and its effect on the hydraulic behaviour of the well. Neglecting the effect of the drill pipe resistance in the well has a significant effect on the calculated flow rates, substantially increasing the calculated figures above what would actually result with the drill pipe present.

The Maximus models described above were used to investigate the hydraulic effect on the predicted flow rate of the two geometries described in Figure C-1 plus a "no drill pipe" geometry equivalent to the one Dr. Liao used and implicit in Dr. Griffiths' calculations.

On 15th July 2010 the capping stack generated sufficient data to determine an estimate of the well flow rate; Dr. Griffiths calculates a value of approximately 55 Mstb/d for a PT-B pressure of approximately 3600 psia.⁹ All hydraulic models can be history matched to this point to provide a better model for extrapolating to flow rates on earlier dates. However, different

⁸ BP-HZN-2179MDL04920969.

⁹ Griffiths Report.pdf – see page 4 of Dr. Griffiths' report.

models may provide different results for the flow rates on earlier dates, depending on how physically realistic they are.

The Maximus model could be history-matched by altering the roughness, a factor on the multiphase frictional pressure drop, a factor on the multiphase gravitational pressure drop, or by altering the well PI. As the values of all of these parameters are well known apart from that of the PI (as the well was not completed), the PI was altered for the Maximus model such that the predicted flow rate matched that for the capping stack period. Table C-2 shows the PIs needed to match either 50,000 or 55,000 stb/d when the reservoir pressure is 10,310 psia and PT-B is 3600 psia. As can be seen, the flow rate is relatively insensitive to PI in this range; *i.e.*, the PI must be increased by 70% to increase the flow rate by 10%.

As the capping stack flow rate estimate is not precise, the PI could have been anywhere between 34 and 59 stb/d/psi. I assumed that the PI for the well is 59 or 57 stb/d/psi for the "Drill Pipe High" or "Drill Pipe Low", respectively, to be consistent with Dr. Griffiths' model (matching 55 Mstb/d when PT-B is 3600 psia on 15th July 2010), though both values are considered high for a PI. These values were selected only to provide a comparison with Dr. Griffiths' model; I do not believe the PI during the capping stack time period was that high.

Capping Stack Flow Rate Estimate (stb/d)	Required PI for the Flow Rate Estimate (stb/d/psi)	
	Drill Pipe High	Drill Pipe Low
50,000	34	34
55,000	59	57

Table C-2. Well PIs required to Match Capping Stack Flow Rate Estimate on 15th July 2010

To help explain the difference between different models, Figure C-3 is a set of performance curves for the system showing the well flow rate (Mstb/d) as a function of PT-B pressure. To show how these performance curves can change between models, even though they are all tuned to results from the 15th July 2010, two sets of curves have been generated in Figure C-3, one using Dr. Griffiths' methods and one for the Maximus/OLGAS model:

- 15th July 2010 [in red] is the well performance curve for the system on 15th July 2010 tuned to the capping stack data, as mentioned above. The dashed line is generated using Dr. Griffiths' methods using his best estimate model parameters; the solid line is for the Maximus "Drill Pipe High" model, as described above.
- 8th May 2010 [in blue] are the two performance curves predicted for the first day when PT-B data is available; both the Maximus (solid) and Dr. Griffiths' (dashed) methods assumed that the PI was the same as the 15th July 2010 value.

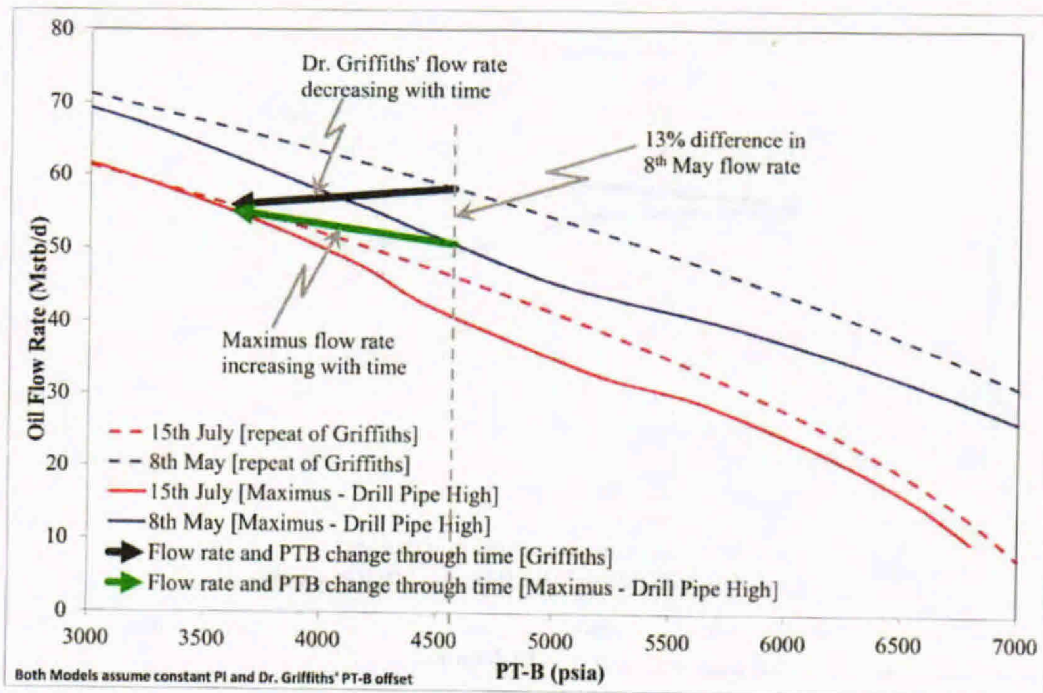


Figure C-3. Well Performance Curves at Start and End of PT-B Data: Drill Pipe High

Also shown in Figure C-3 are the values for the well flow rate and PT-B pressure between 8th May and 15th June 2010, using Dr. Griffiths' assumed offsets to correct the PT-B sensor readings to reflect actual pressures. The black arrow is the path (values for the well flow rate and PT-B pressure) predicted using Dr. Griffiths' methods, the green arrow is the path (values for the well flow rate and PT-B pressure) the Maximus "Drill Pipe High" case follows.

By closely examining the slope of these paths one can determine if the flow from the well was increasing or decreasing between 8th May and 15th June 2010. Using Dr. Griffiths' assumption that the general trend in the PT-B pressure between 8th May 2010 to 15th July 2010 was a decrease from 4560 to 3600 psia, then Dr. Griffiths' methods predict a **decrease** in flow rate from 58 to 55 Mstb/d. However, the more physically detailed Maximus model, which models the effect of the drill pipe in the well, predicts a general **increase** in flow rate from 50 to 55 Mstb/d.

Figure C-4 compares the performance curves for the "Drill Pipe Low" Maximus model with our results for Dr. Griffiths' methods. The "Drill Pipe Low" scenario predicts only a small increase in flow rate between 8th May 2010 and 15th July 2010 (54 to 55 Mstb/d). Again, the absolute magnitude of the flow rates (54 to 55 Mstb/d) are a result of adopting Dr. Griffiths' models' assumptions about the final flow rate on 15th July 2010, they do not necessarily represent the actual flow rate during the capping stack period.

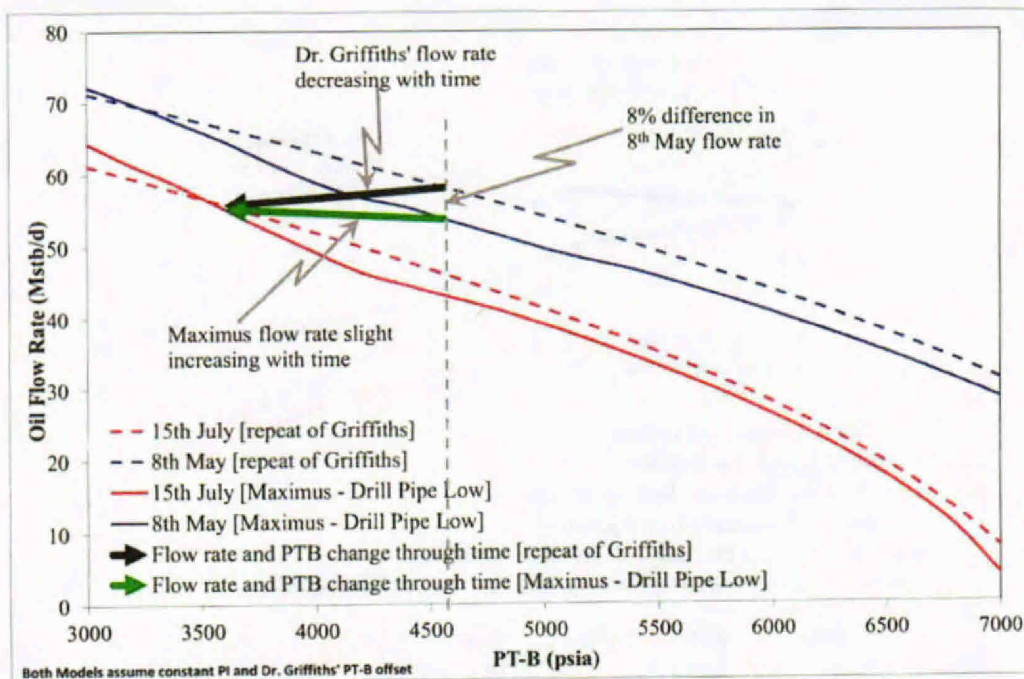


Figure C-4. Well Performance Curves at Start and End of PT-B Data: Drill Pipe Low

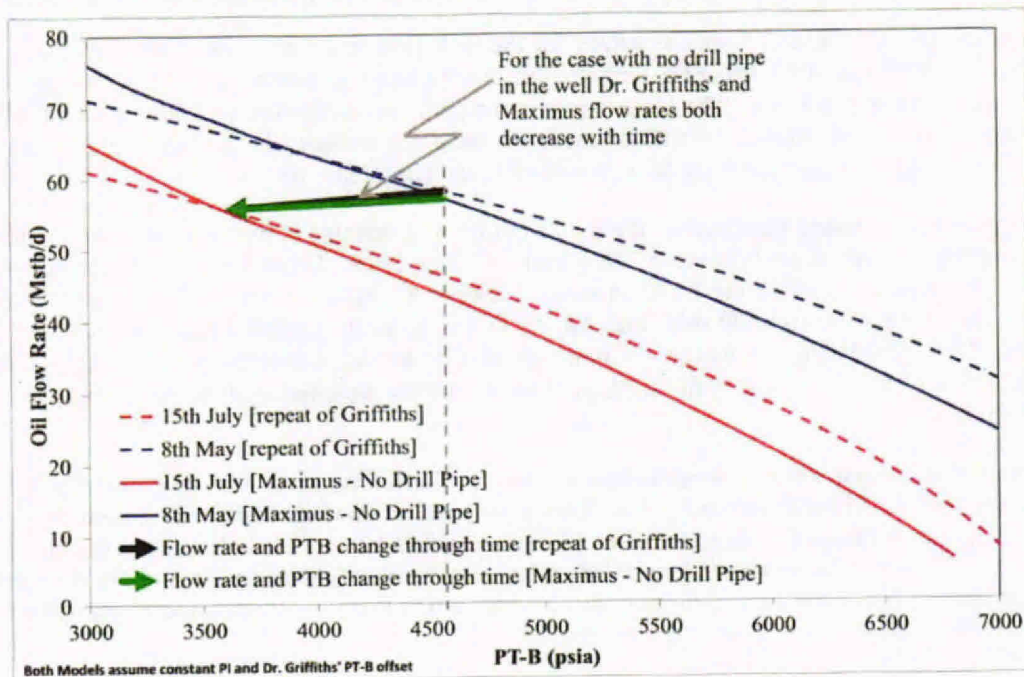


Figure C-5. Well Performance Curves at Start and End of PT-B Data: No Drill Pipe

The well performance curves for the models without a drill pipe are plotted in Figure C-5. As can be seen, the Maximus/OLGAS model agrees with Dr. Griffiths' methods for the well **if there was no drill pipe in it and the PI was constant**, just as Dr. Liao assumed in his model. However, if Dr. Griffiths had a more realistic model representing the drill pipe in either the high or the low position (*i.e.*, capturing correctly the multiphase effects and differences in frictional and gravitational pressure drop between the two flow paths), the result would be early days flow rates (when PT-B was 4565 psia¹⁰) that are 8% to 13% lower than his current model. This can be determined by comparing the flow rates from either the Drill Pipe High or Drill Pipe Low cases (Figure C-3 and C-4) at PT-B pressures within this range with the flow rates from Figure C-5 (Drill Pipe Ignored).

¹⁰ MC252_PT_B_301_1 (BP-HZN-2179MDL06743478) (native), MC252_PT_B_301_2 (BP-HZN-2179MDL06744885) (native), Skandi_MC252_PT_B_301_1 (BP-HZN-2179MDL06742965) (native), Skandi_MC252_PT_B_301_2 (BP-HZN-2179MDL06744773) (native) and Q4000_MC252_PT_B_301 (BP-HZN-2179MDL06742613) (native).



Appendix D

Physical Evidence Examination

I inspected the physical evidence held at the NASA Michoud Assembly Facility near New Orleans, Louisiana on 11th and 12th September 2012.

My inspection was carried out by visual examination and documented by photograph and video. The key information gleaned from the inspection is as follows:

1. There was limited erosion around the sides of the VBRs/Test Ram (see Figures D-1 to D-3), suggesting that other flowpaths through the VBRs/Test Ram or drill pipe existed.

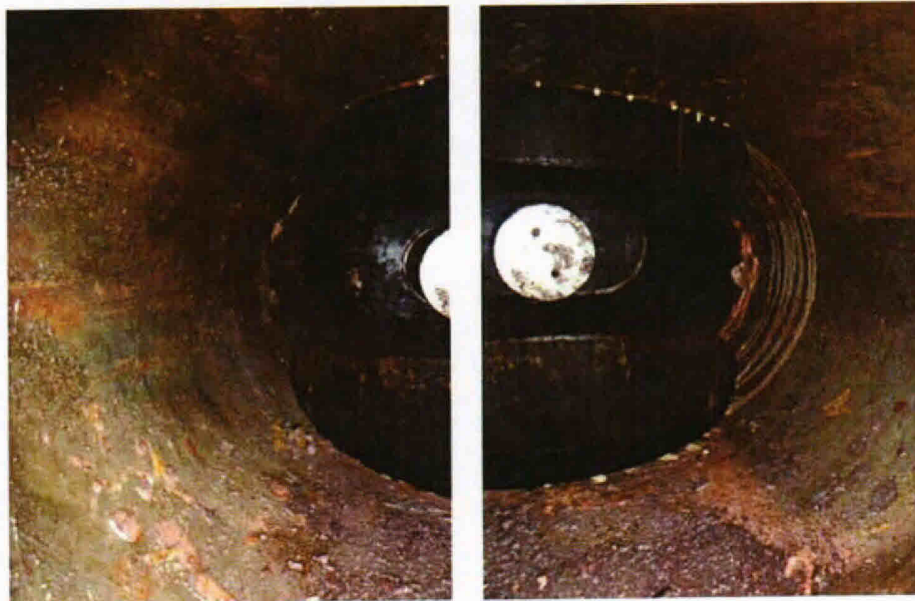


Figure D-1. Test Ram Housing

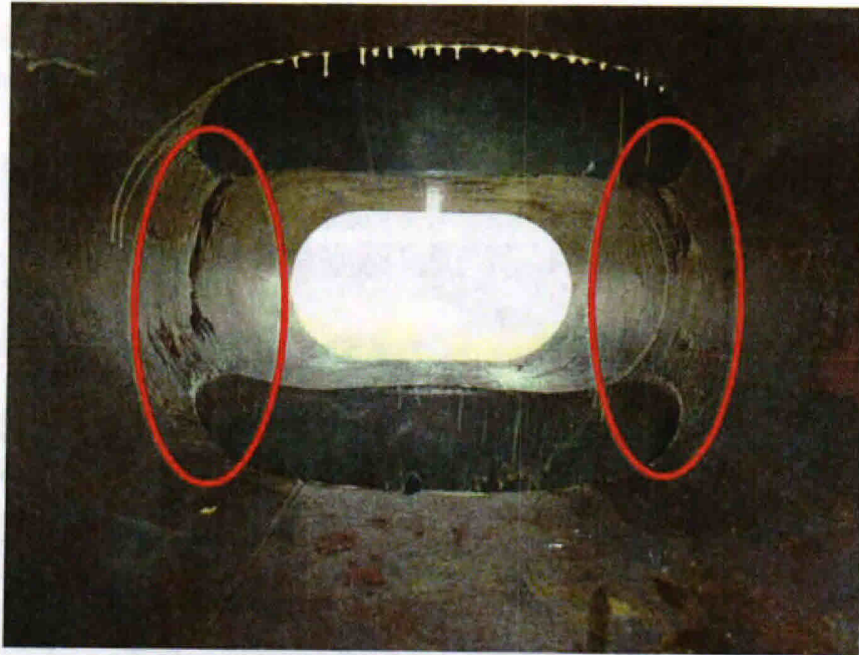


Figure D-2. MVBR Housing

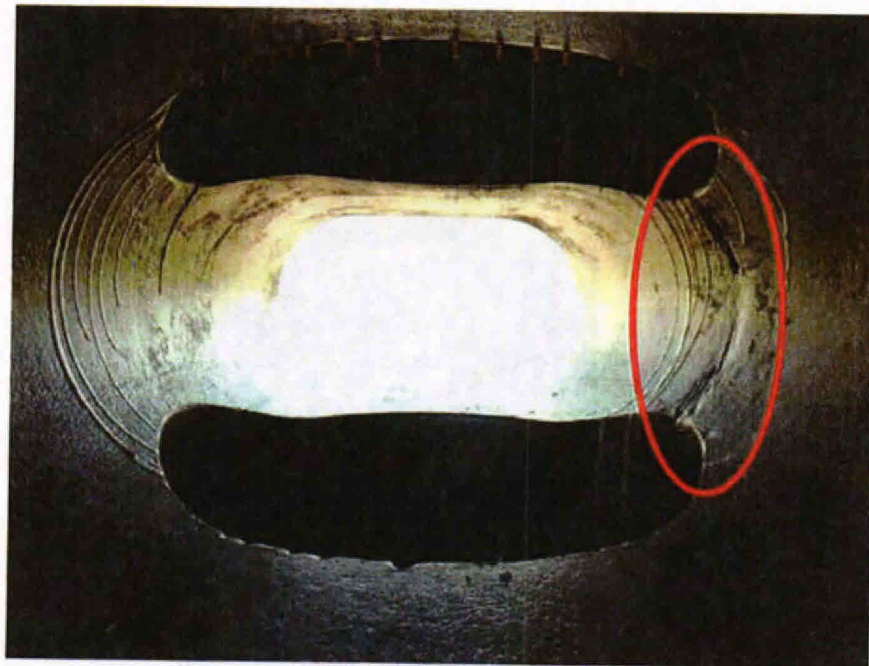


Figure D-3. UVBR Housing

2. There was limited erosion of the housing around the sides of the CSR (see Figures D-4 and D-5), suggesting that other flowpaths through the CSR existed.

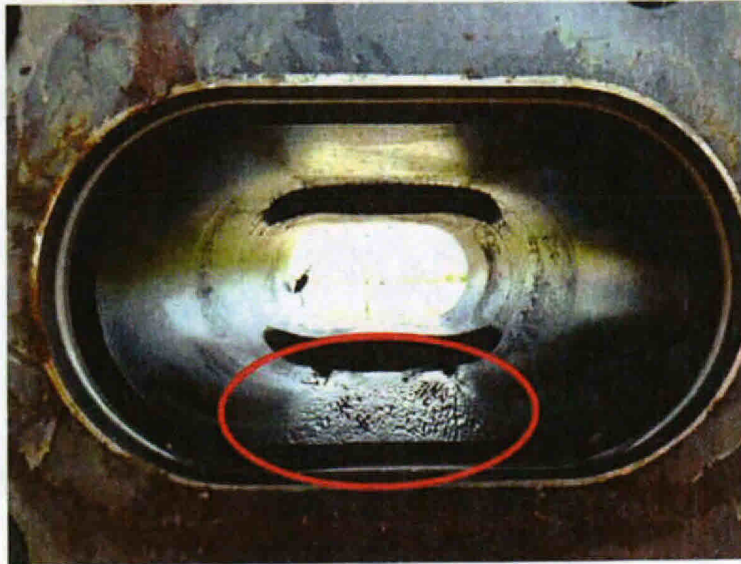


Figure D-4. CSR Housing

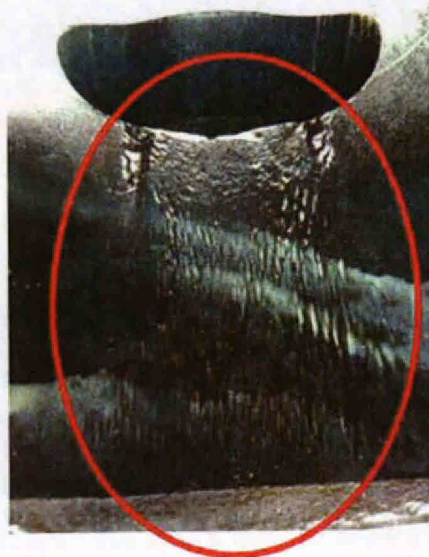


Figure D-5. CSR Housing Detail

3. There was erosion around the sides of the BSR housing (see Figures D-6 and D-7) suggesting that flow was restricted through other parts of the BSR. This, in turn, suggests that the BSR was largely closed at the time of the incident when erosion occurred.

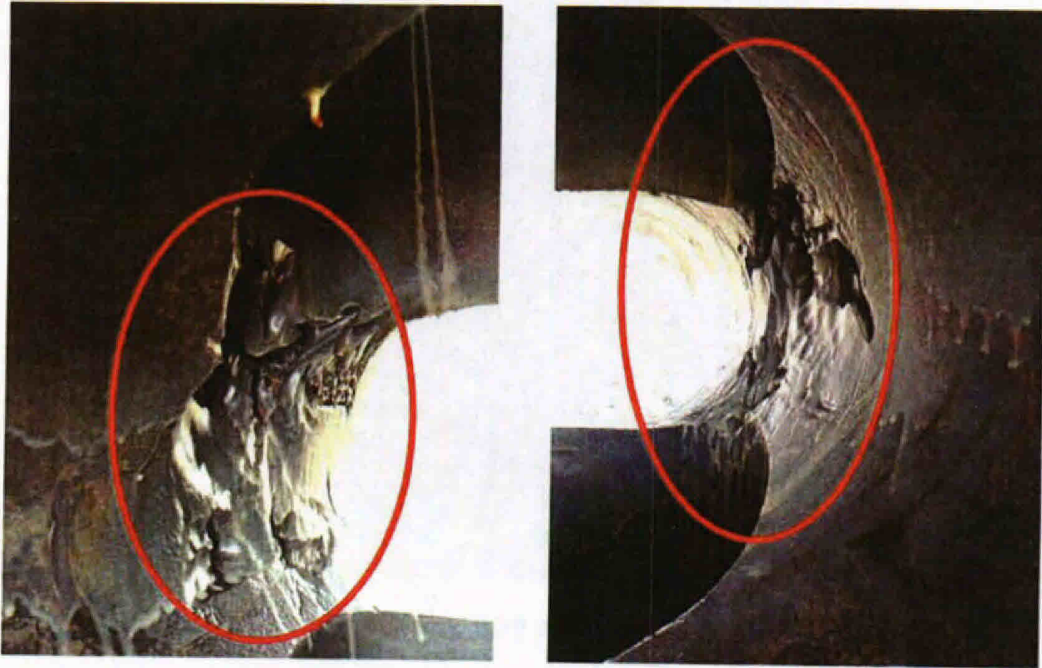


Figure D-6. BSR Housing

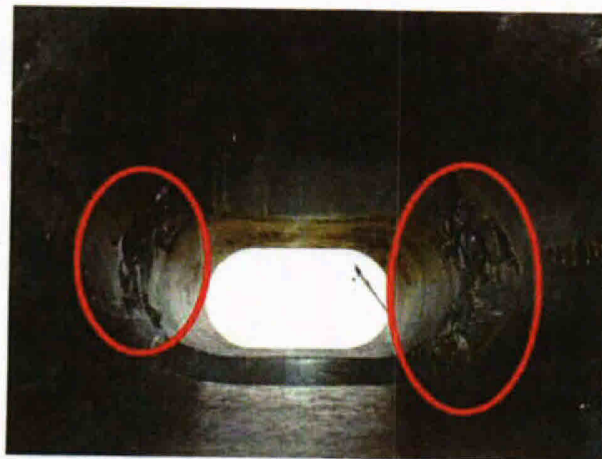


Figure D-7. BSR Housing

4. There was no other obvious damage to the bore of the BOP (see Figure D-8).

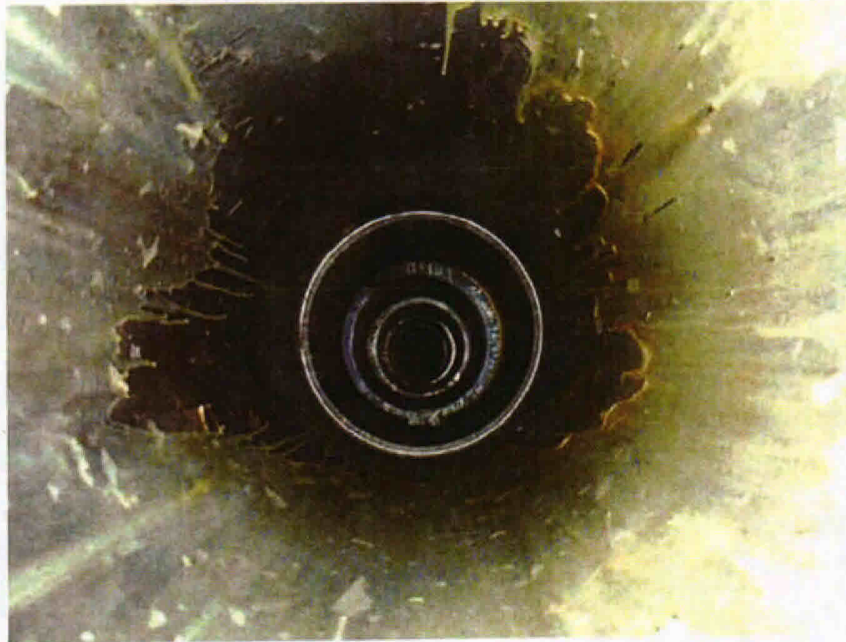


Figure D-8. BOP Main Bore

5. The holes at the kink (see Figure D-9) were caused by erosion resulting from the flow in the gaps on either side of each piece of the two squashed pieces of drill pipe that were trapped in the kink. Other parts of the riser also showed limited signs of erosion, suggesting that the flow cross-sectional area was reasonably large compared to that at the kink. Video evidence¹ shows the start of the kink leaks on 28th April 2010 at 15:33. The erosion of the one-inch thick riser wall therefore occurred over the period between 10:22 on 22 April 2010, when the DWH sank, and the time of the start of the kink leaks. This equates to an average rate of erosion of approximately 1500 mm/yr (59 in/yr) which suggests solids present in the flow.

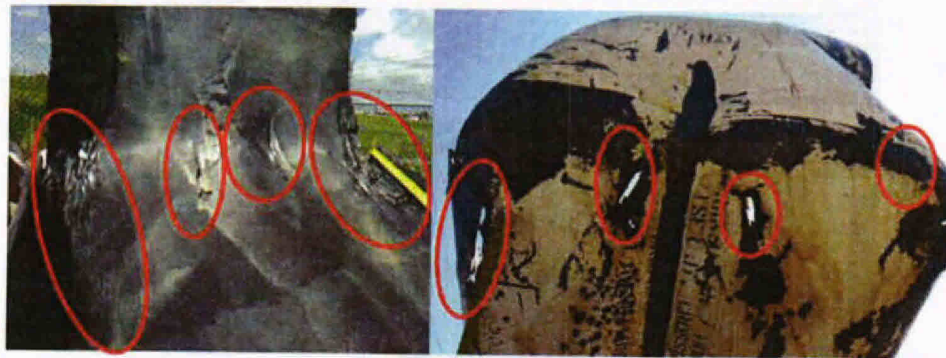


Figure D-9. Kink Erosion – Riser

¹ ROV footage BOS-7677 - OI3_Millennium42_DVD20_BOS-007677a.

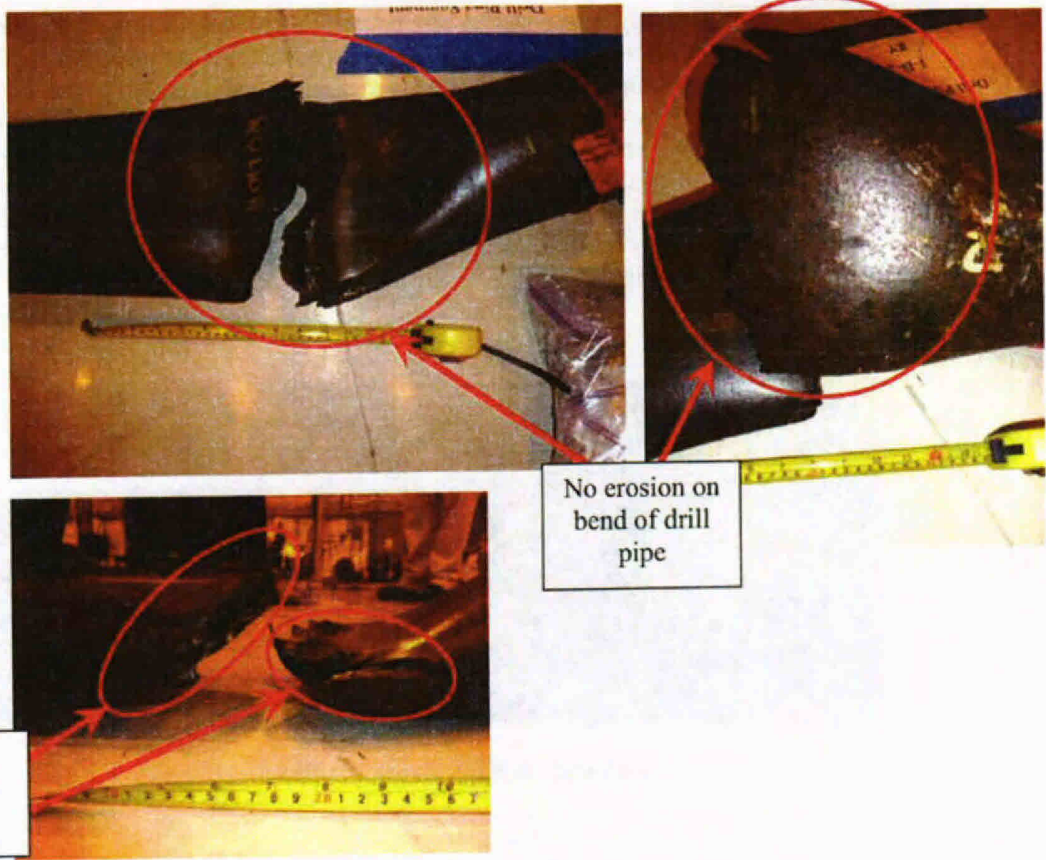


Figure D-10. Kink Erosion – Drill Pipe 1-B-2

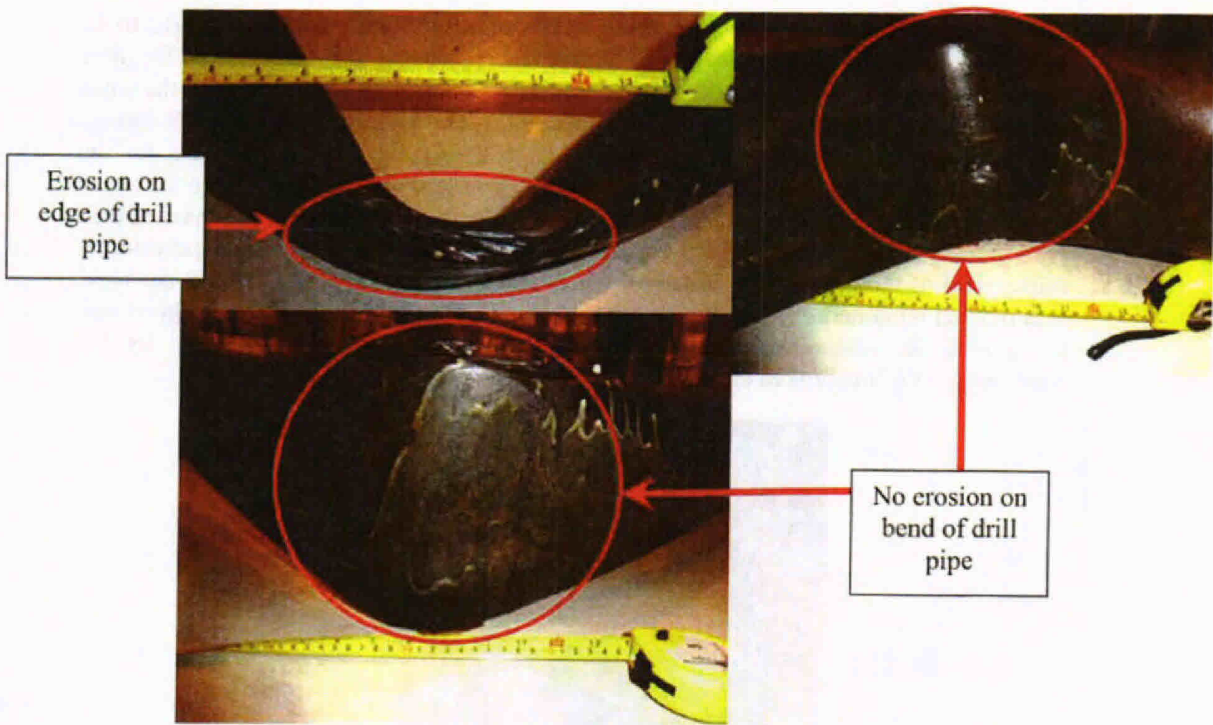


Figure D-11. Kink Erosion – Drill Pipe 1-A-1

6. There was erosion of the drill pipe at the VBRs and Test Ram (see Figures D-12 to D-14), suggesting that they were not fully sealing around the drill pipe all of the time through the incident (see the timeline of the ram closures in section 4.4 of the main report). The drill pipe in the well was detached at the Test Ram (pipe section 148 was the part at the bottom of the BOP that remained in the BOP). The likely cause for the detachment of the drill pipe is erosion of the pipe by the flow to a point where the stress on the pipe at the bottom of the BOP was greater than the yield stress.² The mass of drill pipe in the well is estimated as approximately 58,000 lb, and this would be expected to cause yield of the pipe at the Test Ram when approximately 20% of the cross-sectional area of steel remained. Also, examination of the end of the broken drill pipe suggests that the pipe broke sometime before the flow over it ceased. This is indicated by the smoothing off of the broken ends.

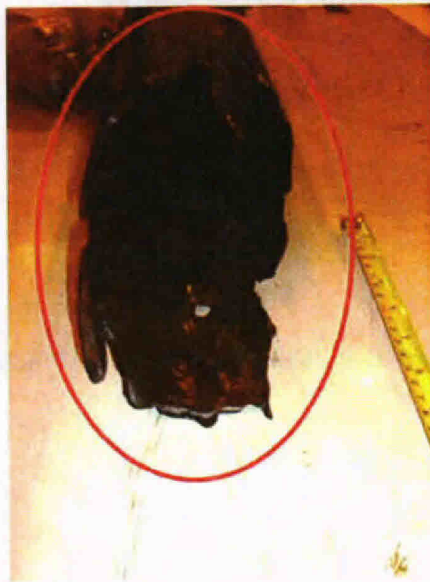


Figure D-12. Drill Pipe Erosion – Test Ram

² The yield stress of a material is the stress required to cause permanent deformation of the material and will lead to the material breaking if the stress continues to be applied.



Figure D-13. Drill Pipe Erosion – MVBR

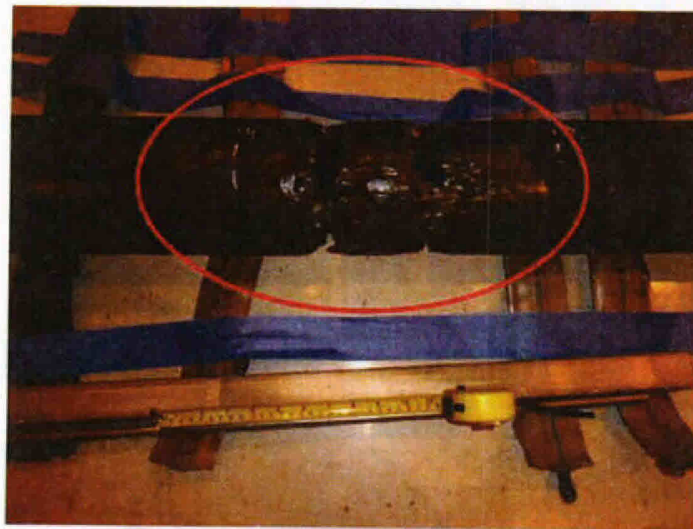


Figure D-14. Drill Pipe Erosion – UVBR

7. The VBRs were in pieces, and the polymer part of the VBRs missing (the polymer is assumed to have traveled downstream in the system, potentially causing blockages). Most of the VBR elements for the MVBR and UVBR were present (see Figure D-16), but only two of the Test Ram elements were present. This suggests that the Test Ram fell apart *in situ*. Most of the Test Ram elements were not recovered.



Figure D-15. A VBR – OEM Example

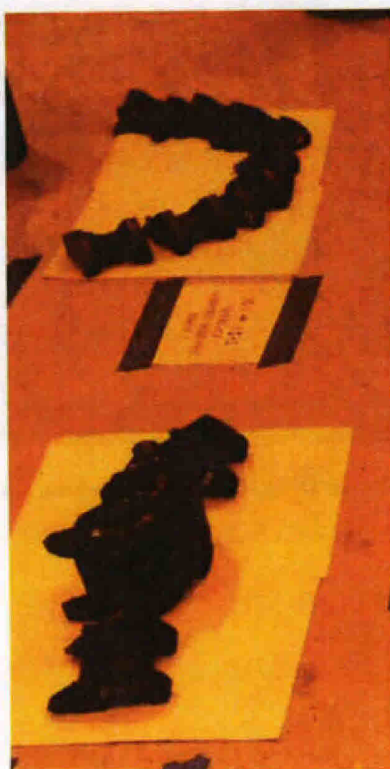


Figure D-16. MVBR (bottom) and UVBR Elements

8. Figure D-17 shows a VBR/Test Ram element and some top kill material that were found jammed approximately one foot up inside pipe section 148 (*i.e.*, just above where the pipe broke). It is likely that this element came from the Test Ram. This suggests that the Test Ram disintegrated after the drill pipe broke. An estimate of the stream velocity required to lift a VBR/Test Ram element gives a result of between 3 m/s and 5 m/s, depending on the assumptions of drag on the element. From the Maximus model, the velocity in the casing below the drill pipe is 6.5 m/s but immediately below the BOP the velocity around the drill pipe is about 22 m/s and in the drill pipe is about 14 m/s. Therefore, it is unlikely that VBR/Test Ram elements would have fallen down the well while it was flowing, suggesting the idea that the VBR/Test Ram element jammed in the drill pipe 148 is from the Test Ram.

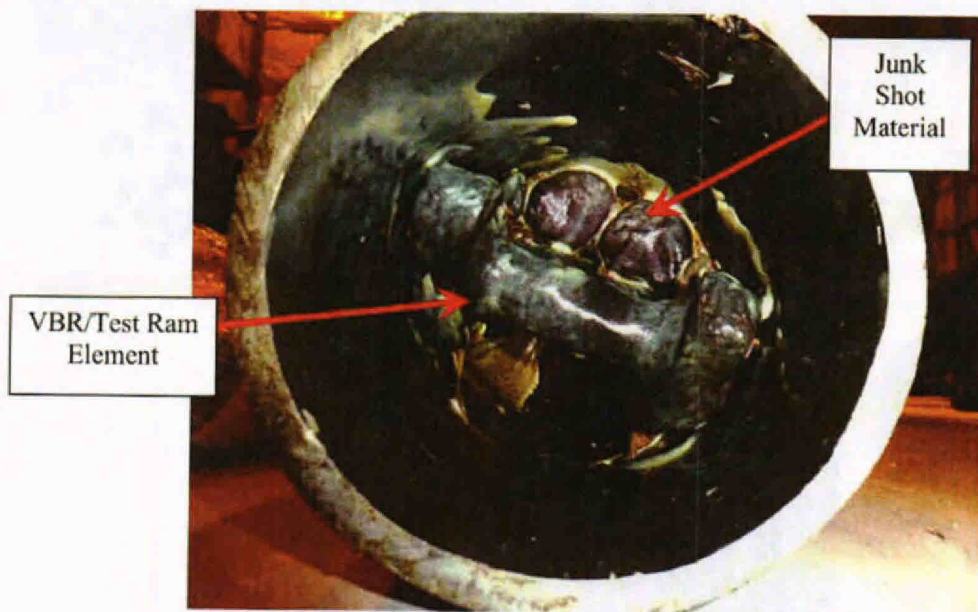


Figure D-17. VBR/Test Ram Element in Pipe 148

9. Top Kill material was found above the jammed VBR/Test Ram element, but below the CSR, in pipe section 148 (see Figure D-18). The junk shot material could have fallen back through the open CSR when flow ceased at the end of the incident, but this seems unlikely.³ It is more probable that the top kill material in pipe 148 arrived there during top kill and before the VBR/Test Ram element became jammed in the pipe. This, combined with the effectiveness of the Test Ram after top kill, as demonstrated by the fact that it continued to produce a considerable pressure drop when closed, suggests that the Test Ram did not disintegrate until some time after Top Kill. Also, some of the debris extracted from pipe section 148 (see Figure D-18, top left) had the appearance of cement suggesting that changes were occurring at bottom hole late into the incident.



Figure D-18. Material Between Test Ram Element and CSR

³ This would have required the drill pipe to be in just the right position below a partially open CSR for this to occur.

10. The CSR rams were open until activated on 29th April 2010. There was a clear circular erosion pattern where flow had been traveling up the drill-pipe below the CSR and impinging on the bottom of the upper CSR ram.

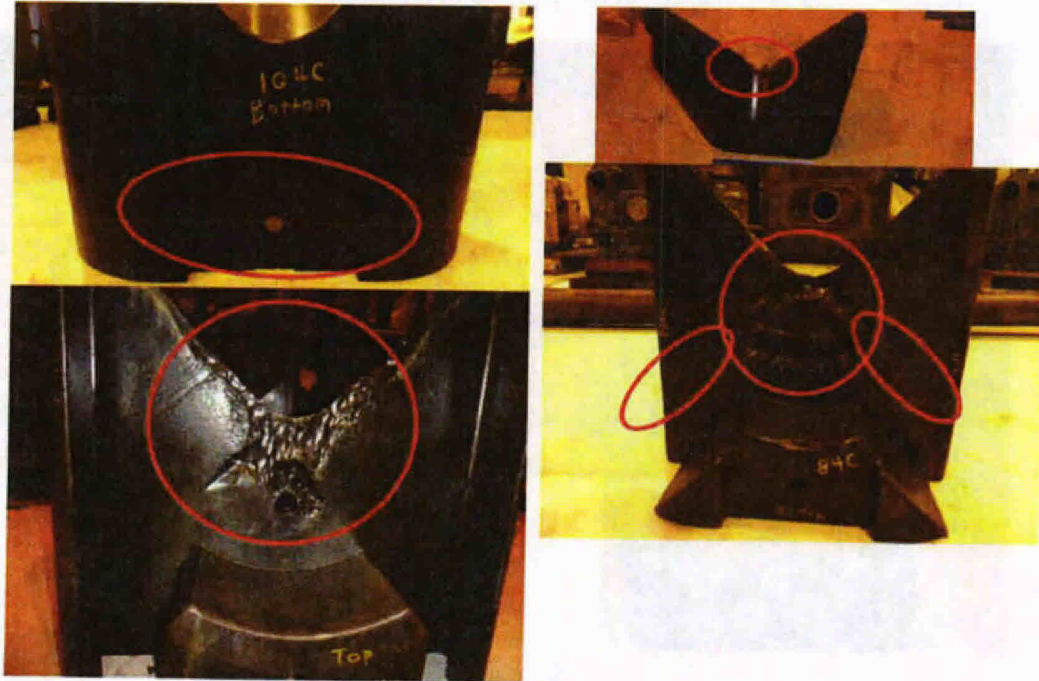


Figure D-19. CSR Rams

11. There was erosion on the BSR rams (see Figure D-20) as well as housing around the BSR rams – see Figures D-6 and D-7 above. Again, this is likely due to the fact that the BSR latched (almost) closed so the flow path was restricted. It is likely that the restriction of the BSR would have changed over the period of the incident.



Figure D-20. BSR Rams

12. The seal on the base of top hat had disintegrated but there were no signs of erosion on the top hat (see Figure D-21) suggesting that velocities at the top hat skirt were low.



Figure D-21. Top Hat and Seal

13. The LAP only showed signs of normal wear and tear (it was not closed during the incident). The elastomer of the UAP was destroyed and the fingers suffered limited damage due to erosion. Figure D-22 shows the elements of the UAP arranged in the as-built order. The elastomer parts could have formed blockages in the BOP and riser and these blockages could have changed with time.

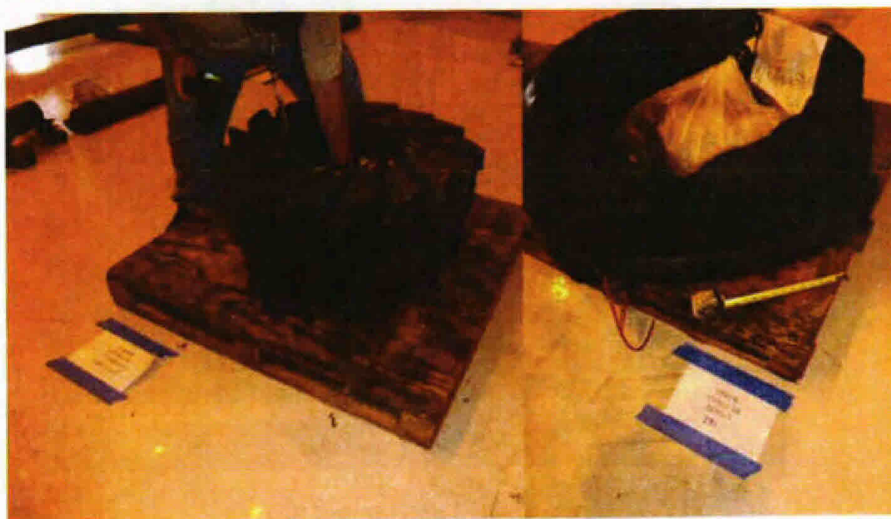


Figure D-22. UAP Elements (arranged in as-built order) and UAP Donut



Figure D-23. OEM UAP Sample

14. It is likely that the UAP formed a significant restriction when first closed (as evidenced by the erosion of the drill pipe at the UAP position). However, when recovered, the UAP was in separate pieces with obvious damage to elastomer parts. Given the flowpaths that must have existed through the UAP at some period in the incident, it is not believed that the UAP formed a significant restriction throughout the whole incident.

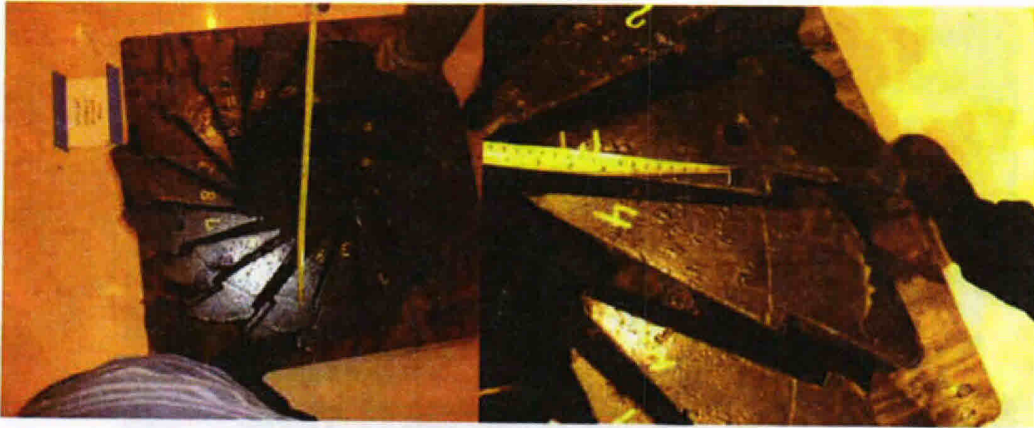


Figure D-24. UAP Element Erosion Patterns

15. There was uniform erosion of the inside of the casing hanger (see Figure D-25). The outside of the casing hanger and casing (see Figures D-25 and D-26) were in pristine condition (apart from light rust) suggesting that there was no (or minimal) flow on the outside of the casing. My conclusion is therefore that the flow was not in the annulus outside of the casing.

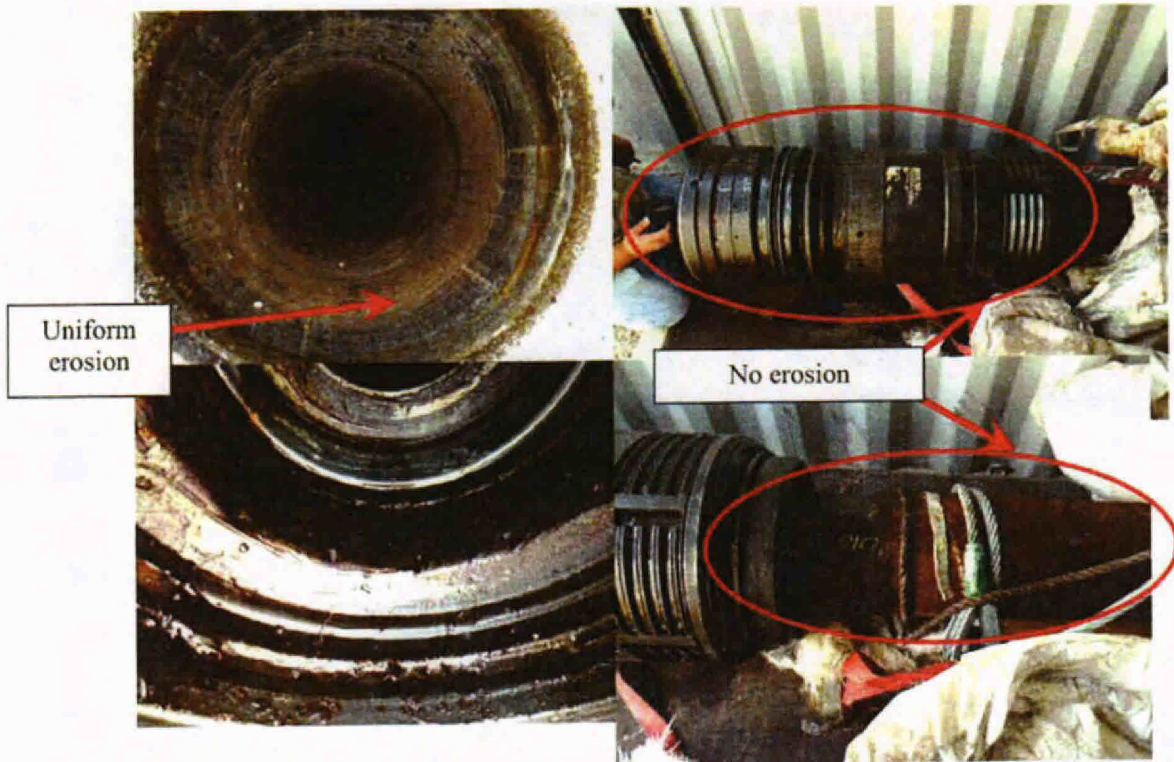


Figure D-25. Inside and Outside of Casing Hanger

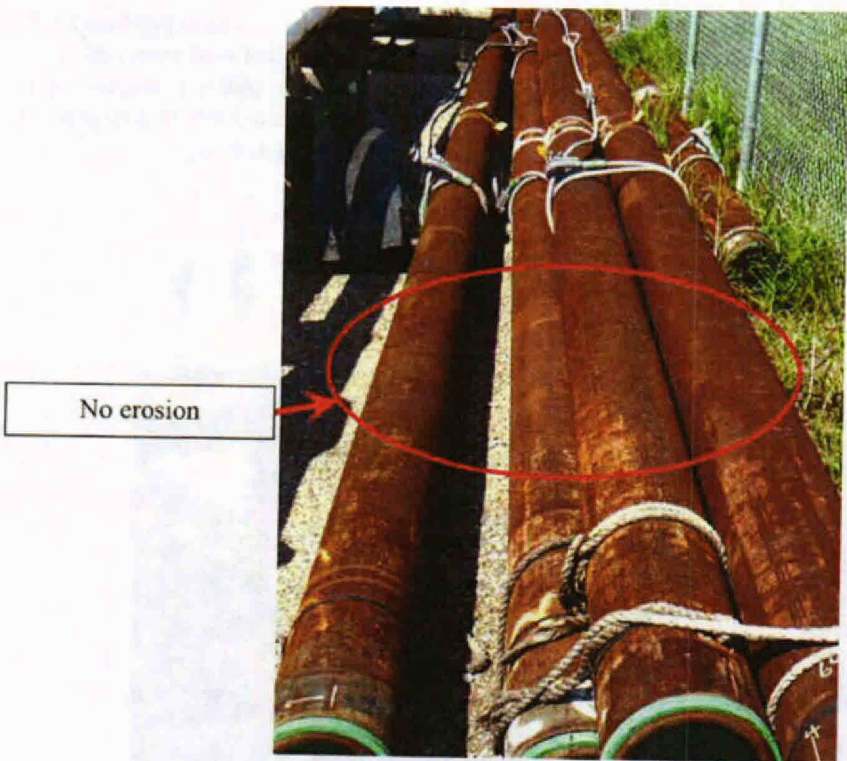


Figure D-26. Outside of Casing

16. The RITT was reported to have been damaged during insertion and thus produced little restriction of the flow out of the end of the fallen riser. The RITT as received at the evidence yard (see Figure D-27) had none of the polymer discs, put in place during its manufacture to limit the amount of oil escaping from the end of the riser, still in place. It is likely that discs were either damaged during insertion or during service.

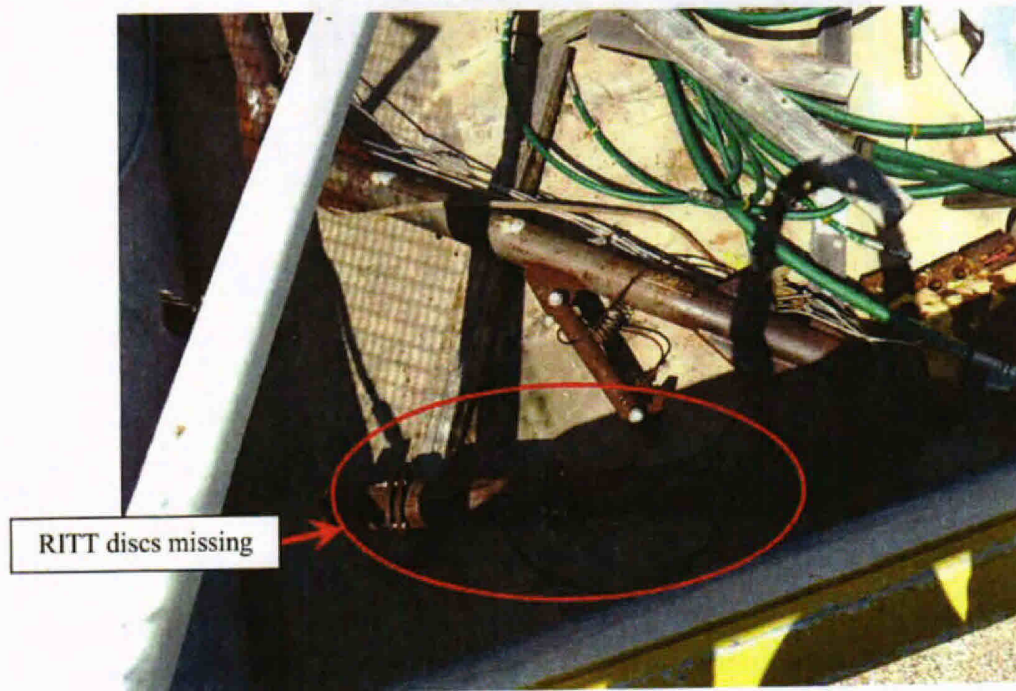


Figure D-27. RITT

The implications from the examination of the evidence at Michoud are:

1. Flow path through the well, BOP, and riser/drill-pipe is not constant through time.
2. There were many sources of blockage material, which could explain variations in PTB readings. Disintegration of the VBRs/Test Ram and the UAP, along with the top kill materials, could explain changes in apparent blockages and variations in the PTB readings.
3. The BSR erosion (rams and housing) was the most severe for all the metal BOP parts recovered. This erosion suggests changing restrictions to flow.
4. The drill pipe broke at the bottom of the BOP before the flow ended on 15th July 2010.
5. There was no, or at most minimal, flow on the outside of the casing, suggesting the flow path was not on the outside of the casing.
6. The RITT did not greatly restrict flow from the end of the fallen riser, at least for some of the time it was used, as the polymer discs were totally absent from the recovered item.
7. The average rate of erosion of the riser wall at the kink was approximately 1500 mm/yr (59 in/yr) which suggests solids presence in the flow.

Appendix E

Evaluation of Dr. Dykhuizen's Top Kill Calculations

This appendix presents an evaluation of Dr. Dykhuizen's calculations of a lower bound oil flow rate based on BOP pressure data and mud flow rate. Dr. Dykhuizen's analysis ignores better top kill data available for 26th May 2010, a period during which junk shot material had not yet been used in the top kill procedures. To correct Dr. Dykhuizen's calculations, I first updated the mixture densities using Multiflash and volume factors for 28th May 2010. Second, I repeated Dr. Dykhuizen's 28th May 2010 calculations using his own densities and the new Multiflash densities. Finally, I recalculated the lower bound flow rate for the top kill attempt on 26th May 2010.

Calculation for 28th May 2010 Top Kill Period

Table E-1 presents a comparison of the values used by Dr. Dykhuizen in his calculations and those I obtained via Multiflash.

	PT-B	P_amb	Temp	Dr. Dykhuizen's Results			Results Using Multiflash			Mud den.
				Mix inlet den.	Mix outlet den.	Eff. Mix den.	Mix inlet den.	Mix outlet den.	Eff. Mix den.	
	psia	psia	°F	kg/m ³	kg/m ³	kg/m ³	kg/m ³	kg/m ³	kg/m ³	kg/m ³
Normal Time	4350	2200	200	518	326	411	472	305	359	-
Idle Time	3500	2200	200	461	326	388	422	305	380	-
Kill Time	5500	2200	74	642	464	546	594	424	502	1965

Table E-1. Comparison of Oil and Gas Mixture Densities During 28th May 2010 Top Kill Events

Table E-2 illustrates the different volume factors calculated for each of the periods identified by Dr. Dykhuizen in his report.¹ Note that I use the stock tank oil density (from Multiflash) of 851.6 kg/m³ (rather than 838 kg/m³ used by Dr. Dykhuizen) and mass fraction of stock tank oil (again from Multiflash) of 0.627 (rather than 0.65 used by Dr. Dykhuizen) to calculate the volume factor. I calculated the volume factor by flashing² the fluid from pressure and temperature conditions at the top kill period to stock tank (*i.e.*, standard) conditions. The

¹ These are defined on page 11 of Dr. Dykhuizen's report.

² Decreasing the pressure and temperature from the top kill conditions to the stock tank conditions.

resulting volume factor is the ratio of the oil present at top kill conditions and the oil present at stock tank conditions.

Period	Dr. Dykhuizen's Volume factor	Recalculated Volume factor
Normal Time	0.319	0.279
Idle Time	0.301	0.264
Kill Time	0.423	0.370

Table E-2. Volume Factor Comparison

Using equation 6 on page 13 of Dr. Dykhuizen's report, I calculated the flow rates in Table E-3 below.

	Dr. Dykhuizen's Flow Rate (stb/d)	Recalculated Flow rate (stb/d)
Idle time	47,753	43,580
Normal Time (<i>i.e.</i> , corrected for increased PT-B pressure) ³	43,170	39,397

Table E-3. Comparison of Calculations of Zero Flow Estimates

Calculation for 26th May 2010 Top Kill Period

Dr. Dykhuizen's analysis uses data from 28th May 2010, a period which includes the presence junk shot material. The purpose of junk shot material is to block the BOP and restrict flow. As a result, the presence of junk shot material would be expected to have a significant effect on the loss coefficient through the BOP, greatly increasing the uncertainty and error bands on calculations that rely on these data. Dr. Dykhuizen ignores better top kill data available for 26th May 2010, a period during which junk shot material had not yet been used in the top kill procedures. Figure E-1, below, illustrates the PT-B readings (corrected using the BP PT-B correction of +966 psi) along with the mud flow rates associated with the 26th May 2010 top kill attempt.⁴

³ I corrected for higher PT-B pressure at normal time consistent with Dr. Dykhuizen's approach in his report on page 15.

⁴ Houston rev 1 (BP-HZN-2179MDL05723217) (native).



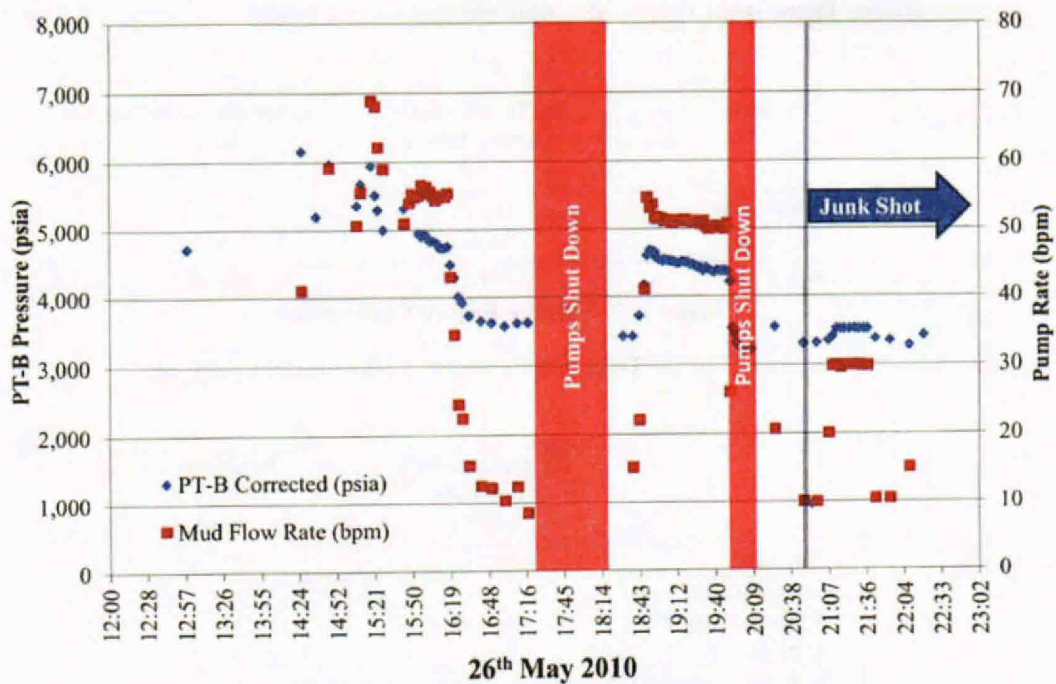


Figure E-1. PT-B Readings and Mud Flow Rates

The highlighted regions (red) in Figure E-1 indicate times at which the mud pumps were shut down. The blue line and arrow indicate times at which junk shot were introduced into the BOP.⁵

On 26th May 2010, within the period 18:55 - 19:50, the PT-B readings and mud flow rates are fairly steady. I repeated Dr. Dykhuizen's calculations for the pressures and flow rates recorded for one of the data points from this period. The data point I selected is 19:22 on 26th May 2010, a data point approximately half-way through the period, with a PT-B reading of 4660 psia and mud flow rate of 51 bpm. These PT-B readings and mud flow rates are representative of this period.

⁵ Ref. Houston rev 1 (BP-HZN-2179MDL05723217) (native).



Table E-4 presents a comparison of pressure, temperature and density values calculated from Dr. Dykhuizen's spreadsheet and those I obtained via Multiflash for the 26th May 2010 top kill attempt.

	PT-B	P_amb	Temp	Results Using Dr. Dykhuizen's Method			Results Using Multiflash			Mud den.
				Mix inlet den.	Mix outlet den.	Eff. Mix den.	Mix inlet den.	Mix outlet den.	Eff. Mix den.	
	psia	psia	°F	kg/m ³	kg/m ³	kg/m ³	kg/m ³	kg/m ³	kg/m ³	kg/m ³
Normal Time	4350	2200	200	518	326	411	472	305	359	-
Idle Time	3500	2200	200	461	326	388	422	305	380	-
Kill Time	4460	2200	90	618	437	519	562	401	475	1965

Table E-4. Oil Densities Comparison During 26th May 2010 Top Kill Events

Table E-5 illustrates the different volume factors calculated for each of the periods identified by Dr. Dykhuizen in his report.⁶ As with my recalculations of Dr. Dykhuizen's 28th May 2010 results, I use the stock tank oil density (from Multiflash) of 851.6 kg/m³ (rather than 838 kg/m³ used by Dr. Dykhuizen) and mass fraction of stock tank oil (again from Multiflash) of 0.627 (rather than 0.65 used by Dr. Dykhuizen) to calculate the volume factor.

	Dr. Dykhuizen's Volume factor	Recalculated Volume factor
Normal Time	0.319	0.279
Idle Time	0.301	0.264
Kill Time	0.403	0.349

Table E-5. Volume Factor Comparison

⁶ These are defined on page 11 of Dr. Dykhuizen's report.

Using equation 6 from page 13 of Dr. Dykhuizen's report, I calculated the lower bound flow rate results for 26th May 2010 shown in Table E-6.

	Dr. Dykhuizen's Flow Rate (stb/d)	Recalculated Flow rate (stb/d)
Idle time	36,164	33,003
Normal Time (<i>i.e.</i> , corrected for increased PT-B pressure) ⁷	32,693	29,835

Table E-6. Comparison of Calculations of Zero Flow Estimates

⁷ I corrected for higher PT-B pressure at normal time consistent with Dr. Dykhuizen's approach in his report on page 15.

Appendix F

Ambient Sea Pressures

The calculation of flow rates requires the use of accurate ambient sea pressures. Dr. Dykhuizen's, Dr. Griffiths' and my calculations all rely on ambient sea pressure as an important input. However, from the values presented by Dr. Dykhuizen and Dr. Griffiths in their respective reports it appears that they are not using the most accurate data for determining these pressures.

Calculation of an accurate sea pressure requires knowledge of the sea water density and the depths of key points on the BOP and riser including, for example, fallen riser exit, kink leak, BOP pressure gauges, and riser cut at the top of the LMRP.¹ I determined sea water density for my sea pressure calculation from the highly accurate Paroscientific pressure sensor and depth data obtained in August 2010.² The density was calculated according to the following equation:

$$\rho_s = \frac{P_s - P_a}{h_w \cdot g} \quad (F1)$$

Where:

- ρ_s is the average sea water density
- P_s is the ambient sea pressure
- P_a is the atmospheric pressure at the sea surface
- h_w is the depth of water to the key points
- g is acceleration due to gravity

The average readings for the Paroscientific pressure sensors are shown in Table F-1.

Depth (ft)	Pressure at Depth (psia)	Coincident Surface Pressure sensor (psia)
4915.77	2193.73	15.45
4908.73	2190.61	15.46
0	14.92	15.67

Table F-1. Paroscientific Averaged Pressure Readings

Based on the surface pressure sensor readings illustrated in Table F-1, I calculated the atmospheric pressure relative to the pressure sensor that was mounted on the ROV. The atmospheric pressure relative to the pressure sensor on the ROV is necessary to account for the

¹ BP-HZN-2179MDL01945241 - Copy of Pressure measurement reconciliation rev 3.

² MDL 2179 Deposition Exhibit 8682. The Paroscientific pressure gauge was mounted on an ROV, controlled from the *MSV Olympic Challenger*, and the depth gauge for the readings was taken from the UHD31 depth gauge on the ROV.

effects of changing atmospheric pressure on the Paroscientific readings on the ROV. The average atmospheric pressure relative to the pressure sensor on the ROV is 14.70 psia.³

I calculated the average seawater density as 1022.1 kg/m³. The Paroscientific averaged pressure readings at two depths are plotted in Figure F-1, along with the calculated ambient pressures at various locations associated with the equipment at the top of the well.

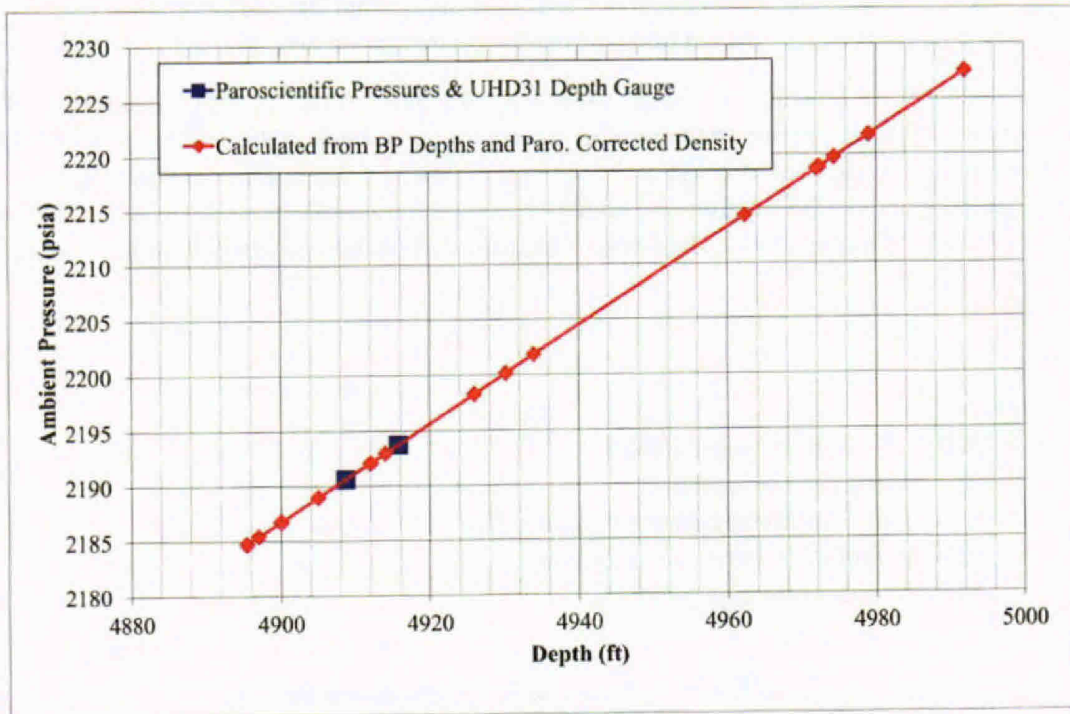


Figure F-1. Calculated Ambient Sea Pressures and Paroscientific Average Pressure Data

Based on my calculated average sea water density and the known depth at the key points, I calculated the ambient sea pressure at the key points by the following equation:

$$P_s = P_a + (h_w \cdot \rho_s \cdot g) \quad (F2)$$

The depths and resulting ambient sea pressures that I calculated are given in Table F-2. The calculations in Table F-2 assumes that the end of the drill pipe is 10 feet above the seabed (at the end of riser location), and the end of the fallen riser has self-excavated by 2 feet.

³ This value is slightly lower than the coincident sensor values in Table F-1 due to a slight offset between the surface Paroscientific reading and the ROV Paroscientific reading.

Location	Water Depth		Water Column Pressure	Ambient Pressure
	ft	m	psi	psia
Sea surface	0.0	0.0	0.0	14.7
Point 1 Along Riser	4895.5	1492.1	2170.0	2184.7
Capping Stack Choke Line Exit	4897.0	1492.6	2170.7	2185.4
Top of Capping Stack	4900.0	1493.5	2172.0	2186.7
Capping Stack Kill Line Exit	4905.0	1495.0	2174.3	2189.0
Capping Stack Body Pressure, PT-3K-2	4912.0	1497.2	2177.4	2192.1
Pancake Flange	4914.0	1497.8	2178.2	2192.9
Riser Kink	4930.2	1502.7	2185.4	2200.1
Riser Adapter Flange	4926.0	1501.4	2183.6	2198.3
PT-M	4934.0	1503.9	2187.1	2201.8
End of drill pipe	4962.4	1512.5	2199.7	2214.4
Bottom of BOP Pressure, PT-B	4972.0	1515.5	2204.0	2218.7
Seabed at End of Drill Pipe and Riser	4972.4	1515.6	2204.1	2218.8
End of Riser	4974.4	1516.2	2205.0	2219.7
Top of Wellhead	4979.0	1517.6	2207.1	2221.8
Seabed at BOP	4992.0	1521.6	2212.8	2227.5

Table F-2. Calculated Ambient Sea Pressures and Depths

Appendix G

Pressure Calculations Near the Bottom Hole

This appendix provides the result of calculations using the Maximus model to calculate pressures in the casing at a depth of 18,056 ft TVD (True Vertical Depth). These calculations were performed for various pressures at the top of the well and assumed well flow rates. Input data was given in terms of top of well pressure (PT-B) at various times and assumed flow rates at different times. The pressure results were generated for each PT-B pressure time. The pressure at the depth of 18,056 ft was calculated in Maximus using the OLGAS 2 phase correlation. Frictional and gravitational pressure losses up the well were calculated taking into account the flow regime predicted by OLGAS. There were two flowpaths in the well, one up the casing and the other up the drill pipe within the casing. The frictional and gravitational pressure losses in each of these flow paths were calculated and these added to the PT-B pressure to arrive at a pressure at the depth of 18,056 ft.

These cases are grouped in two batches, called "OPTION 1" and "OPTION 2". Both files have the same format and are called "OPTION1 P and Q for Translation (26-04-13) with BHPs.xlsx" and "OPTION2 P and Q for Translation (26-04-13) with BHPs.xlsx". Calculations were done using the Maximus model described in Appendix C of my report with the following changes:

- Simulations for times before 15th July 2010 were done assuming steady state, with a U value (the overall heat transfer coefficient defining the rate of energy loss from the well to its surroundings) changing with time to represent the warm-up of the well.
- For the last day of the incident, as the well is being shut-in over a relatively short duration compared to the thermal dynamics of wells, it was assumed that the well was constantly warm throughout this day. For this day the temperature profile of the well was set to the steady state temperature profile of a high flow rate (the first time on 15th July 2010). This was called the "warm well" assumption and was done by setting the ambient temperature to the target temperature profile and setting the overall heat transfer coefficient of the casing to a high value (200 BTU/hr/ft²/°F).

The Excel files for these cases are in the following format:

Input:

- Column F gives the times.
- Column G gives the pressure at top of the well.
- Column N gives the well flow rate.

Output:

- Column H gives the pressure at 18,056 ft TVD assuming the Drill Pipe High geometry, as described in Appendix C of my report.
- Column I gives the pressure at 18,056 ft TVD assuming the Drill Pipe Low geometry, as described in Appendix C of my report.

Appendix H

Materials Considered

Produced Documents

AE-HZN-2179MDL00060126
AE-HZN-2179MDL00064585
AE-HZN-2179MDL00078658
BP-HZN-2179MDL00004086
BP-HZN-2179MDL00063016
BP-HZN-2179MDL00063084
BP-HZN-2179MDL00154331
BP-HZN-2179MDL00161580
BP-HZN-2179MDL00255269
BP-HZN-2179MDL00255270
BP-HZN-2179MDL00255271
BP-HZN-2179MDL00258893
BP-HZN-2179MDL00269156
BP-HZN-2179MDL00309089
BP-HZN-2179MDL00322248
BP-HZN-2179MDL00328855
BP-HZN-2179MDL00330291
BP-HZN-2179MDL00331248
BP-HZN-2179MDL00412974
BP-HZN-2179MDL00427260
BP-HZN-2179MDL00477088
BP-HZN-2179MDL01088589
BP-HZN-2179MDL01088594
BP-HZN-2179MDL01513892
BP-HZN-2179MDL01514053
BP-HZN-2179MDL01514072
BP-HZN-2179MDL01530342
BP-HZN-2179MDL01567488
BP-HZN-2179MDL01594162
BP-HZN-2179MDL01608483
BP-HZN-2179MDL01608973
BP-HZN-2179MDL01644245
BP-HZN-2179MDL01872218
BP-HZN-2179MDL01945241
BP-HZN-2179MDL02172464
BP-HZN-2179MDL02208359
BP-HZN-2179MDL02355409
BP-HZN-2179MDL02393883
BP-HZN-2179MDL03198892
BP-HZN-2179MDL03349164
BP-HZN-2179MDL03676655

BP-HZN-2179MDL03742328
BP-HZN-2179MDL03807359
BP-HZN-2179MDL03830472
BP-HZN-2179MDL04366973
BP-HZN-2179MDL04440100
BP-HZN-2179MDL04440168
BP-HZN-2179MDL04440192
BP-HZN-2179MDL04440249
BP-HZN-2179MDL04440262
BP-HZN-2179MDL04440263
BP-HZN-2179MDL04440268
BP-HZN-2179MDL04440368
BP-HZN-2179MDL04440382
BP-HZN-2179MDL04440456
BP-HZN-2179MDL04440466
BP-HZN-2179MDL04440557
BP-HZN-2179MDL04440584
BP-HZN-2179MDL04440613
BP-HZN-2179MDL04440614
BP-HZN-2179MDL04440689
BP-HZN-2179MDL04440732
BP-HZN-2179MDL04440733
BP-HZN-2179MDL04440775
BP-HZN-2179MDL04440804
BP-HZN-2179MDL04440968
BP-HZN-2179MDL04440969
BP-HZN-2179MDL04440977
BP-HZN-2179MDL04440978
BP-HZN-2179MDL04549798
BP-HZN-2179MDL04549799
BP-HZN-2179MDL04569961
BP-HZN-2179MDL04569964
BP-HZN-2179MDL04569966
BP-HZN-2179MDL04578057
BP-HZN-2179MDL04784574
BP-HZN-2179MDL04799584
BP-HZN-2179MDL04802942
BP-HZN-2179MDL04824968
BP-HZN-2179MDL04826982
BP-HZN-2179MDL04830442
BP-HZN-2179MDL04830628
BP-HZN-2179MDL04833555
BP-HZN-2179MDL04833558
BP-HZN-2179MDL04833559
BP-HZN-2179MDL04833560
BP-HZN-2179MDL04833561
BP-HZN-2179MDL04833562
BP-HZN-2179MDL04833563

BP-HZN-2179MDL04833564
BP-HZN-2179MDL04833565
BP-HZN-2179MDL04833566
BP-HZN-2179MDL04833567
BP-HZN-2179MDL04833568
BP-HZN-2179MDL04833569
BP-HZN-2179MDL04833570
BP-HZN-2179MDL04833571
BP-HZN-2179MDL04833572
BP-HZN-2179MDL04833573
BP-HZN-2179MDL04833574
BP-HZN-2179MDL04833575
BP-HZN-2179MDL04834293
BP-HZN-2179MDL04851876
BP-HZN-2179MDL04869503
BP-HZN-2179MDL04877807
BP-HZN-2179MDL04884261
BP-HZN-2179MDL04884262
BP-HZN-2179MDL04884263
BP-HZN-2179MDL04884264
BP-HZN-2179MDL04884268
BP-HZN-2179MDL04897017
BP-HZN-2179MDL04908488
BP-HZN-2179MDL04908567
BP-HZN-2179MDL04910290
BP-HZN-2179MDL04920969
BP-HZN-2179MDL04926107
BP-HZN-2179MDL04926108
BP-HZN-2179MDL04927171
BP-HZN-2179MDL04931374
BP-HZN-2179MDL04934351
BP-HZN-2179MDL04940401
BP-HZN-2179MDL04996564
BP-HZN-2179MDL04996568
BP-HZN-2179MDL04996569
BP-HZN-2179MDL04996572
BP-HZN-2179MDL04996573
BP-HZN-2179MDL04996574
BP-HZN-2179MDL04996575
BP-HZN-2179MDL04996576
BP-HZN-2179MDL04996577
BP-HZN-2179MDL05022893
BP-HZN-2179MDL05048308
BP-HZN-2179MDL05058495
BP-HZN-2179MDL05086823
BP-HZN-2179MDL05086932
BP-HZN-2179MDL05187231
BP-HZN-2179MDL05187232

BP-HZN-2179MDL05368302
BP-HZN-2179MDL05497207
BP-HZN-2179MDL05497212
BP-HZN-2179MDL05497215
BP-HZN-2179MDL05698790
BP-HZN-2179MDL05698791
BP-HZN-2179MDL05723217
BP-HZN-2179MDL05728432
BP-HZN-2179MDL05735114
BP-HZN-2179MDL05758379
BP-HZN-2179MDL05758380
BP-HZN-2179MDL05782192
BP-HZN-2179MDL05782193
BP-HZN-2179MDL05782198
BP-HZN-2179MDL05796332
BP-HZN-2179MDL05809601
BP-HZN-2179MDL05809602
BP-HZN-2179MDL05830311
BP-HZN-2179MDL05861781
BP-HZN-2179MDL05871047
BP-HZN-2179MDL06004627
BP-HZN-2179MDL06005945
BP-HZN-2179MDL06005948
BP-HZN-2179MDL06005969
BP-HZN-2179MDL06009619
BP-HZN-2179MDL06089077
BP-HZN-2179MDL06094683
BP-HZN-2179MDL06096211
BP-HZN-2179MDL06096290
BP-HZN-2179MDL06096346
BP-HZN-2179MDL06096360
BP-HZN-2179MDL06099691
BP-HZN-2179MDL06099692
BP-HZN-2179MDL06099693
BP-HZN-2179MDL06099694
BP-HZN-2179MDL06114509
BP-HZN-2179MDL06123290
BP-HZN-2179MDL06124324
BP-HZN-2179MDL06124325
BP-HZN-2179MDL06124348
BP-HZN-2179MDL06144176
BP-HZN-2179MDL06314451
BP-HZN-2179MDL06330450
BP-HZN-2179MDL06336851
BP-HZN-2179MDL06393411
BP-HZN-2179MDL06424832
BP-HZN-2179MDL06474846
BP-HZN-2179MDL06475244

BP-HZN-2179MDL06536400
BP-HZN-2179MDL06599701
BP-HZN-2179MDL06599702
BP-HZN-2179MDL06666023
BP-HZN-2179MDL06741948
BP-HZN-2179MDL06742178
BP-HZN-2179MDL06742179
BP-HZN-2179MDL06742232
BP-HZN-2179MDL06742233
BP-HZN-2179MDL06742234
BP-HZN-2179MDL06742238
BP-HZN-2179MDL06742239
BP-HZN-2179MDL06742608
BP-HZN-2179MDL06742609
BP-HZN-2179MDL06742613
BP-HZN-2179MDL06742614
BP-HZN-2179MDL06742720
BP-HZN-2179MDL06742721
BP-HZN-2179MDL06742965
BP-HZN-2179MDL06742966
BP-HZN-2179MDL06742968
BP-HZN-2179MDL06742969
BP-HZN-2179MDL06742970
BP-HZN-2179MDL06742973
BP-HZN-2179MDL06742974
BP-HZN-2179MDL06743166
BP-HZN-2179MDL06743280
BP-HZN-2179MDL06743284
BP-HZN-2179MDL06743478
BP-HZN-2179MDL06743479
BP-HZN-2179MDL06743482
BP-HZN-2179MDL06744009
BP-HZN-2179MDL06744010
BP-HZN-2179MDL06744011
BP-HZN-2179MDL06744066
BP-HZN-2179MDL06744067
BP-HZN-2179MDL06744204
BP-HZN-2179MDL06744773
BP-HZN-2179MDL06744880
BP-HZN-2179MDL06744882
BP-HZN-2179MDL06744883
BP-HZN-2179MDL06744884
BP-HZN-2179MDL06744885
BP-HZN-2179MDL06744992
BP-HZN-2179MDL06745326
BP-HZN-2179MDL06745327
BP-HZN-2179MDL06745329
BP-HZN-2179MDL06746267

BP-HZN-2179MDL06746268
BP-HZN-2179MDL06890645
BP-HZN-2179MDL06902305
BP-HZN-2179MDL06903151
BP-HZN-2179MDL06907946
BP-HZN-2179MDL06907947
BP-HZN-2179MDL06907948
BP-HZN-2179MDL06907949
BP-HZN-2179MDL06947350
BP-HZN-2179MDL06947352
BP-HZN-2179MDL06947353
BP-HZN-2179MDL07001148
BP-HZN-2179MDL07001149
BP-HZN-2179MDL07014306
BP-HZN-2179MDL07014311
BP-HZN-2179MDL07014314
BP-HZN-2179MDL07033640
BP-HZN-2179MDL07066615
BP-HZN-2179MDL07114100
BP-HZN-2179MDL07119924
BP-HZN-2179MDL07119926
BP-HZN-2179MDL07129522
BP-HZN-2179MDL07147962
BP-HZN-2179MDL07241912
BP-HZN-2179MDL07241913
BP-HZN-2179MDL07241914
BP-HZN-2179MDL07265827
BP-HZN-2179MDL07265866
BP-HZN-2179MDL07265901
BP-HZN-2179MDL07265944
BP-HZN-2179MDL07265965
BP-HZN-2179MDL07266071
BP-HZN-2179MDL07266154
BP-HZN-2179MDL07266155
BP-HZN-2179MDL07266172
BP-HZN-2179MDL07266193
BP-HZN-2179MDL07266256
BP-HZN-2179MDL07279438
BP-HZN-2179MDL07279439
BP-HZN-2179MDL07279440
BP-HZN-2179MDL07279441
BP-HZN-2179MDL07279442
BP-HZN-2179MDL07279443
BP-HZN-2179MDL07279444
BP-HZN-2179MDL07279445
BP-HZN-2179MDL07279446
BP-HZN-2179MDL07279447
BP-HZN-2179MDL07279448

BP-HZN-2179MDL07279449
BP-HZN-2179MDL07279450
BP-HZN-2179MDL07291675
BP-HZN-2179MDL07291679
BP-HZN-2179MDL07307994
BP-HZN-2179MDL07352418
BP-HZN-2179MDL07354167
BP-HZN-2179MDL07383106
BP-HZN-2179MDL07383107
BP-HZN-2179MDL07383108
BP-HZN-2179MDL07383109
BP-HZN-2179MDL07556778
BP-HZN-2179MDL07557142
BP-HZN-2179MDL07574314
BP-HZN-2179MDL07576153
BP-HZN-2179MDL07576154
BP-HZN-BLY00000001
BP-HZN-BLY00000194
BP-HZN-BLY00000195
BP-HZN-BLY00000201
BP-HZN-BLY00000202
BP-HZN-BLY00000203
BP-HZN-BLY00000204
BP-HZN-BLY00000208
BP-HZN-BLY00000220
BP-HZN-BLY00000232
BP-HZN-BLY00000237
BP-HZN-BLY00000242
BP-HZN-BLY00000276
BP-HZN-BLY00000304
BP-HZN-BLY00000371
BP-HZN-BLY00000373
BP-HZN-BLY00000375
BP-HZN-BLY00000384
BP-HZN-BLY00000386
BP-HZN-BLY00000393
BP-HZN-BLY00000402
BP-HZN-BLY00000407
BP-HZN-BLY00000526
BP-HZN-BLY00000586
BP-HZN-BLY00000593
BP-HZN-BLY00000597
BP-HZN-BLY00000758
BP-HZN-BLY00082874
BP-HZN-BLY00134336
BP-HZN-BLY00138899
BP-HZN-BLY00269184
BP-HZN-MBI00180471

BP-HZN-SEC00365348
BP-HZN-SEC00365349
CAM_CIV_0000116
CAM_CIV_0018107
CAM_CIV_0020865
CAM_CIV_0020866
CAM_CIV_0028270
CAM_CIV_0148046
DSE031-001794
IGS076-000671
IMV147-021123
LAL134-003719
LAL248-009068
LDX005-0023459
LNL067-006068
LNL075-013264
SDX009-0004236
SES-00065846
SNL007-003654
SNL007-006691
SNL007-006872
SNL007-006878
SNL007-013271
SNL007-013281
SNL007-013376
SNL007-013378
SNL007-013382
SNL007-013386
SNL007-013413
SNL007-014386
SNL007-014405
SNL007-014426
SNL008-014169
SNL008-014301
SNL022-007753
SNL043-005774
SNL043-005950
SNL043-007022
SNL043-007023
SNL043-007034
SNL043-007524
SNL044-002450
SNL046-000421
SNL046-082105
SNL059-000136
SNL061-007297
SNL066-013744
SNL075-004401

SNL086-006516
SNL087-001156
SNL087-001206
SNL087-015349
SNL088-072912
SNL105-014853
SNL105-014885
SNL109-004876
SNL110-002263
SNL110-002730
SNL111-002483
SNL111-002485
SNL129-004883
TRN-HCEC-00026904
TRN-INV-00008580
TRN-INV-00835166
TRN-INV-01275508
TRN-INV-01544188
TRN-INV-01871788
TRN-INV-01871789
TRN-INV-02887797
TRN-INV-02956057
TRN-MDL-01065224
TRN-MDL-01851720
WHOI-000752
WW-MDL-00022601
WW-MDL-00030514
BP Barcode BP-032413, Copy of DNV6M-V006 Video, Photolibrary_Houston_External HDD (previously made available to all parties on a sharepoint site)
BP Barcode BP-032631, DNV Data Copy of PM-V006, Video Photo Library BP-023634 (previously made available to all parties on a sharepoint site)
BP Barcode BP-032646, DVD Data, Copy of DNVMN-V006, Video Photolibrary_Houston_External HDD BP-023858 (previously made available to all parties on a sharepoint site)

BP Barcode BP-032687, Det_Norske_Veritas_(DNV) Houston_External HDD BP-029549 (previously made available to all parties on a sharepoint site)
BP Barcode BP-034258, Det_Norske_Veritas_Houston_ExternalHDD_ BP-029902 (previously made available to all parties on a sharepoint site)
DNV2011061504 - P-T Sensor Test Data

Publicly Available Documents

Article - Composition and fate of gas - C.M. Reddy.pdf	MDL Dep. Ex. 9012
Azzopardi - Two-Phase Flow Patterns in Large	Two-Phase Flow Patterns in Large Diameter Vertical Pipes at High Pressures, N.K. Ombere- lyari and B.J. Azzopardi, AIChE Journal, Vol.53, No. 10, Oct. 2007
BOP Further Forensic Testing - Handwritten.pdf	
BP Fact Sheet (http://www.bp.com/liveassets/bp_internet/globalbp/globalbp_uk_english/incident_response/STAGI/NG/local_assets/downloads_pdfs/RITT_Factsheet_5-13-10)	
Bushnell N - 003.06 - Fundamentals of Multiphase Flows.pdf	XSGX004-000932
Bushnell N - Pg 21 - Irrecoverable Pressure Loss Coefficients.pdf	Irrecoverable Pressure Loss Coefficients for Two Out-of-Plane Piping Elbows at High Reynolds Number, R.D. Coffield et al, http://www.osti.gov/bridge/servlets/purl/7647-8LcJVH/webviewable/7647.pdf
Camilli - Acoustic Measurement of the Deepwater Horizon Macondo Well Flow Rate	MDL Dep. Ex. 9006
Camilli - Acoustic Measurement Supporting Information	MDL Dep. Ex. 9006
Camilli - Composition and Fate of Gas and Oil Released	MDL Dep. Ex. 9012
CL68379-DEC-EOS20120322.MFL	
CL68379-EOS20120322.MFL	
CL68379-EOS20120322.out	
CL68508-DEC-EOS20120322.MFL	
CL68508-EOS20120322.MFL	
D.S. Miller, Internal Flow Systems, 2nd ed. 1990.	
DNV BOP Report Addendum	
DNV BOP Report Volume I	
DNV BOP Report Volume II Appendices	

DNV BOP Testing Phase I	
DNV2011062210 - Laser Scanning Tracking Sheet	
Doc 2016-1 (Approved Protocol)	Deepwater Horizon Blowout Preventer (BOP) Final Protocol Points Regarding Further Forensic Testing, Document No. 2016-1, Filed Apr. 19, 2011
DOE-NL -- DJB marked with proprietary marked OOU -SAND Report on Flow Analysis Studies 12-08-10	MDL Dep. Ex. 8621
DOE-NL DWH Oil Re (Griffiths)_(18699619_1)	SNL144-016043
EOS parameters 20120924.xls	
FRTG - Assessment of Flow Rate Estimates for the Deepwater Horizon-Macondo Oil Spill - (Combined)	MDL Dep. Ex. 9005
Government Update (http://www.restorethegulf.gov/release/2010/05/16/update-riser-insertion-tube-tool-progress)	SNL144-016043
Griffiths - 017 - June 2011 Sandia Report.pdf	MDL Dep.Ex.9890
Griffiths - 065.01 - Collection rates during well integrity test w_Vx.xlsx	BP-HZN-2179MDL04801508
Griffiths - 070 - SAND2011-3800.pdf	TREX-21174
Griffiths_Revised_6_2011	MDL Dep.Ex.9890
Hewitt, G.F., and Roberts, D.N., "Studies of Two-Phase Flow Patterns by Simultaneous X-ray and Flash Photography," AERE-M 2159, HMSO, 1969	
INTERTEK-DEC-EOS20120322.MFL	
INTERTEK-EOS20120322.MFL	
Kelkar M - 006 - Macondo EOS.pdf	Zick Expert Report, Appendix D
Kelkar M - 028 - Use of Data.pdf	Morris Muskat, Use of Data on the Build-up of Bottom-hole Pressures, Fort Worth Meeting, 1936
Kelkar M - 029 - Understanding.pdf	V.C. Larson, Understanding the Muskat Method of Analysing Pressure Build-up Curves, Journal of Canadian Petroleum, Page 136 (April 1963)
Multiflash Notes.txt	
Oil Release from Well MC252 Following the Deepwater Horizon Accident	Stewart K. Griffiths, Oil Release from Macondo Well MC252 Following the Deepwater Horizon Accident (Just Accepted Manuscript), Environ. Sci. Technol., April 16, 2012 (downloaded from http://pubs.acs.org on April 24, 2012)
Oldenburg_PNAS.pdf	Numerical simulations of the Macondo well blowout reveal strong control of oil flow by reservoir permeability and exsolution of gas, Curtis M. Oldenburg et al, www.pnas.org/cgi/doi/10.1073/pnas.1105165108
P.B. Whalley -- "Boiling, Condensation and Gas-Liquid Flow" Oxford University Press, pp 52 - 59, 1987	
Pabon Declaration No. 4	Declaration of Martin J.Pabon, Doc. No.3149-2, Filed July 6, 2011
PNAS-2011-Reddy-1101242108	MDL Dep. Ex. 9012

PresComm - BP Comments to Oct 6 Working Paper No 3 - Amount and Fate of Oil	MDL Dep. Ex. 10338
PresComm - Flow Rate - Amount and Fate of Oil	MDL Dep. Ex. 10762
Procedure 4209	BP-HZN-2179MDL06746270
R.W. Lockhart and R.C. Martinelli, "Proposed correlation of Data for Isothermal, Two Phase, Two Component Flow in Pipes" Chem. Eng. Prog., Vol. 45. 1949, pp. 39-48	
Revised_Ratzel_9_2011	MDL Dep. Ex. 8621
S.K. Griffiths, Env. Sci. Tech 46(10) 5616.pdf	Stewart K. Griffiths, Oil Release from Macondo Well MC252 Following the Deepwater Horizon Accident (Just Accepted Manuscript), Environ. Sci. Technol., April 16, 2012 (downloaded from http://pubs.acs.org on April 24, 2012)
SLB-118-DEC-EOS20120322.mfl	
SLB-118-EOS20120322.MFL	
Sperry-Sun drilling data	BP-HZN-BLY00061169
Staff Working Paper No. 3, Oct, 2010.pdf	http://www.oilspillcommission.gov/sites/default/files/documents/Updated%20Amount%20and%20Fate%20of%20the%20Oil%20Working%20Paper.pdf
Supporting Information, Oil Release from Macondo Well MC252 Following the Deepwater Horizon Accident, Stewart K. Griffiths	

ROV Video Footage

BP-HZN-2179MDL04569966,
BP-HZN-2179MDL00330291,
BP-HZN-2179MDL04569961,
BP-HZN-2179MDL04569964,
BP-HZN-2179MDL06004627,
BP-HZN-2179MDL02378370,
BP-HZN-2179MDL02360288,
BP-HZN-2179MDL03096374,
BP-HZN-2179MDL03096378,
BP-HZN-2179MDL03096381,
BP-HZN-2179MDL03096433,
BP-HZN-2179MDL03096434,
BP-HZN-2179MDL03096476,
BP-HZN-2179MDL03096483,
BP-HZN-2179MDL03096490,
BP-HZN-2179MDL03096491,
BP-HZN-2179MDL03096492,
BP-HZN-2179MDL03096493,
BP-HZN-2179MDL03096494,
BP-HZN-2179MDL03096495,
BP-HZN-2179MDL03096496,
BP-HZN-2179MDL03096497,
BP-HZN-2179MDL03096498,
BP-HZN-2179MDL04569876,
BP-HZN-2179MDL04569882,
BP-HZN-2179MDL04569889,
BP-HZN-2179MDL04569895,
BP-HZN-2179MDL04569898,
BP-HZN-2179MDL04569902,
BP-HZN-2179MDL04569903,
BP-HZN-2179MDL04569906,
BP-HZN-2179MDL04569907,
BP-HZN-2179MDL04569908,
BP-HZN-2179MDL04569909,
BP-HZN-2179MDL04569910,
BP-HZN-2179MDL04569911,
BP-HZN-2179MDL04569912,
BP-HZN-2179MDL04569914,
BP-HZN-2179MDL04569915,
BP-HZN-2179MDL04569916,
BP-HZN-2179MDL04569917,
BP-HZN-2179MDL04569918,
BP-HZN-2179MDL04569920,
BP-HZN-2179MDL04569921,
BP-HZN-2179MDL04569922,
BP-HZN-2179MDL04569923,
BP-HZN-2179MDL04569924,
BP-HZN-2179MDL04569926,
BP-HZN-2179MDL04569927,
BP-HZN-2179MDL04569929,
BP-HZN-2179MDL04569930,
BP-HZN-2179MDL04569931,
BP-HZN-2179MDL04569932,
BP-HZN-2179MDL04569934,
BP-HZN-2179MDL04569937,
BP-HZN-2179MDL04569945,

BP-HZN-2179MDL04569946,
BP-HZN-2179MDL06727894,
BP-HZN-2179MDL06727895,
BP-HZN-2179MDL06727896,
BP-HZN-2179MDL06727897,
BP-HZN-2179MDL06727898,
BP-HZN-2179MDL06727899,
BP-HZN-2179MDL06727900,
BP-HZN-2179MDL06727901,
BP-HZN-2179MDL06727902,
BP-HZN-2179MDL06727903,
BP-HZN-2179MDL06727904,
BP-HZN-2179MDL06727905,
BP-HZN-2179MDL06727906,
BP-HZN-2179MDL06727907,
BP-HZN-2179MDL06727908,
BP-HZN-2179MDL06727909,
BP-HZN-2179MDL06727910,
BP-HZN-2179MDL06727911,
BP-HZN-2179MDL06727912,
BP-HZN-2179MDL06727913,
BP-HZN-2179MDL06727914,
BP-HZN-2179MDL06727915,
BP-HZN-2179MDL06727916,
BP-HZN-2179MDL06727917,
BP-HZN-2179MDL06727918,
BP-HZN-2179MDL06727919,
BP-HZN-2179MDL06727920,
BP-HZN-2179MDL06727921,
BP-HZN-2179MDL06727922,
BP-HZN-2179MDL06727923,
BP-HZN-2179MDL04569970,
BP-HZN-2179MDL04569971,
BP-HZN-2179MDL03096573,
BP-HZN-2179MDL03096567,
BP-HZN-2179MDL03096570,
BP-HZN-2179MDL03096571,
BP-HZN-2179MDL03096572,
BP-HZN-2179MDL03096568,
BP-HZN-2179MDL03096574,
BP-HZN-2179MDL06530476,
BP-HZN-2179MDL06530477,
BP-HZN-2179MDL06530478,
BP-HZN-2179MDL06530479,
BP-HZN-2179MDL06530480,
BP-HZN-2179MDL06530481,
BP-HZN-2179MDL06530482,
BP-HZN-2179MDL06530483,
BP-HZN-2179MDL06530484,
BP-HZN-2179MDL06530485,
BP-HZN-2179MDL06530486,
BP-HZN-2179MDL04569866,
BP-HZN-2179MDL04569868,
BP-HZN-2179MDL04569879,
BP-HZN-2179MDL04569928,
BP-HZN-2179MDL04569940,

	BP-HZN-2179MDL04569867, BP-HZN-2179MDL04569891, BP-HZN-2179MDL04569899, BP-HZN-2179MDL04569925, BP-HZN-2179MDL04569897, BP-HZN-2179MDL04569896, BP-HZN-2179MDL04947818, BP-HZN-2179MDL06530487, BP-HZN-2179MDL06530488, BP-HZN-2179MDL04569874, BP-HZN-2179MDL04569872, BP-HZN-2179MDL04569884, BP-HZN-2179MDL04569888, BP-HZN-2179MDL04569893, BP-HZN-2179MDL04569894, BP-HZN-2179MDL04569901, BP-HZN-2179MDL04569904, BP-HZN-2179MDL04569905, BP-HZN-2179MDL04569900, BP-HZN-2179MDL04569869, BP-HZN-2179MDL04569877, BP-HZN-2179MDL04569870, BP-HZN-2179MDL04569871, BP-HZN-2179MDL04569880, BP-HZN-2179MDL04569886, BP-HZN-2179MDL04569887, BP-HZN-2179MDL04569881, BP-HZN-2179MDL04569878, BP-HZN-2179MDL04569885, BP-HZN-2179MDL04569962, BP-HZN-2179MDL04569963, BP-HZN-2179MDL06625855; BP-HZN-2179MDL06625854
--	--

Other Documents

Consideration Materials List of Mohan Kelkar and Rajagopa Raghavan
Consideration Materials List of Mohan Kelkar and Rajagopa Raghavan (Revised)
Consideration Materials List of Nathan Bushnell
Consideration Materials List of Ronald Dykhuizen
Consideration Materials List of Ronald Dykhuizen (Revised)
Consideration Materials List of Stewart Griffiths
Deposition of A. Ratzel
Deposition of M. Gochnour
Deposition of M. Levitan
Deposition of R. Dykhuizen
Deposition of S. Griffiths
Deposition of T. Lockett
Deposition of T. Lockett (Corrected)
Deposition of T. Liao
Deposition of A. Ratzel

Deposition of R. Lynch
Deposition of S. McArthur
Dykhuizen_relied upon modeling runs
Expert Report of Forrest Earl Shanks
Expert Report of Greg Childs (Transocean)
Expert Report of J. J. Azar, Ph. D
Expert Report of Mehran Pooladi-Darvish
Expert Report of Mohan Kelkar and Rajagopal Raghavan
Expert Report of Morten Emilsen
Expert Report of Nathan Bushnell
Expert Report of Ronald Dykhuizen
Expert Report of Stewart Griffiths
Griffiths_relied upon modeling runs
Kelkar_relied upon modeling runs
MDL 2179 Deposition Exhibit 0604 [oversized]
MDL 2179 Deposition Exhibit 0620 [oversized]
MDL 2179 Deposition Exhibit 6138
MDL 2179 Deposition Exhibit 8682
MDL 2179 Deposition Exhibit 9361
MDL 2179 Deposition Exhibit 9012
Rebuttal Expert Report of Forrest Earl Shanks (BP)
Spreadsheet - "Topkill#3 (Autosaved).xism" from Dykhuizen modeling runs
Stipulation Mooting BP's Motion for Partial Summary Judgment Against the United States, Document 8620, Filed Feb. 19, 2013
TREX-63059